AD-A183 538 SCRIBE (STRATOSPHERIC CRYOGENIC INTERFEROMETER BALOON EXPERIMENT) DATA SU..(U) OPTIMETRICS INC BURLINGTON MA W O GALLERY ET AL. 16 FEB 87 OMI-201 AFGL-TR-87-0061 1/2

UNCLASSIFIED F19628-86-C-0102 F/G 4/1 NL

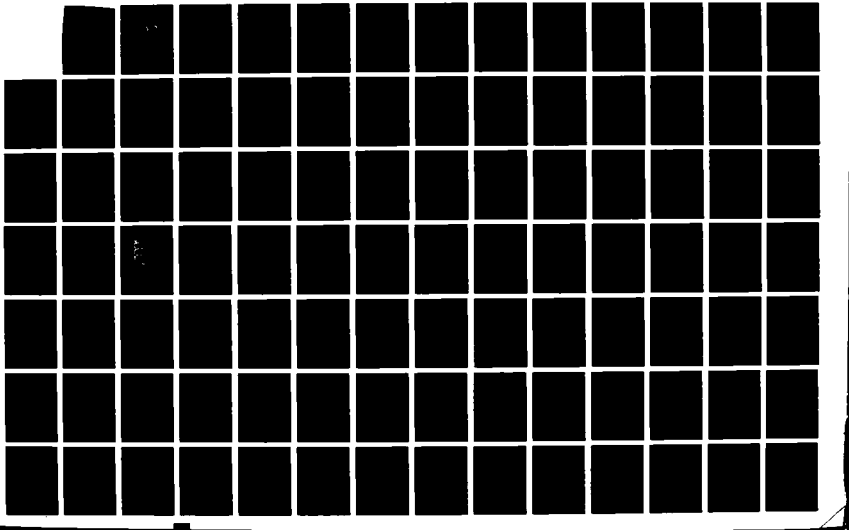

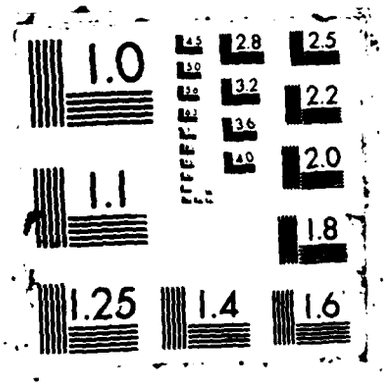
1.0
1.1
1.25
1.4
1.6
2.8
3.2
3.6
4.0
2.5
2.2
2.0
1.8

AFGL-TR-87-0061

OMI-201

SCRIBE Data Survey and Validation

W. O. Gallery
D. L. Longtin
G. Tucker

OptiMetrics, Inc.
121 Middlesex Turnpike
Burlington, MA 01803

16 February 1987

Final Report
July 1986 - January 1987

APPROVED FOR PUBLIC RELEASE; DISTRIBUTION UNLIMITED

AIR FORCE GEOPHYSICS LABORATORY
AIR FORCE SYSTEMS COMMAND
UNITED STATES AIR FORCE
HANSCOM AIR FORCE BASE, MASSACHUSETTS 01731

SECURITY CLASSIFICATION OF THIS PAGE A183532

REPORT DOCUMENTATION PAGE

1a REPORT SECURITY CLASSIFICATION Unclassified	1b RESTRICTIVE MARKINGS
2a SECURITY CLASSIFICATION AUTHORITY	3 DISTRIBUTION / AVAILABILITY OF REPORT Approved for public release Distribution unlimited
2b DECLASSIFICATION / DOWNGRADING SCHEDULE	
4 PERFORMING ORGANIZATION REPORT NUMBER(S) OMI-201	5 MONITORING ORGANIZATION REPORT NUMBER(S) AFGL-TR-87-0061
6a NAME OF PERFORMING ORGANIZATION OptiMetrics, Inc. — 6b OFFICE SYMBOL (If applicable)	7a NAME OF MONITORING ORGANIZATION Air Force Geophysics Laboratory
6c ADDRESS (City, State, and ZIP Code) 121 Middlesex Turnpike Burlington, MA 01803	7b ADDRESS (City, State, and ZIP Code) Hanscom AFB Massachusetts 01731
8a NAME OF FUNDING / SPONSORING ORGANIZATION — 8b OFFICE SYMBOL (If applicable)	9 PROCUREMENT INSTRUMENT IDENTIFICATION NUMBER F19628-86-C-0182
8c ADDRESS (City, State, and ZIP Code)	10 SOURCE OF FUNDING NUMBERS

PROGRAM ELEMENT NO.	PROJECT NO.	TASK NO.	WORK UNIT ACCESSION NO
65502F	5502	03	AF

11 TITLE (Include Security Classification)
SCRIBE Data Survey and Validation

12 PERSONAL AUTHOR(S)
W. O. Gallery, D. L. Longtin, and G. Tucker

13a TYPE OF REPORT	13b TIME COVERED	14 DATE OF REPORT (Year, Month, Day)	15 PAGE COUNT
Final Report	FROM 7/86 TO 1/87	1987 February 16	132

16 SUPPLEMENTARY NOTATION

17 COSATI CODES		
FIELD	GROUP	SUB-GROUP

18 SUBJECT TERMS (Continue on reverse if necessary and identify by block number)
Atomospheric Radiance,
Infrared Radiation,
Stratospheric Composition,

19 ABSTRACT (Continue on reverse if necessary and identify by block number)

The Stratospheric CRyogenic Interferometer Balloon Experiment (SCRIBE) is a 0.06 cm^{-1} resolution infrared interferometer spectrometer measuring emission from a stratospheric balloon platform. Three successful operational flights so far have produced a significant body of data. Two different groups the University of Denver and the University of Massachusetts have processed the interferograms from two of these flights into calibrated spectra covering the region from 600 cm^{-1} to 1200 cm^{-1} and beyond. This report examines and critically evaluates these spectra in terms of the calibration and the presence of channel spectra or other modulation. The evaluation is based upon model calculations and physical considerations which limit the expected range of the measured radiance. The result is a set of verified spectra which may be further analyzed for scientific information. Significant differences between the measured spectra and FASCODE (over)

20 DISTRIBUTION / AVAILABILITY OF ABSTRACT	21 ABSTRACT SECURITY CLASSIFICATION
☐ UNCLASSIFIED/UNLIMITED ☐ SAME AS RPT ☐ DTIC USERS	Unclassified

22a NAME OF RESPONSIBLE INDIVIDUAL	22b TELEPHONE (Include Area Code)	22c OFFICE SYMBOL
George Vanasse	617-337-3655	AFGL/OPI

DD FORM 1473, 84 MAR — 83 APR edition may be used until exhausted. All other editions are obsolete.

SECURITY CLASSIFICATION OF THIS PAGE

19. (cont.)
calculations are reported. Recommendations are made for future flights.

Keywords: —> - fac(

Preface

The authors gratefully acknowledge the assistance of Aaron Goldman, David G. Murcray, Frank H. Murcray, and Frank J. Murcray, of the Department of Physics of the University of Denver, for providing the data from the July 1984 SCRIBE flight in advance of publication, and for valuable discussions and assistance. We also wish to thank Dr. H. Saki of the University of Massachusetts, Amherst for his valuable discussions.

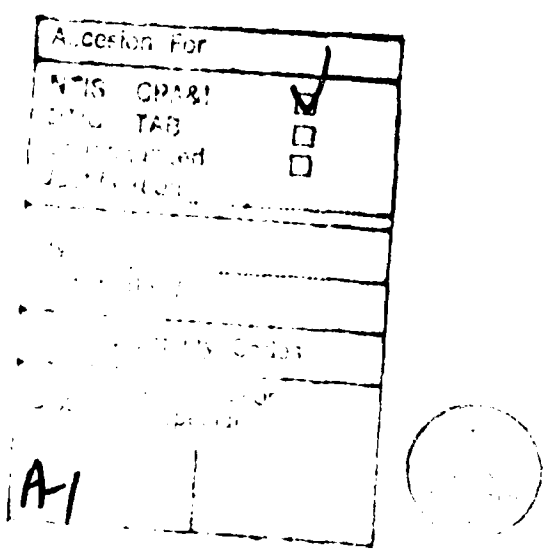

Contents

Contents (cont.)

Tables

Illustrations

1. INTRODUCTION

The Stratospheric CRyogenic Interferometer Balloon Experiment (SCRIBE) is a high resolution spectrometer which measures atmospheric emission in the stratosphere from a balloon platform. The data from SCRIBE are unique among radiometric measurements of the atmosphere in combining the following characteristics:

1. Measurement of emission, rather than absorption,
2. Absolute radiometric calibration,
3. Spectral coverage from 600 cm^{-1} to 1400 cm^{-1} at a resolution of 0.06 cm^{-1},
4. Optical paths including downlooking paths and limb views with tangent heights in the stratosphere.

The measurements are of scientific interest as they relate to models of atmospheric radiative transfer and to the presence of minor gases in the atmosphere. In the first instance, the measurements can be used to validate models of background atmospheric radiance used by the Air Force to predict and evaluate the performance of electro-optical systems. These measurements can also be used to test new methods for the remote sounding of temperature. Finally, the measurements can be used to detect the presence of minor gases in the stratosphere and to determine their abundance. This subject is of intense interest due to the importance of these gases in the photochemistry of the stratosphere and in the radiation balance and its influence on climate.

SCRIBE has completed its development phase and has been successfully flown three times. Spectra from two of these flights have been processed and are available for analysis.

It was considered advisable to critically examine and evaluate these spectra and their supporting measurements before further analysis and any further flights. The evaluation reported here will check the radiometric and spectroscopic calibration, the presence of noise and spurious signals and the general shape of the spectra. The criteria will be based upon model calculations and upon physical considerations which limit the expected range of measured radiance. Supporting measurements will be evaluated in terms of their accuracy and precision, plus how they represent the state of the atmosphere. The result of this evaluation is a set of validated spectra which can be analyzed with confidence for scientific content. The evaluation will also lead to recommendations for reducing the data from future flights and for the conduct of the flights themselves.

This report is organized as follows: Section 2 gives an overview of the SCRIBE project, including a brief history and an inventory of all the data produced to date. Section 3 describes the method of evaluating the SCRIBE spectra, including model calculations of the expected values, physical constraints on range of the radiance values and uncertainties in the supporting measurements. Section 4 presents a survey and first cut evaluation of all the available SCRIBE spectra. Section 5 presents a detailed comparison between selected spectra and model calculations. Conclusions and recommendations are given in Section 6.

2. THE SCRIBE PROGRAM: AN OVERVIEW

This section provides a broad overview of the SCRIBE program, including a brief description of the instrument, a history of the SCRIBE flights to date, a discussion of the procedures to record and reduce the data, an inventory of the data obtained so far and a summary of the results obtained from analyzing the SCRIBE data.

2.1 The SCRIBE Instrument

SCRIBE is a balloon-borne, high resolution Fourier transform spectrometer (FTS) designed to measure atmospheric emission at stratospheric altitudes. The SCRIBE instrument was designed to accommodate the requirements of high resolution (0.06 cm^{-1}), high sensitivity and to operate at altitudes up to 40 km. The following discussion applies to the instrument as it was flown in 1983. Modifications for specific flights are described in the next section.

Optical alignment over a wide temperature range was accomplished by choosing a cat's eye interferometer optical system and by fabricating all mechanical parts from the same low expansion coefficient material. Mirror position is determined by a mechanical transducer and by HeNe laser fringes. The optical path difference can vary between -0.1 to +10 cm, corresponding to a mirror travel of 5 cm. In practice, a total used optical path difference is about 8.3 cm, corresponding to an interferogram of $131072 = 2^{17}$

points. The nominal unapodized instrument function is then a sinc function with distance to the first zero of 0.060 cm^{-1}. About 400 points before the central maximum at the zero path difference are recorded to allow the interferogram to be phase corrected.

The FTS is mounted in a large dewar, equipped with an uncooled ZeSe window of low emissivity. The entire dewar is tipped to allow viewing from about -6 degrees to about +7 degrees above horizontal. A flat mirror can be inserted for nadir viewing and an ambient temperature blackbody can also be inserted to aid in calibration. The detector is copper doped germanium operating at liquid helium temperatures. The detector signal is sampled by a 12-bit analog to a digital converter whose output, along with a variety of housekeeping signals, is fed to a custom pulse code modulation (PCM) encoder. The PCM encoder generates a 72-bit frame at a rate of 10^4 frames per second. The data are relayed to a ground station via an S-band telemetry link. The exact form of the PCM stream will be considered in more detail in Section 2.4.

2.2 Program History

In 1973, at the initiation of Dr. George Vanasse, the Air Force Geophysics Laboratory (AFGL) entered into a contract with James L. Pritchard of Idealab, Inc. for the development of a cryogenically cooled interferometer. At the conclusion of this contract in 1976, the basic SCRIBE

interferometer as it exists today had been constructed. In its initial form, the interferometer utilized a LN_2 cooled HgCdTe detector and needed major modifications before it could be flown. Under a contract from AFGL, the Department of Physics at the University of Denver undertook the tasks of making SCRIBE flight-ready and of conducting a flight program[1]. The modifications made included replacing the HgCdTe detector with a liquid helium cooled HgGe detector, interfacing the analog-to-digital converter to the PCM encoder, repacking all electronics to ensure operation at 40 km, mounting the dewar in a gondola with provisions for tilting the dewar and introducing a mirror or a blackbody into the field-of-view. On October 8, 1980 SCRIBE was flown for the first time from Holloman Air Force Base, in New Mexico. Unfortunately, problems with the interferometer's drive and the loss of laser fringes limited the data obtained to a few noisy spectrum taken at low altitude. The instrument was again flown on October 7, 1981[2] and on June 16, 1982; in each case, problems limited the value of the measurements obtained. These three flights however, served to demonstrate the potential of the inter-

1. Murcray, F. H., F. J. Murcray , D. G. Murcray, and W. J. Williams (1981) Stratospheric Cryogenic Infrared Balloon Experiment, Air Force Geophysics Laboratory, Hanscom AFB, MA, AFGL-TR-81-0186, AD-A104 168.

2. Sakai, H. and G. A. Vanasse (1983) Atmospheric Infrared Emission Observed at Altitude of 27000 to 28000 m, SPIE Publ. 366, p165-172, AD-A133 472.

ferometer[3,4,5] and to point out flaws in the system which were subsequently corrected[6].

On October 23, 1983 the SCRIBE instrument (as described in the previous section) was successfully launched from Holloman AFB, New Mexico at 0510 MST (1210 GMT)[7]. All systems worked well during the ascent, and the float altitude of 30.7 km above mean sea level was reached at 0650 MST. Unfortunately, the balloon developed a leak, and after 30 minutes at float altitude it began to descend. While at float altitude, a series of scans at various look angles plus blackbody measurements were obtained. During the descent a series of nadir viewing scans were taken. The flight was terminated when the balloon descended to 18 km.

---

3. Sakai, H., T. C. Li, J. Pritchard, F. J. Murcray, F. H. Murcray, J. Williams, and G. A. Vanasse (1981) Measurement of Atmospheric Emission using a Balloon - Borne Cryogenic Fourier Spectrometer SPIE Publ. 289, p196-198, AD-A111 343.

4. Sakai, H., W. Barowy, S. Pulchtopek, J. Pritchard, F. J. Murcray, F. H. Murcray, and G. A. Vanasse (1982) Study of Atmospheric Infrared Emission Using a Balloon-Borne Cryogenic Fourier Spectrometer, SPIE Publ. 364, p38-45.

5. Vanasse, G. A. (1981) Stratospheric Cryogenic Interferometer Balloon Experiment (SCRIBE), Air Force Geophysics Laboratory, Hanscom AFB, MA, AFGL-TR-81-0048, AD-A100 218.

6. Sakai, H. (1981) SCRIBE I DATA ANALYSIS Air Force Geophysics Laboratory, Hanscom AFB, MA, AFGL-TR-81-0129, AD-A102 262.

7. Murcray, F.H., F. J. Murcray, D. G. Murcray, J. Prichard, G. A. Vanasse, and H. Sakai (1984) Liquid Nitrogen Cooled Fourier Transform Spectrometer System for Measuring Atmospheric Emission At High Altitudes, J. Atm. and Oceanic Tech., 1., p351-357, AD-A152 450.

Based on the results of this flight, an optical filter was added to the optical path in order to reduce the source noise from the strong 15 micrometer CO_2 band. This modification resulted in improved performance in the higher wavenumber region. The modified instrument was again launched from Roswell, New Mexico on July 5, 1984 at 0451 MST and reached float altitude, 31.3 km msl, at 0645 MST[8]. All systems worked well, with the only problem being strong winds at float which limited the time the balloon was in telemetry range. Good data were obtained on ascent and for approximately 1 1/2 hours at float altitude.

After the 1984 flight, the primary goal of obtaining high resolution atmospheric emission spectra at a variety of observation angles had been accomplished. Consequently, it was then possible to plan flights designed to make measurements of specific compounds which were thought to play key roles in atmospheric photochemistry. The initial compound to be studied was N_2O_5. Its presence is predicted as a result of reactions between NO_x and ozone. The interferometer was optimized for the 1250 cm^{-1} spectral region where N_2O_5 has a major band.

SCRIBE was again launched from Roswell on June 21, 1985. Launch was at 0155 MDT in order to be at float just before dawn, at which time N_2O_5 was predicted to peak[8]. An

---

8. Murcray, F.H., F. J. Murcray, D. G. Murcray, and A. Goldman (1986) Measurement of Atmospheric Emission Spectra at High Altitudes, Air Force Geophysics Laboratory, Hanscom AFB, MA, AFGL-TR-86-0061, AD-A170 143.

unexpected wind change just after inflation began made for a difficult launching. Just after release, the payload struck the ground damaging the package and causing a loss of command and balloon control links. Although the interferometer telemetry link instrument still functioned, the elevation angle and detector bias could not be changed. With the instrument locked in an upward viewing geometry and the bias at the low setting, very little useful data were obtained.

After this flight, major modifications were undertaken to narrow the field-of-view of the instrument, to provide better control of the viewing angle and to visually verify the emission source. This was accomplished by adding an uncooled telescope and a ground-controlled steering mirror to the optical path and by adding a bore-sighted television camera to the system. An operator viewing a television monitor could control the view using a joystick. The new system, designated SCRIBE-99, was successfully flown on August 10, 1986 from Roswell. The balloon was launched at 0600 MST and reached a planned float altitude of 76,000 feet. All systems operated successfully and a large number of horizontal and nadir scans were acquired. None of the spectra from this flight were available for evaluation in this report.

2.3 Data Recording

The measurement data from SCRIBE is transmitted over an S-band telemetry link to a ground recording station. There AFGL records all the data (interferograms plus houskeeping channels) on analog tape, while the Denver group edits the data stream in real-time and records only the interferograms on digital tape. This section describes the recording processes used by both groups.

Understanding the format of the analog tapes and the problems associated with them requires a discussion of the data system onboard the SCRIBE package. The analog output of the detector preamplifier is fed through a 12-bit analog-to-digital converter whose output is sampled by a custom-built PCM encoder. An interface between the A/D converter and the encoder is necessary because the time required between interferogram samples is slower than the rate at which the encoder outputs its data words. Since it is crucial that a sample not be recorded twice, a signal from the encoder clears the A/D outputs and sets a data valid bit to zero. Any frames sent before a new measurement is made contain 12 zero data bits. When a new measurement is made the data-valid bit is reset to one. The 12-bit interferogram sample is combined with four status bits to form a 16-bit word. Bit 13 is tied to ground, bit 14 shows drive direction (1=forward), bit 15 indicates the detector amplifier gain (1=high gain) and bit 16 indicates if the data are valid (1=valid).

The PCM encoder generates 72-bit frames at a rate of approximately 10^4 frames/sec. Each frame consists of two 8-bit sync words, an 8-bit counter, the 16-bit interferogram/status word, two 8-bit words indicating carriage position and speed, and two 8-bit words containing auxiliary data. Because the auxiliary measurements do not require as high a sampling rate as the interferometer, they are commutated, allowing 30 data channels to be sampled at a rate of 700 samples per second. Among the measurements on these channels are detector impedance, amplifier gain, laser fringe amplitude, various internal and external temperatures, elevation angle and instrument azimuthal position. Other data were recorded on these channels but it varied from flight to flight. The University of Denver has the channel assignments as well as the calibration data which allows these digital signals to be interpreted.

On the ground, AFGL passes the telemetry signal through a bit synchronizer along with millisecond resolution time code (IRIGB) data, and then records the combined signal on analog 1/2" magnetic tapes at a speed of 60 inches per second (ips). Generally, AFGL has at least two ground stations making analog recording of each flight.

At the same time that AFGL is recording the analog tapes, the Denver group passes the output of the parallel bit synchronizer to a Nova 1200 computer (acting as a decommutator). There the interferogram words are removed from the data stream, redundant samples discarded and the

resulting interferograms formatted and stored on digital magnetic tapes. By recording the data in this way, the Denver group provides a backup to the analog recording. In addition, the digital tapes are immediately available for a quick look at the data. Denver has copies of the analog tapes and can read them as necessary to obtain the housekeeping data.

Measurements of the physical state of the atmosphere are provided by radiosonde flights either from White Sands Missile Range or from Holloman AFB. Ground radar stations also record the balloon's X, Y and Z coordinates.

2.4 Data Reduction

The first step in data reduction for the analog tapes is to decommutate them to produce digital tapes. This step involves playing back the tapes through an analog tape recorder and feeding the output through a decommutator to a digital tape recorder. Both the interferograms and the housekeeping data can be recovered. However, decommutating the analog tapes has has proved difficult for a number of reasons (see Section 2.5), resulting in major delays in processing the data. The digital tapes recorded directly by Denver were available immediately but contained only the interferograms.

Reducing the digital data tapes to calibrated spectra requires a number of separate steps. First, the interferograms must be corrected for gain changes that occur

during and between scans. These changes are necessary because of the widely varying radiance levels observed and the limited resolution of the 12-bit A/D converter. The first gain change occurs in each interferogram at approximately 800 points, where the gain is increased by a factor of 10.91 to allow the region beyond zero path difference to be sampled at a reasonable resolution. During the flight, the peak amplitude of each interferogram is monitored. If the signal falls outside the optimum range, the gain is automatically adjusted up or down by a factor of 2 as required, before the next scan is performed. These gain changes are recorded as one of the auxiliary data channels on the PCM encoder. Finally, whenever the instrument views the blackbody or the nadir, the gain is reduced by changing the detector bias by a factor of 2.1.

After the gain corrections are made, the interferograms must be examined for spurious spikes which are far above the normal signal levels. The spikes are believed to be caused by cosmic rays. If the spikes are not removed, the resulting spectrum will exhibit strong modulation. These spikes are removed by zeroing out the affected part of the interferogram.

A channel spectrum caused by the ZeSe window is also often present and will also cause modulation in the resulting spectrum if not removed. Removing the spikes and channel spectra is a tedious process since each interferogram must be examined individually.

Because of non-linear dispersion in the optical train, the recorded interferogram is not symmetric around the zero path difference. The interferogram is phase corrected by using the short, two-sided portion of the interferogram around the zero path point to generate the phase curve[9]. The resulting symmetrized interferogram is transformed into an uncalibrated spectrum using a Fast Fourier Transform.

Experience has shown that the spectra show a small frequency shift which varies linearly with frequency. It is the same for all spectra from the same flight but varies from flight to flight. The shift is determined by comparing the measured position of certain absorption lines with their known positions as listed in the AFGL Atmospheric Line Parameters Compilation[10]. The lines of the 10.6 micrometer CO_2 laser bands are typically used for this calibration. The measured spectra are corrected by multiplying the nominal wavenumber with a correction factor which is linear in wavenumber.

The final step in the data processing is the radiometric calibration. At some point during the flight, a blackbody operating at ambient temperature is positioned in front of the instrument and a number of interferograms recorded. The blackbody temperature is recorded on one of

---

9. Vanasse, G. A. and H. Sakai (1967) "Fourier Spectroscopy" in ,Progress in Optics (E. Wolf ed.), Vol VI, North Holland Publishing Co., Amsterdam.

10. Rothman, L. S. (1986) HITRAN, The Molecular Absorption Database, in the Sixth Conference on Atmospheric Radiation, Williamsburg, Virginia, May 13-16, 1986, p137-140.

the housekeeping channels. The system's response function is obtained from the spectrum of the blackbody and from the known blackbody temperature. This function is applied to the atmospheric spectra to obtain radiometricaly calibrated spectra.

The ZeSe window contributes a small but finite emission through reflection and by scattering internal radiation back into the instrument[11]. The Denver group corrects for this emission by subtracting an emission equal to the blackbody radiance at the internal instrument temperature times an effective window emissivity. This emissivity is estimated from measured emission in the window region for upward looking spectra taken at high altitude. Calculations show that this emission should be negligible so that any measured emission is caused by the window. The emissivity is assumed to be spectrally flat and has a typical value of 5 percent. The product of this final correction is a spectrum which is calibrated absolutely both radiometricaly and in frequency.

2.5 An Inventory of SCRIBE Data

This section lists all of the SCRIBE data which have been processed into interferograms or spectra and are available for further analysis. As mentioned previously, the data from the first three flights were of poor quality and none are listed here. The June 1985 flight also produced no data and the data from the August 1986 flight

11. A. Goldman, private communication.

have not yet been processed. The two flights of October 23, 1983 and July 5, 1984 did produce large numbers of spectra which are listed here.

The SCRIBE data have been processed independently by two groups: the Denver group consisting of the Murcrays (David, Frank H. and Frank J.) and Aaron Goldman, all at the Department of Physics of the University of Denver, and by Dr. H. Sakai of the Amherst Astronomy Research Facility of the University of Massachusetts. Dr. Sakai worked with the analog tapes but encountered problems processing them due to the low signal levels and variations in the speeds of the recording and playing tape recorders. Although these problems caused significant delays, Dr. Sakai was able to read and process tapes from both the October 1983 and the July 1984 flights. For a complete discussion of the University of Massachusetts effort, see references[2,3,4,6,12,13,14,15]. The Denver group had both the

---

12. Sakai, H., and G. A. Vanasse (1982) SCRIBE II DATA ANALYSIS, Air Force Geophysics Laboratory, Hanscom AFB, MA, AFGL-TR-82-0150, AD-A116 250.

13. Sakai, H., anD G. A. Vanasse (1983) SCRIBE Data of October 23, 1983, Air Force Geophysics Laboratory, Hanscom AFB, Ma., AFGL-TR-84-0208, AD-A154 862.

14. Sakai, H., G. A. Vanasse, F. H.Murcray, and F. J. Murcray, (1984) Detector-Nose-Limited Sensitivity of Fourier Spectroscopy Plus Stratospheric Emission Measurements and Observed Trace Gas Spectra, Proceedings of the 13th Congress of the International Commission for Optics, p550-551.

15. Sakai, H., (1985) Processing of Scribe Data, Air Force Geophysics Laboratory, Hanscom AFB, MA, AFGL-TR-85-0279, AD-A165 226.

analog tapes and the digital interferogram tapes they had recorded in real time.

Table 1 lists all the calibrated spectra produced by Dr. Sakai for the October 1983 flight. Table 2 lists a subset of these spectra which Dr. Sakai considers to be of superior quality and which are available on tape at AFGL. All the spectra are unapodized and have a resolution of 0.06 cm^{-1}. The Denver group has produced the spectra listed in Table 3 for this flight. The spectra correspond to the time period after the balloon started to leak and began to descend. Because the individual spectra were relatively noisy, 6 to 8 spectra were co-added and the resulting spectra smoothed to 0.24 cm^{-1} resolution.

It would be useful to directly compare calibrated spectra produced by the different groups from the same interferograms. Unfortunately, this is not possible since none of the spectra processed by the two groups coincide.

Dr. Sakai also processed spectra from the July 5, 1984 flight but because of severe and unexplained modulation in the blackbody spectra, he could not perform a calibration. Table 4 lists all the spectra processed, while Table 5 lists those available at AFGL. The Denver group has delivered to AFGL the interferograms from the July 5, 1984 flight listed in Table 6. These interferograms have not been corrected for gain, bias or phase. From this set, Aaron Goldman has produced a set of four calibrated spectra which represent

Table 1. Calibrated Spectra from the October 23, 1983 SCRIBE Flight Processed by the University of Massachusetts, Amherst

File Names	Time (GMT)	Altitude (kft)	Elevation Angle (deg)
SP830A1-A7	12:16	10	7.5
" M1-M7	12:20	20	7.5
" N1-N7	12:25	25	7.5
" O1-O7	12:30	30	7.5
" 11-17	13:15	70	1.7
" 21-27	13:45	95	-90.0
" V1-V7	13:50	95	-90.0
" W1-W7	13:54	95	-90.0
" B1-B7	14:00	95	-90.0
" C1-C7	14:05	95	-90.0
" D1-D7	14:08	95	-90.0
" 31-37	14:13	95	-0.4
" E1-E7	14:17	95	-0.4
" F1-F7	14:20	95	-0.4
" G1-G7	14:24	95	*-0.4/2.9
" H1-H7	14:27	95	-2.9
" I1-17	14:30	95	-2.9
" J1-J7	14:33	95	*-2.9/-5.4
" K1-K7	14:37	95	-5.4
" L1-L7	14:40	95	-5.4
" 41-47	14:45	95	-5.4
" 61-67	14:48	95	-5.4
" 71-77	14:53	95	Blackbody
" 81-87	14:55	95	Blackbody
" 91-97	15:02	95	7.5
" P1-P7	15:06	95	*7.5/-90.0
" Q1-Q7	15:10	95	-90.0
" R1-R7	15:15	90	-90.0
" S1-S7	15:18	90	-90.0
" T1-T7	15:22	90	-90.0
" U1-U7	15:25	90	-90.0

Notes:
1. Spectra are unapodized with a resolution of 0.06 cm^{-1}.
2. * Indicates the quantity changes during the interval.
3. A Blackbody calibration was applied to all spectra.
4. Times and altitudes are aproximate. Altitudes are above the ground.
5. These files are stored on magnetic tape at the University of Massachusetts, Amherst.

Table 2. Selected Calibrated Spectra from the October 23, 1983 SCRIBE Flight Processed by the University of Massachusetts, Amherst and Available at AFGL

File Names	Time (GMT)	Altitude (kft)	Elevation Angle (deg)
SP830M4	12:20	20	7.5
N1	12:25	25	7.5
O1	12:30	30	7.5
V3	13:50	95	-90.0
W1	13:54	95	-90.0
B1-B7	14:00	95	-90.0
C1-C5	14:05	95	-90.0
D1	14:08	95	-90.0
31,36	14:13	95	-0.4
E1	14:17	95	-0.4
F6	14:20	95	-0.4
G1,G3	14:24	95	*-0.4/-2.9
H1,H2	14:27	95	-2.9
I1,I2	14:30	95	-2.9
J2,J7	14:33	95	*-2.9/-5.4
K3,K7	14:37	95	-5.4
L1,L2	14:40	95	-5.4
41-47	14:45	95	-5.4
95-97	15:02	95	7.5
P1,P3	15:06	95	*7.5/90.0
Q1	15:10	95	-90.0

Notes:

1. Spectra are unapodized with a resolution of 0.06 cm^{-1}.
2. * Indicates the quantity changes during the interval.
3. A Blackbody calibration was applied to all spectra.
4 Times and altituded are aproximate.
5. File names are from U. Mass.
6. These files are available at AFGL on tape FTHY06.

Table 3. Calibrated Spectra From the October 23, 1983 SCRIBE Flight Processed by the University of Denver and Available at AFGL

File No.	Co-Added Files	Altitude (km msl)
1	Tape 4 Files 86, 87, 88, 90, 91, 92	28.1
2	Tape 5 Files 2, 3, 4, 5, 6, 7, 8, 9	27.2
3	Tape 5 Files 10, 11, 12, 13, 14, 15, 16, 17	26.8
4	Tape 5 Files 18, 19, 20, 21, 22, 23, 24, 26	26.6
5	Tape 5 Files 27, 28, 29, 30, 32, 33, 35, 36	26.2
6	Tape 5 Files 37, 38, 39, 40, 41, 42, 43, 44	25.6
7	Tape 5 Files 45, 46, 47, 48, 49, 50, 51, 52	25.1
8	Tape 5 Files 53, 55, 56, 57, 58, 61, 62, 63	24.4
9	Tape 5 Files 64, 66, 67, 68, 69, 61, 72, 73	23.3
10	Tape 5 Files 74, 75, 76, 77, 78, 79, 80, 81	21.8
11	Tape 6 Files 2, 3, 4, 5, 6, 7, 8, 9	19.0

Notes:

1. All spectra are Nadir views.
2. These spectra were obtained during decent and were relatively noisy due to balloon rotation. They were degraded to a resolution of 0.24 cm^{-1} to reduce the noise.
3. A blackbody calibration was applied to all spectra.
4. Altitudes are approximate because the balloon was descending during this period.
5. The co-added file designation indicates the individual spectra used in the co-adding. The tape and file numbers are the notatation used at U. Denver.
6. The spectra are archived on magnetic tape and floppy disk at the AFGL.

Table 4. Uncalibrated Spectra from the July 5, 1984 SCRIBE Flight Processed by the University of Massachusetts, Amherst

Time (GMT)	File Names	Elevation Angle (deg)	Gain	Bias
12:21-12:22	MI-MK	4.9	1	2.1
12:24-12:33	QE,QF,QL,PE QJ,QK,PF,PC	4.9	2	2.1
12:50-13:45	KA-KL,LA-LI, LK,LL,MA,MB, ME,HI,HK,HL, IA-IL,JA-JL	1.9	2	2.1
13:58-14:05	GA,GB,GD-GJ	-0.6	2	2.1
14:10-14:35	HA-HH,TA-TH, UA-UH	-3.2	1	2.1
14:47-14:58	AA-AL,BA,BB, BD-BF	-3.7	1	2.1
15:06-15:12	DA-DH	-1.2	2	2.1
15:28-15:30	EA-ED	Blackbody	1	1
15:45	RB	-1.2	1	1
15:48	RF	-90.0	2	1
15:50-15:53	RH-RL	-90.0	1/2	1

Notes:

1. Spectra are unapodized with a resolution of 0.06 cm^{-1}.
2. No blackbody calibration was performed.
3. These files are stored on magnetic tape at the University of Massachusetts, Amherst. The file designations are those of U. Mass.

Table 5. Uncalibrated Spectra from the July 5, 1984 SCRIBE Flight Processed by the University of Massachusetts, Amherst and available at AFGL

File Name	GMT	Altitude (kft msl)	Elevation Angle (deg)	Gain	Bias
847MJ	12:22	40	4.9	1	2.1
847QA	12:45	60	1.9	1	2.1
847LC	13:01	70	1.9	2	2.1
847HJ	13:21	75	1.9	2	2.1
847IA	13:24	80	1.9	2	2.1
847IK	12:33	85	1.9	2	2.1
847JB	13:36	90	1.9	2	2.1
847JI	13:43	94	1.9	2	2.1
847FA	13:49	100	1.9	2	2.1
847GB	13:58	100	-0.6	2	2.1
847HB	14:11	100	-3.2	2	2.1
8475C[TC]	14:22	100	-3.2	2	2.1
847UC	14:31	100	-3.2	1	2.1
847AC	14:48	100	-3.7	1	2.1
847BF	14:58	100	-1.2	1	2.1
846DC	15:05	100	-1.2	2	2.1

Notes:

1. Resolution of all scans is 0.06 cm^{-1}.
2. No blackbody calibration was applied to the spectra.
3. File 8475C[TC] was obtained from a co-add of eight interferograms.
4. These files are available at AFGL on tape FTHY85.

Table 6. Interferograms from the July 5, 1984 Flight Collected by the University of Denver

Tape No.	Files	Elevation Angle (deg)	Altitude (km msl)	Gain	Bias
1	2-66	4.9	*	0.5	1
1	67-100	4.9	*	1	2.1
1	101-125	4.9	*	2	2.1
2	2-6	4.9	*	2	2.1
2	12-113	1.9	*	2	2.1
3A	2-74	1.9	*	2	2.1
3A	78-112	-0.6	31.2	2	2.1
4A	2-10	-3.2	31.2	2	2.1
4A	11-73	-3.2	31.2	1	2.1
4A	79-98	-3.7	31.2	1	2.1
5A	2-39	-3.7	31.2	1	2.1
5A	43-97	-1.2	31.2	2	2.1
6A	5-7	-1.2	31.2	2	2.1
6A	11-46	Blackbody	31.2	1	1
6A	51-83	-90.0	31.2	0.5	1
6A	87-96	-1.2	*	*	*

Notes:

1. * indicates the quantity varied during the interval.
2. The interferograms have not been corrected for phase, gain or bias.
3. These interferograms are stored on magnetic tape at AFGL.
4. Files are not included where the data was questionable, for example, when the interferometer was being moved to a new elevation angle.

co-added spectra of 10 to 13 individual spectra. These spectra are listed in Table 7.

AFGL encountered great difficulty in reading the analog tapes. After considerable effort, the problem was traced to a faulty playback tape recorder which has since been repaired. AFGL has successfully read all 30 tapes from the August 1986 flight and can process tapes from past flights as needed.

2.6 Data Analysis

Although data reduction has accounted for most of the effort to date, data analysis has resulted in several interesting results.In the the 1983 spectra, Dr. Sakai found the expected features due to CO_2, O_3, HNO_3, H_2O and N_2O [14]. The Q branch of the ν_2 band of CO_2 at 667 cm^{-1}, which is very opaque, was used to measure temperature in the vicinity of the balloon. The values obtained were about 10 K higher than those measured in a less opaque spectral region for the atmosphere at a similar altitude some distance from the instrument. Dr. Sakai attributed this discrepancy to a mass of warm air carried along with the balloon on its ascent. The HNO_3 features were verified as the ν_5 and $2\nu_9$ bands. He also compared SCRIBE spectra to synthetic spectra generated from the AFGL Atmospheric Line Compilation (HITRAN database).

Table 7. Calibrated Co-Added Spectra for the July 5, 1984 Flight from the University of Denver

File Name	Elevation Angle (deg)	Altitude (km msl)	No. Co-added Spectra
SC84-1	-90.0	31.3	12
SC84-2	-3.7	31.3	10
SC84-3	-3.2	31.3	12
SC84-4	1.9	31.3	13

Notes:

1. Spectra are unapodized with a resolution of 0.06 cm^{-1}.
2. A blackbody calibration has been applied.

The University of Denver group performed a similar analysis[7,16], and in addition to the molecules mentioned earlier, also identified features due to $CFCl_3$ (freon 11) and CF_2Cl_2 (freon 12). They also obtained a laboratory absorption spectrum of HNO_3. By comparing this spectrum with the SCRIBE data, the assignment of HNO_3 features in the SCRIBE spectra were verified. In addition, the laboratory spectrum was used to confirm that the resolution of the SCRIBE interferometer is 0.06 cm^{-1} (FWHM). They concluded that the instrument has sufficient sensitivity to measure atmospheric emission at high altitudes at its full resolution. Also at the University of Denver, Dr. Aaron Goldman prepared comparisons of simulated and SCRIBE spectra[17]. He generally found good agreement of his model with the observed radiance, but noted major inadequacies in the 830 cm^{-1} window region.

Dr. Goldman has also prepared similar comparisons for the 1984 flight [18,19]. These comparisons were made for elevation angles of 1.9, -3.2, -3.7 and 90.0 degrees while

---

16. Murcray, D. G., F. H. Murcray, F. J. Murcray and G. A. Vanasse (1985) Measurements of Atmospheric Emission at High Spectral Resolution, J. of Met. Soc. Japan, 63, p320-324, AD-A159 338.

17. Goldman, A. (1986) Atmospheric Radiance in the 8.6 - 13.6 Micrometer Region-an Update, Scientific Report, Dept of Physics, U. of Denver, Denver CO.

18. Goldman, A. (1985) Cold Interferometer July 5 1984 Flight Scientific Report, Dept. of Physics, U. of Denver, Denver, CO.

19. Goldman, A. (1985) Preliminary Qualitative Comparison of Calculated and Experimental Cold Interferometer Spectra, Scientific Report, Dept of Physics, U. of Denver, Denver CO.

the interferometer was at float. Again, reasonable agreement was found but a number of adjustments to the model were necessary before this could be accomplished.

Dr. Laurence Rothman of AFGL has compared the 1983 downlooking spectra obtained at 61, 70, 81 and 88 kft with synthetic spectra generated by the FASCODE modeling program from the AFGL line parameter file. Preliminary results indicate that there is a major discrepancy between the spectra in the region of the CO_2 ν_2 Q branch at 667 cm^{-1}. This discrepancy is not yet understood and additional analysis is being undertaken with a more complete set of spectra.

3. METHOD OF VALIDATION OF THE SCRIBE DATA

The criteria for judging the spectra must be established before attempting to evaluate them. This section discusses the methods and procedures used to evaluate the spectra, and it discusses the uncertainties in the process.

The spectra which will be evaluated are all the SCRIBE spectra available at AFGL which have been absolutely calibrated and are at the maximum instrument resolution of 0.06 cm^{-1}. The inventory in Section 2 identified the spectra which meet these requirements as those listed in Tables 2 and 7. (The other available spectra are either uncalibrated [Table 5], or are at reduced resolution [Table 3].) These spectra include the 47 spectra from the October 23, 1983 flight, as processed by Dr. Sakai and the four co-added spectra from the July 5, 1984 flight as processed by the University of Denver. It would be useful to be able to compare spectra from the two different groups which were derived from the same interferogram, but unfortunately there are none.

The evaluation consists of two steps. First, all the spectra are examined for gross errors in shape and for unreasonable radiance levels. Second, spectra which pass this test are subjected to a detailed comparison with model calculations.

3.1 Survey of All the Data

The first step in the evaluation is to visually inspect the spectra for gross errors in shape and level. A SCRIBE spectrum between 600 and 1200 cm^{-1} at maximum resolution (0.06 cm^{-1}), contains 10,000 points and when plotted as a whole, the fine detail overwhelms the large scale features. Therefore, the measured spectrum is first degraded with a triangular instrument function with a half width at half maximum (HWHM) of 1.0 cm^{-1}. The degraded spectrum is plotted both on a radiance scale and on an equivalent brightness temperature scale. The brightness temperature scale is useful because it allows the observer to easily relate the different parts of the spectrum to temperatures in the atmosphere. In particular, for downward looking spectra, the brightness temperature in the window regions is related to the temperature of the ground. For this evaluation, the spectral extent is limited to 600 to 1200 cm^{-1} because the system response falls off very quickly below 600 cm^{-1} and the signal-to-noise ratio becomes relatively large above 1200 cm^{-1}. The spectra do however extend out to about 1500 cm^{-1}.

While the exact shape of the spectra should vary with altitude and look angle, the general shape should contain certain features. Figure 1 shows two calculated spectra which model the extreme cases of the SCRIBE spectra for the October 1983 flight. The upper curve corresponds to the case of a downward looking spectrum (zenith angle of 180

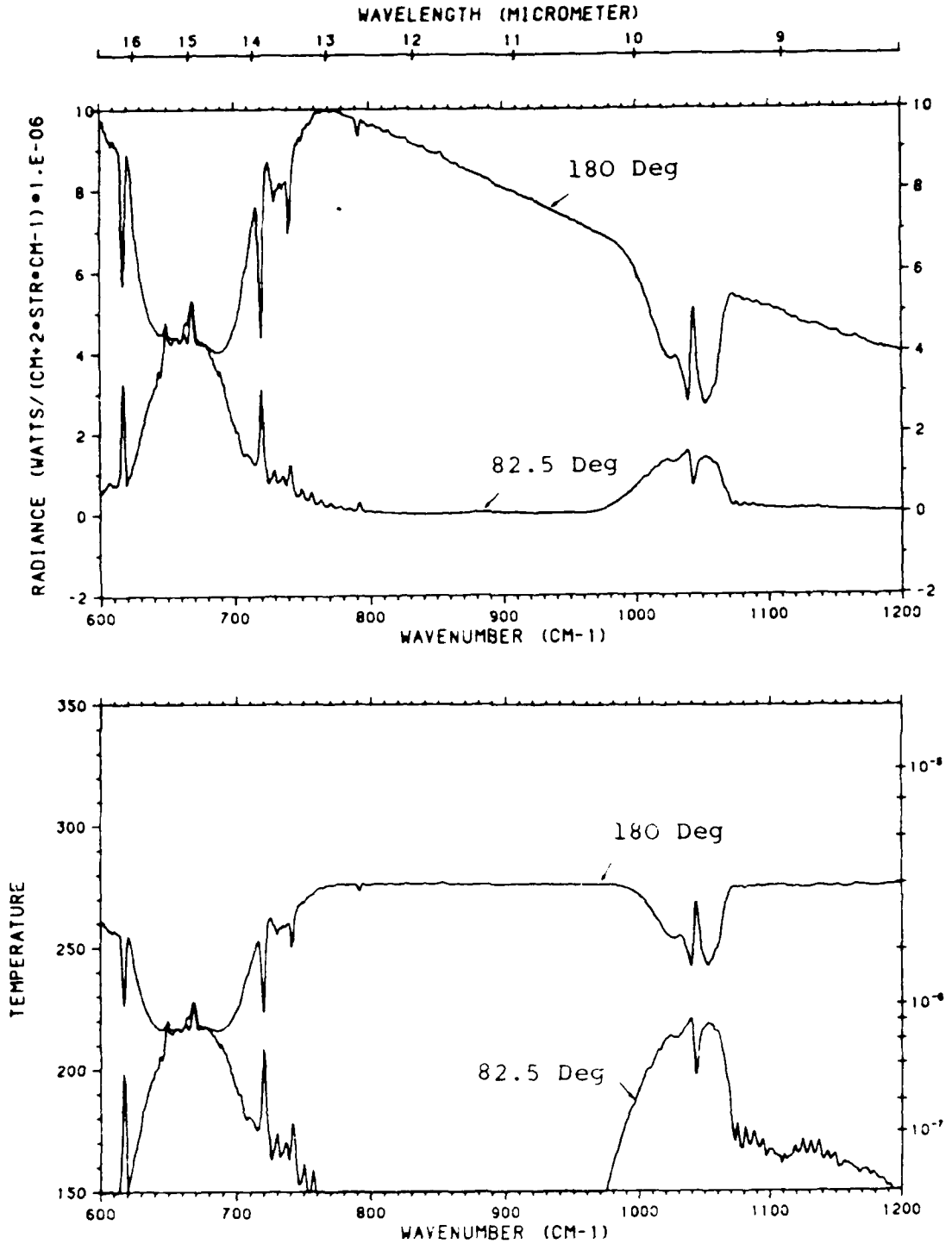

Figure 1. Calculated Radiance from 600 cm^{-1} to 1200 cm^{-1} Degraded to 1.0 cm-1 Resolution for Zenith Angles of 180 and 82.5 Deg: a. Radiance, b. Brightness Temperature. This Figure Shows the Overall Shape and the Prominant Features Expected in the SCRIBE Spectra.

degrees), while the lower curve is for the case of looking 7.5 degrees above the horizon (zenith angle of 82.5 degrees) Both spectra assume a float altitude of 30.7 km. The spectra were calculated using FASCOD2[20]. The spectra were degraded with a triangular instrument function of 1.0 HWHM so as to smooth out the fine detail leaving only the overall shape and broad features.

The three prominent features seen in these spectra are the 15 micrometer CO_2 band centered at 667.cm^{-1}, the 10.6 micrometer ozone band centered at 1040 cm^{-1} and the window regions between about 800 and 970 cm^{-1} and beyond 1080 cm^{-1}. In looking at the 15 micrometer CO_2 band first, note that in the downward looking case, this feature is seen in absorption, while in the uplooking case it is seen in emission. This is because in the downward looking case, the cold CO_2 is seen against the warm earth background, while in the upward looking case it is seen against the colder background of space. The ozone band around 1040 cm^{-1} exhibits the same kind of behavior but not as strongly since the absorption by ozone is less than that of CO_2. In the window regions between these bands, the downward looking case essentially sees the blackbody radiance at the temperature of the ground, modified only slightly by the absorption and re-emission of the intervening atmosphere.

---

20. Clough, S. A., F. X. Kneizys, E. P. Shettle, and G. P. Anderson (1986) Atmospheric Radiance and Transmittance: FASCODE 2, in the Sixth Conference on Atmospheric Radiation, Williamsburg, Virginia, May 13-16, 1986

This effect is best seen in Figure 1b where the spectra are plotted in terms of brightness temperature. Here the spectrum in the windows is flat at a temperature close to the ground temperature. For the upward looking case, the radiance level in the windows is very small.

These two spectra show the extreme limits of the expected SCRIBE spectra. Measured spectra taken at a zenith angle between these two limits, such as viewing the limb below the horizon, will show characteristics somewhere between the these two.

In addition to the low resolution plots of the measured spectra, plots are also made at full resolution for the regions between 665 and 675 cm^{-1}, and between 800 and 820 cm^{-1}. These plots are examined for specific features as follows.

The center of the ν_2 band of CO_2 at 667 cm^{-1} is so opaque that the radiance originates from 1 km or less of the path. This point is illustrated in Figure 2 which shows the calculated transmittance between 665 and 675 cm^{-1} for various path lengths from 10 m to 2 km. The calculation assumes a horizontal path at 30 km and is degraded to match the spectral resolution or SCRIBE. This figure shows that at the center of the Q branch between 667.4 and 667.8 cm^{-1}, the transmittance for a 1 km path is less than 1 percent, so that over 99 percent of the radiance originates within the first kilometer; similarly, 50 percent originates within the first 50 m. The measured brightness temperature within this

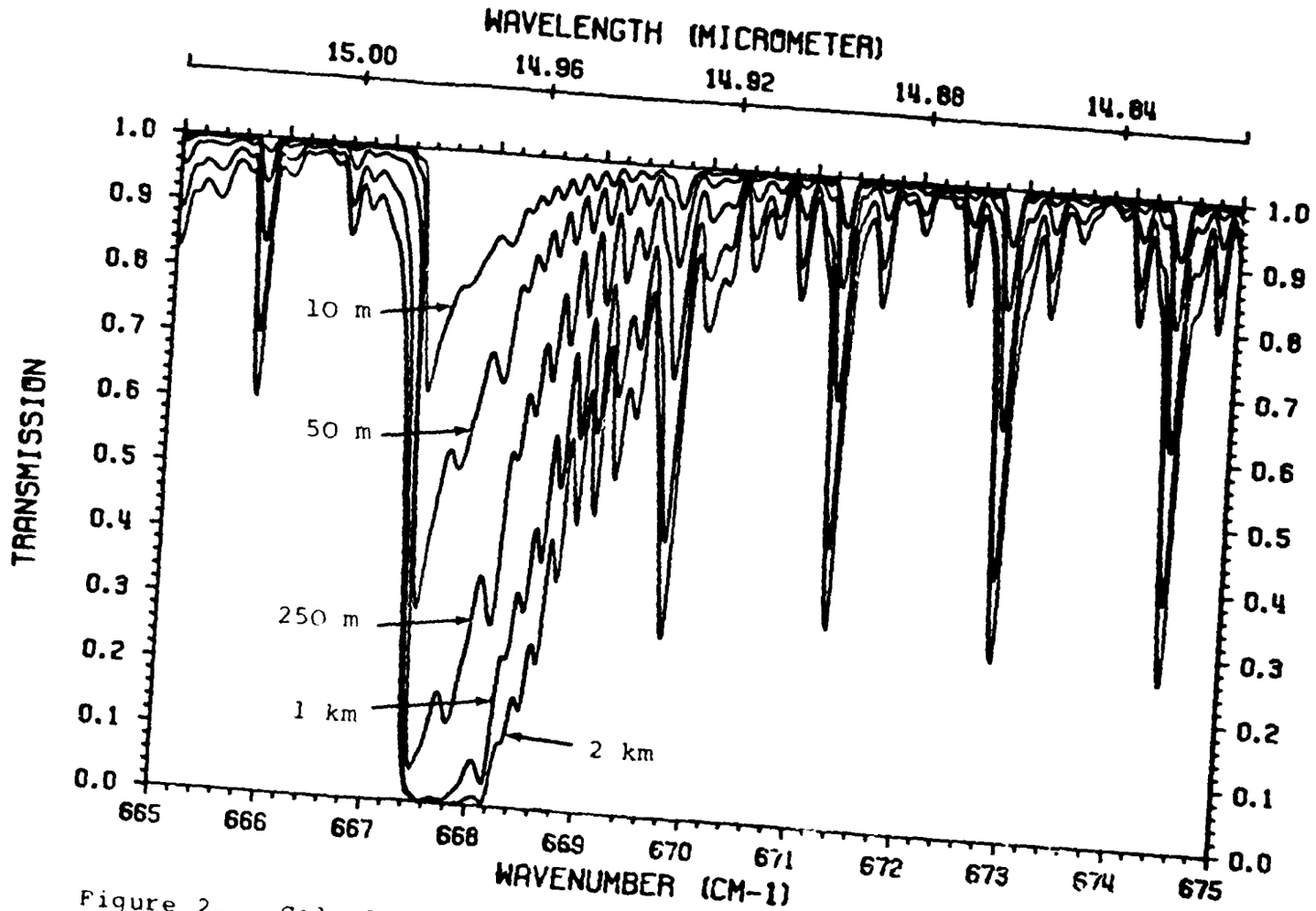

Figure 2. Calculated Transmittance Between 665 and 675 cm^{-1} for a Horizontal Path at 30 km for 5 Different Ranges: 10 m, 50 m, 250 m, 1 km, and 2 km.

region should therefore be essentially the same as the temperature of the air at the same altitude as the sensor. This is true regardless of the look angle of the sensor as demonstrated in Figure 3. This figure shows the calculated radiance in about the same region for three different zenith angles ranging from downward looking to above the horizon. Between 667 and 668 cm^{-1} the three spectra all show essentially the same brightness temperature of 230 K. The peaks of the P and R branch lines on either side of the Q branch are also close to this temperature. Therefore, the measured radiance at 667 cm^{-1} should compare favorably with the measured air temperature at the altitude of the sensor.

As part of the evaluation process, the brightness temperature at 667.5 cm^{-1} is read from the high resolution plots and compared to the air temperature at the corresponding altitude taken from the radiosonde profile. Large differences are indicative of problems with the spectra. There is however, a degree of uncertainty in this comparison due to such factors as the uncertainty in the measured temperature profile and in the sensor altitude. These factors will be evaluated later in this section.

Finally, Figure 4 shows a detailed calculation of the transmittance between 800 and 820 cm^{-1} for the two extreme optical paths viewed by SCRIBE. The calculation used a midlatitude summer temperature and humidity profile. The large absorption lines in the downward looking spectra are water vapor, while the smaller, regularly spaced lines are

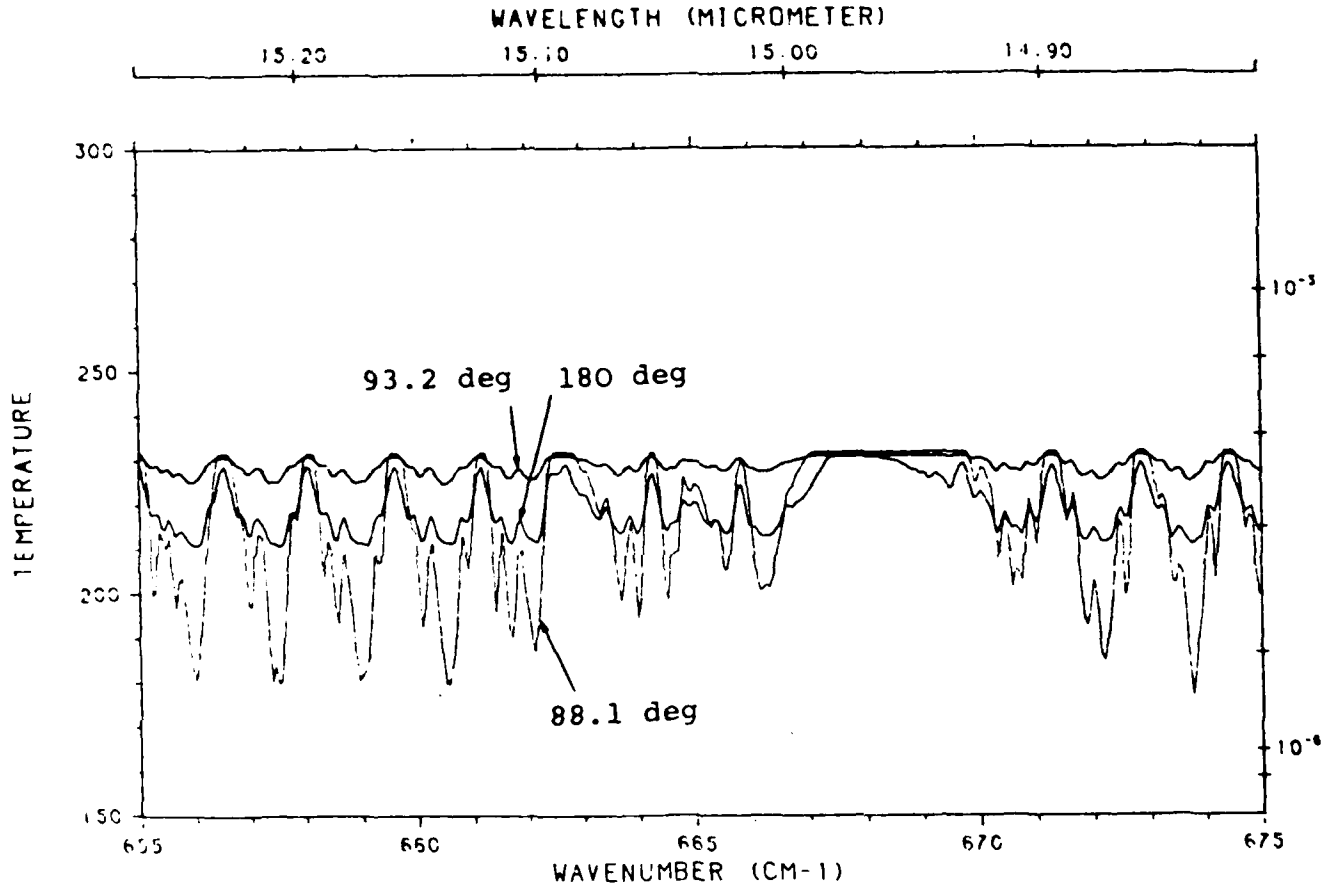

Figure 3. Calculated Brightness Temperature Between 655 and 675 cm^{-1} at 30 km for 3 Zenith Angles: 180 Deg, 93.2 Deg, and 88.1 Deg.

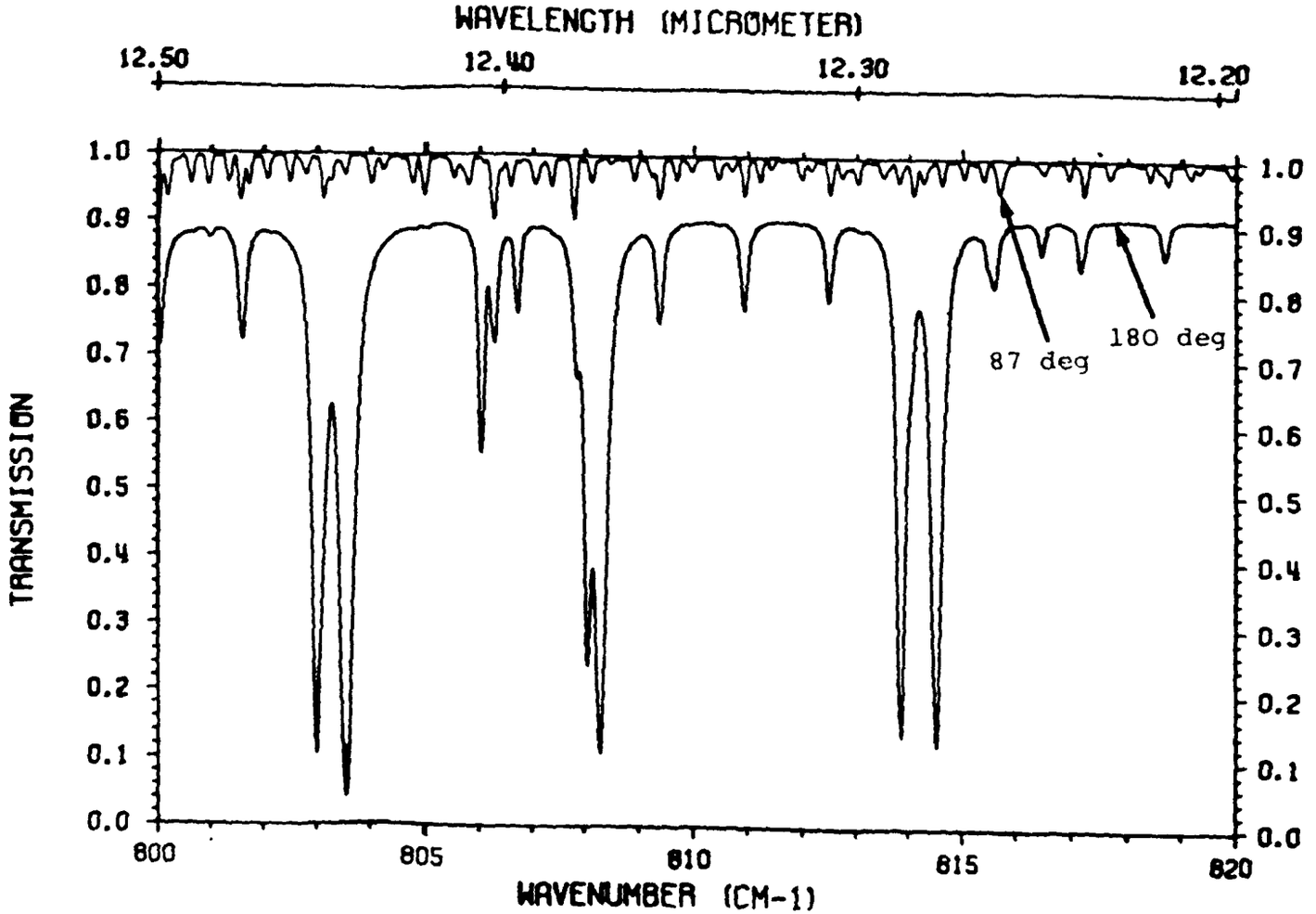

Figure 4. Calculated Transmittance Between 800 and 820 cm^{-1} for 2 paths: 30 km to the Ground at a Zenith Angle of 180 Deg and 30 km to Space at a Zenith Angle of 87 Deg.

CO_2. This figure shows that for the downward looking path, the transmittance to the ground between the absorption lines is about 90 percent. The 10 percent atmospheric absorption is due primarily to the water vapor continuum whose effect is concentrated near the ground. The measured brightness temperature between the lines should therefore be approximately the same as the temperature of the ground, modified by the 10 percent atmospheric absorption. Since most of the atmospheric absorption is near the ground with a temperature not far from the ground temperature, the effect of the atmospheric absorption should be small. For the upward looking case, the atmospheric absorption is small everywhere. Since the stratospheric temperatures are low, the measured radiance in this region should be small also.

As the last part of this step in the evaluation, the radiance between the lines is read from the high resolution plots and checked for consistency with the viewing angle. The values for downward looking spectra should match reasonable ground temperatures, while the values for upward looking spectra should be small.

From this evaluation, a set of spectra are selected which pass all the criteria for overall shape and reasonable radiance values in the different regions. From this set, a spectrum for each zenith angle is chosen for a detailed comparison with a FASCODE calculation.

3.2 Comparisons with FASCODE

The second step of the validation consists of a comparison between each of the selected spectra and a FASCODE calculation. The object of this comparison is to make a detailed radiometric comparison between the measurement and the calculation, and to verify the spectral calibration of the measurements. It should be kept in mind that there are uncertainties in the FASCODE calculations and that disagreement between the measurement and the calculation does not necessarily indicate an error in the measured spectrum.

For this comparison, the latest version of FASCODE, FASCOD2[20], was used. The atmospheric profiles of temperature and humidity were obtained from the measured radiosonde profiles shown in Figures 7 and 8 and listed in Appendix A. The profiles for all the other gases and for water vapor above the highest reported level were interpolated from the profiles compiled in Anderson, et. al.[21]. For the downward looking spectra, the ground temperature was obtained from the measured brightness temperature in the window region (see Section 3.3.2 for a further discussion of this point). The ground temperature

---

21. Anderson, G. P. , S. A. Clough, F. X. Kneizys, J. H. Chetwynd, and E. P. Shettle (1986) AFGL Atmospheric Constituent Profiles (0-120km), AFGL-TR-86-0110, AD-A175 173.

used for the October 23, 1983 flight was 276 K, and for the July 5, 1984 flight was 315 K.

The layering was generated internally by **FASCODE** and the number of layers varied from 16 for the downward looking cases, to eight for the upward looking spectra. The resulting monochromatic spectrum was scanned with a triangular instrument function with both 0.06 cm^{-1} HWHM and 1.0 cm^{-1} HWHM: both resulting spectra were stored. Since a single **FASCODE** calculation is limited to a total of 525 cm^{-1}, the calculation had to be done in two parts, from 600 to 1000 cm^{-1} and from 1000 to 1200 cm^{-1}.

The molecular absorption parameters were from the 1986 version of the AFGL Atmospheric Absorption Line Parameters Compilation (also known as the HITRAN Database[15]). Absorption by all 28 molecules in the database was included.

The **FASCODE** calculations and the measured spectra were plotted on the same graph using an enhancement of the **FASCODE** plotting package[22]. For each case, three graphs were made. The first graph shows the 1.0 cm^{-1} resolution spectra from 600 to 1200 cm^{-1} in both radiance and brightness temperature. The other two graphs show the 0.06 cm^{-1} spectra first from 665 to 675 cm^{-1} and then from 800 to 820 cm^{-1}.

---

22. Gallery, W. O. , J. L. Manning, and D. Tucker (1987) Enhancements to the Atmospheric Transmittance/Radiance Program **FASCODE**, OptiMetrics Inc, OMI 200.

These graphs permit a detailed comparison of the spectra including the large scale spectral features, the radiance levels at 667 cm^{-1} and in the window region, the emission by isolated lines in the 800 cm^{-1} region, the spectral calibration and the level of noise in the measurement. The spectral calibration is easily checked by comparing the positions of the centers of strong lines in both the 667 cm^{-1} and in the 800 cm^{-1} regions. The positions of these lines are well known so that the positions of the calculated lines should be accurate. The noise level can be estimated by looking between the lines in the 800 to 820 cm^{-1} region where the calculations show a flat spectrum. The variance in the measured spectrum should be due to noise.

3.3 Uncertainties in the Method of Validation

There are a number of sources of uncertainty in the comparison between the measurements and the calculations, including errors associated with the SCRIBE package and errors in the supporting meteorological parameters. This section will identify the source of some of these errors and will attempt to estimate the magnitude of their effect.

3.3.1 Effect of Field-of-View and Pointing Error

The field-of-view of SCRIBE is approximately a rectangle with a half width of 0.5 degrees. When viewing the limb, this finite field-of-view causes the instrument to

see a range of tangent heights which is illustrated in Figure 5. This figure shows the tangent height versus depression angle (angle below the horizon) for a sensor at 30.5 km. The dashed lines show the limits of the tangent height corresponding to the limits of the field-of-view. Note that the tangent height for a path with a four degree depression angle is nominally 15 km but the field-of-view actually covers a range of tangent heights from 10 to 20 km. For a 4.5 degree depression angle, the nominal tangent height is five km but the field-of-view includes the ground.

A similar situation exists for the air mass included along the path as illustrated in Figure 6. Air mass here refers to the total amount of air along the path as compared to a vertical path from ground to space and is a measure of the amount of absorbing gas in the path. From Figure 6, the nominal air mass for a 4 degree depression angle is 11 but the field-of-view encompasses values from 6 to 22.

The tangent height and the air mass are important to the validation in so far as they affect the calculated spectrum. The bulk of the gas along the path is located within a layer a few kilometers thick above the tangent height so the temperature of the tangent height determines the emission of this layer. For an optically thin gas, the emission is proportional to the air mass.

In addition to the field-of-view effect there is some uncertainty in the reported look angle. For flights prior

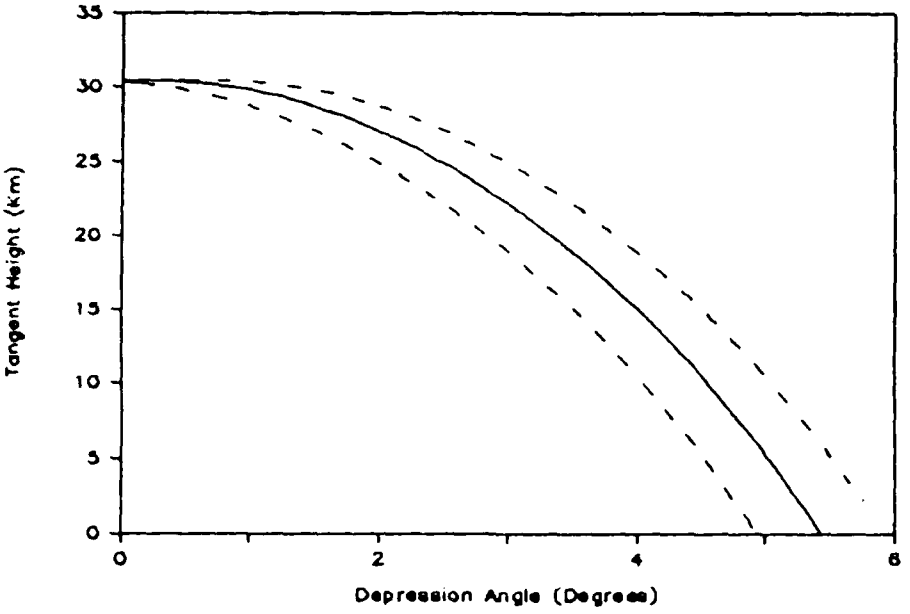

Figure 5. Tangent Height vs. Depression Angle for a Float Altitude of 30.5 km. The Dashed Lines Represent the Tangent Height Corresponding to the Limits of the Instrument Field of View of $\pm$ 0.5 Degrees Half Width at Full Height. Depression Angle is the View Angle Measured Below the Horizontal.

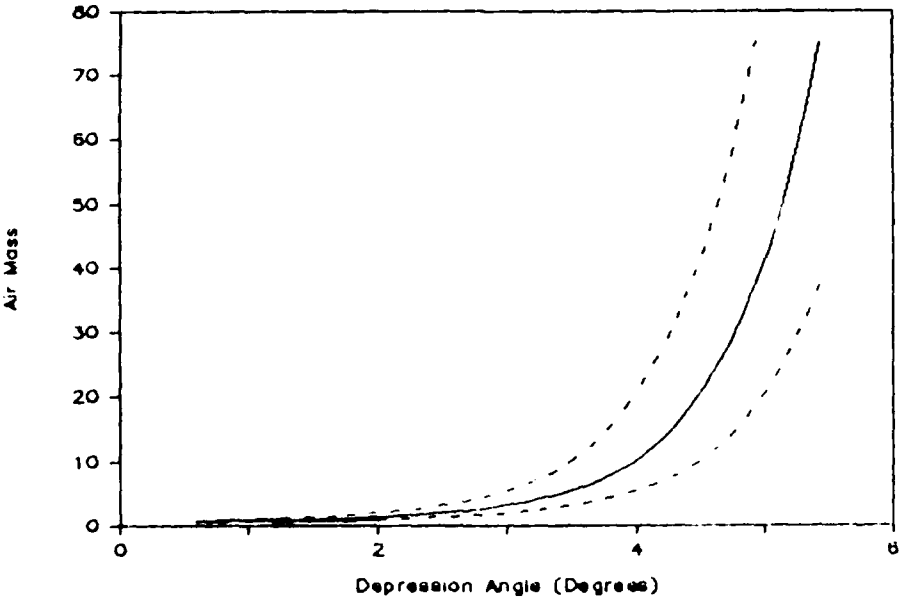

Figure 6. Air Mass vs. Depression Angle for a Float Altitude of 30.5 km. The Dashed Lines Represent the Air Mass Corresponding to the Limits of the Instrument Field of View of $\pm$ 0.5 Degrees Half Width at Full Height. Depression Angle is the View Angle Measured Below the Horizontal.

to 1986, the field-of-view is controlled by tilting the dewar containing the instrument using a screw mechanism. The reported look angle is given by the screw setting. Preflight measurements showed this setting to be quite repeatable but also showed some hysteresis in the setting depending on whether the instrument was scanning up or down[23]. Goldman reports that in order to get good agreement between the measured spectrum and a calculation, the look angle had to be increased by 0.5 degrees over the reported angle[24]. It is clear from Figures 5 and 6 that an error of 0.5 degrees the look angle for low tangents heights will result in a large error in the tangent height and air mass.

The uncertainty due to field-of-view and to pointing error is significant only for limb scanning spectra. The effect on downward looking spectra and those looking above the horizon should be small.

3.3.2 Uncertainty in Atmospheric Parameters

Among the inputs to the **FASCODE** calculation are the atmospheric profiles of temperature, humidity and the concentration of the other absorbing gas amounts, principally CO_2 and ozone. For downward looking spectra, the ground temperature must also be included. The profiles of temperature and humidity used in the **FASCODE** calculation were obtained from radiosonde ascents made during the flights either from Holloman AFB, NM for the October 23,

23. F. J. Murcray, private communication.

24. A. Goldman, private communication.

1983 flight, or from the White Sands Missile Range, NM for the July 5, 1984 flight. The measured temperature profiles are shown in Figures 7 and 8. (These profiles are also listed in Appendix A, along with other parameters from each flight.) Note that maximum altitude reached by the radiosonde for the October 23, 1983 ascent was 27.8 km, while the maximum altitude reached by SCRIBE was 30.5 km. The measured profile therefore had to be extrapolated to higher altitudes by assuming stratopause temperature of 270 K at 1 mb (equal to that of the US Standard Atmosphere), and by extending the profile linearly from the highest measured point to the stratopause. The profile for the July 5, 1984 flight reached 31.3 km, about the same as the maximum altitude reached by SCRIBE. In order to model the upward looking spectra, this profile also had to be extrapolated upward using the same lapse rate.

The radiosonde system used to measure these profiles is known to have significant errors as high as 1 km or more at 30 km[25]. This uncertainty plus the uncertainty from extrapolating the 1983 profile represents a significant uncertainty in comparing the measured and calculated spectra in the 667 cm^{-1} region.

The measured humidity profile is also known to be subject to uncertainties of as much as $\pm$ 20 percent which will be reflected in the calculated spectrum. The most

---

25. Nestler, M. S. (1983) A Comparative Study of Measurements from Radiosondes, Rocketsondes, and Satellites, NASA Contractor Report 168343, April 1983

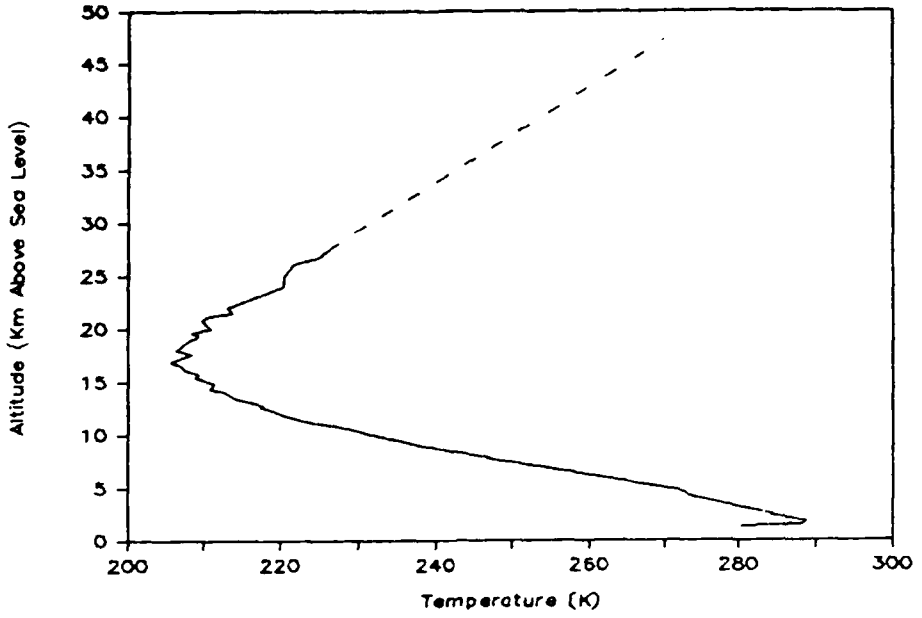

Figure 7. Temperature Profile at Holloman AFB, New Mexico on October 23, 1983 (0700 mst). The Extrapolated Part of the Profile is Indicated by a Dashed Line

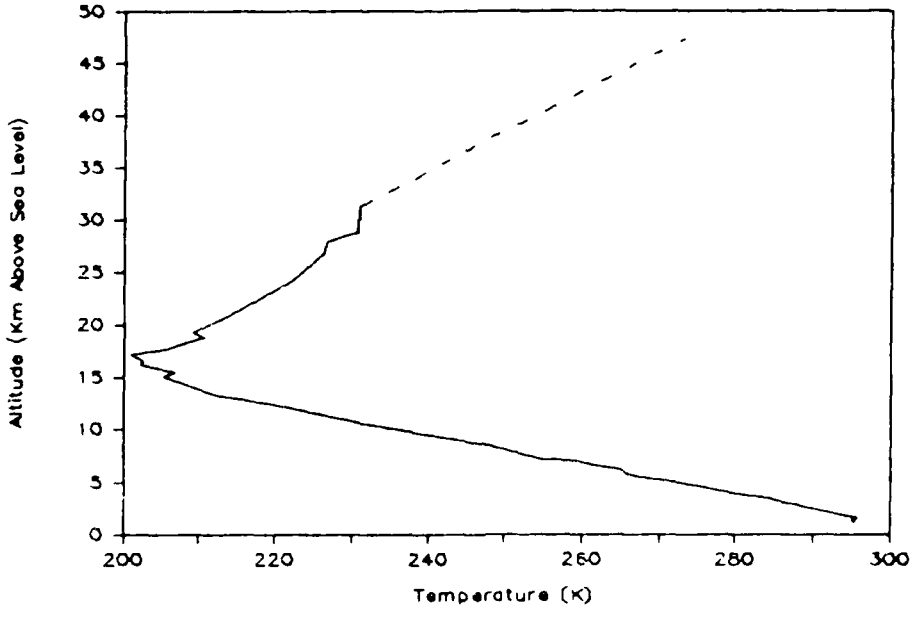

Figure 8. Temperature Profile for White Sands Missile Range, New Mexico on July 5, 1984 at 0700 MST. The Extrapolated Part of the Profile is Indicated by a Dashed Line

significant water vapor absorption in these comparisons however, is caused by the water vapor continuum which is greatest near the ground. This uncertainty will primarily affect the downward looking spectra.

The other significant absorbing gases are CO_2, O_3 and HNO_3. The emission by most other gases is smoothed out in the low resolution spectra and is not seen in the full resolution spectra in the 667 and the 800 cm^{-1} regions. The concentration of CO_2 is relatively uniform and well known and it contributes little uncertainty. **FASCODE** uses a value of 330 ppmv. The profiles of O_3 and HNO_3 are highly variable in time and space and were not measured for these flights. Average profiles for these molecules therefore, had to be assumed, and were taken from the model atmosphere 6 in **FASCODE**.

The last significant atmospheric parameter is the ground temperature. The flight path of SCRIBE extends several hundred kilometers over a variety of desert surfaces while the flight extends from before dawn to several hours after. Therefore, the ground temperature can vary significantly in space and time. It will also, in general, be different from the surface air temperature. The best measure of the ground temperature is actually the measured brightness temperature in the window region. While using this temperature as the ground temperature in the **FASCODE** calculation represents a circular argument, it is the best that can be achieved: this point should be kept in mind when

evaluating the comparison between the measurements and the calculations.

3.3.3 Noise Equivalent Radiance

The brightness temperature is related to the radiance through the blackbody function, which is a highly non-linear function of both temperature and wavenumber. When examining the measured spectra plotted as brightness temperature, the uncertainty due to noise depends upon both the wavenumber and the radiance level. This point is illustrated by Figure 9 which shows the uncertainty in the brightness temperature due to a noise equivalent radiance of 2×10^{-7} Watts/ (cm^{-2} sr cm^{-1}). Note that at 800 cm^{-1} the uncertainty in brightness temperature for a nominal temperature of 200 K is about 3 K, while at 1200 cm^{-1} it is almost 16 K. In other words, the same level of noise on a brightness temperature scale looks much larger at 1200 cm^{-1} than at 800 cm^{-1} for a low nominal or background brightness temperature. For a nominal brightness temperature of 300 K, the effect is almost independent of wavenumber. This effect should be kept in mind when examining the spectra on a brightness temperature scale.

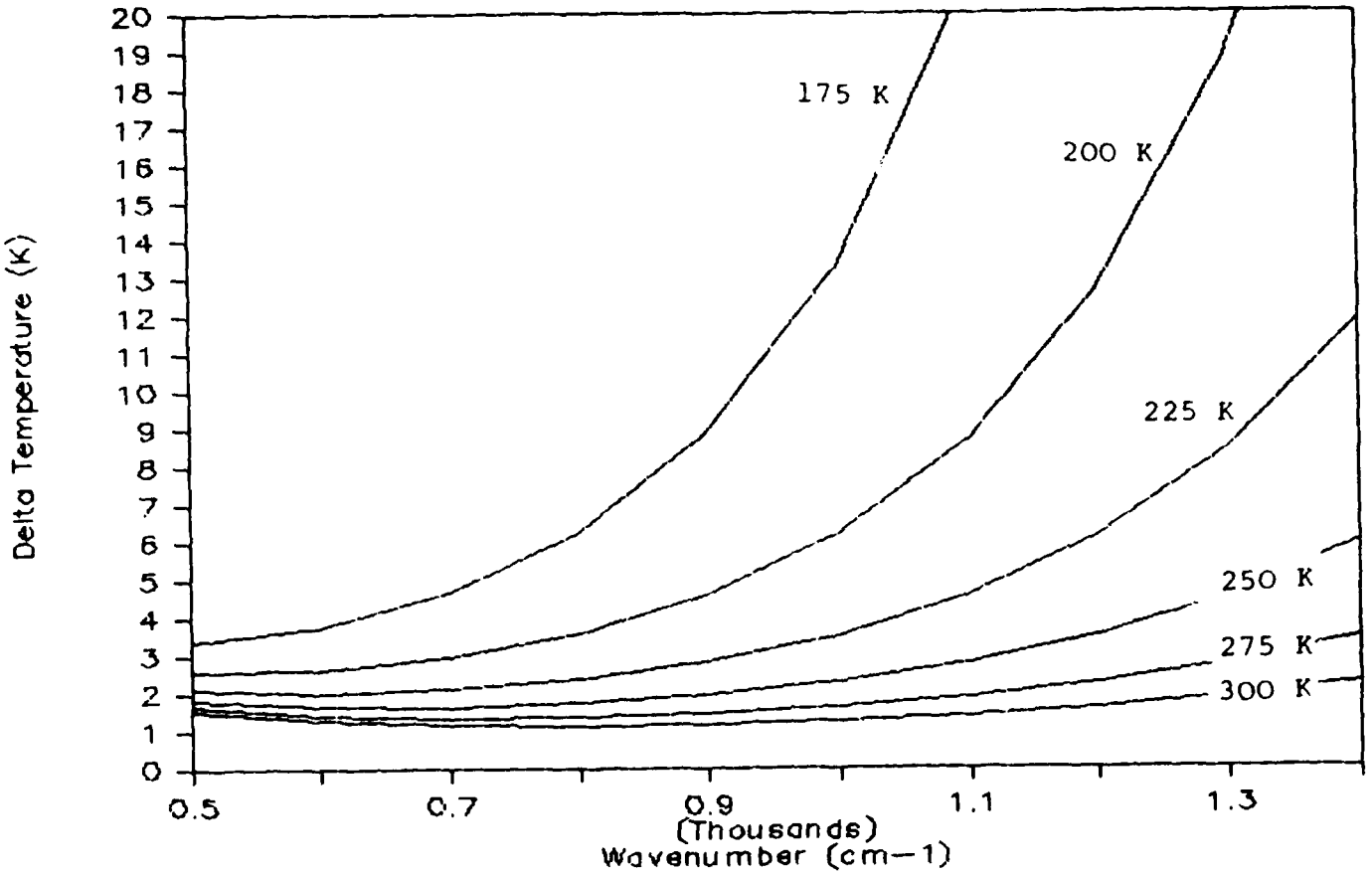

Figure 9. Uncertainity in Brightness Temperature Due to a Noise Equivalent Radiance of 2.0 X 10^{-7} Watts/ (cm^2*str*cm^{-1}). Each Curve Represents a Different Nominal Brightness Temperature.

4. SURVEY OF CALIBRATED SCRIBE DATA

The first step in the evaluation was conducted as described in the previous section. The results are summarized in Table 8. The spectra included in this list are all those from Tables 2 and 7. The various columns in this table were obtained as follows. For the 1983 flight, the times for each spectrum were matched with the list of the radar track of the flight (see Appendix A) to get the exact altitude. The "Zenith Angle" is as reported in Table 2. The "Tangent Height" is given only for selected spectra and is calculated by **FASCODE**. The "Radiosonde Temp. at Altitude" is the air temperature at the balloon altitude from the radiosonde profile. The "667 cm^{-1} Brightness Temperature" is the measured brightness temperature at 667.5 cm^{-1}, obtained from full resolution plots of the measured spectrum. The "800 cm^{-1} Radiance" is the background radiance between 800 and 820 cm^{-1}, again obtained from full resolution plots. The equivalent brightness temperature at 800 cm^{-1} is given only for downward looking spectra. The "comments" column lists observations about the overall shape or radiance level of the spectra. The spectra from the 1984 flight each represent co-added spectra of up to 13 individual spectra. No times are available for these spectra: the altitude is as reported in Table 7.

From this list, the best spectra were selected based upon overall consistency and lack of obvious errors, with

Table 8. Summary of All Calibrated Scribe Spectra Available at AFGL

Name	Minutes After Launch	Altitude Above Sea Level (km)	Zenith Angle (deg)	Tangent Height (km msl)	Radiosonde Temp. at Altitude (K)	667 cm^{-1} Brightness Temp. (K)	800 cm^{-1} Brightness Temp. (K)	800 cm^{-1} Radiance ($W/(cm^2\ sr\ cm^{-1}) \times 10^{-6}$)	Comments
Spectra from the October 23, 1983 Flight Processed by U. Mass									
SP830M4	11.3	5.23	82.5		267	308	-	1.9	A
SP830N1	15.0	6.59	82.5		256	296	-	1.7	A
SP830O1	20.0	8.52	82.5		242	235	-	0.7	B
SP830V3	100.8	30.36	180.0		232	225	270	8.5	
SP830W1*	104.0	30.67	180.0	(grnd)	233	225	272	9.1	
SP830B1	110.0	30.57	180.0		233	207	253	6.5	C
SP830B2	110.4	30.55	180.0		233	211	255	6.7	C
SP830B3	110.8	30.55	180.0		233	208	254	6.5	C
SP830B4	111.3	30.58	180.0		233	207	252	6.4	C
SP830B5	111.7	30.61	180.0		233	210	254	6.6	C
SP830B6	112.1	30.66	180.0		233	207	252	6.4	C
SP830B7	112.5	30.69	180.0		233	206	251	6.3	C
SP830C1	115.0	30.64	180.0		233	204	250	6.2	C
SP830C2	115.4	30.59	180.0		233	206	250	6.2	C
SP830C3	115.8	30.55	180.0		233	203	251	6.1	C
SP830C4	116.3	30.51	180.0		233	203	250	6.2	C
SP830C5	116.7	30.51	180.0		233	204	253	6.4	C
SP830D1	118.0	30.51	180.0		233	203	253	6.4	C
SP83031	123.0	30.67	90.4		233	229	-	0.2	
SP83036	125.1	30.65	90.4		233	228	-	0.2	
SP830E1*	127.0	30.63	90.4	30.47	233	229	-	0.3	
SP830F6	132.1	30.53	90.4		233	226	-	0.3	D
SP830G1	134.0	30.46	90.4		232	226	-	0.6	D
SP830G3	134.8	30.44	-		233	231	-	0.4	B
SP830H1	137.0	30.42	92.9		232	236	-	0.2	B,E
SP830H2	137.4	30.42	92.9		232	228	-	0.5	B
SP830I1	140.0	30.30	92.9		232	230	-	0.8	E
SP830I2*	140.4	30.29	92.9	22.02	232	228	-	0.6	
SP830J2	143.4	30.17	92.9		232	230	-	0.7	
SP830J7	145.5	30.09	95.4		232	224	264	8.2	E
SP830K3	147.8	30.10	95.4		232	-	-	-	F
SP830K7	149.5	30.03	95.4		231	214	254	7.1	G
SP830L1	150.0	30.01	95.4		231	218	262	8.3	G
SP830L2	150.4	29.99	95.4		231	223	267	9.0	G
SP83041	155.0	29.71	95.4		231	223	268	9.2	G
SP83042	155.4	29.67	95.4		231	223	267	9.3	G
SP83043*	155.8	29.64	95.4	(grnd)	231	224	266	9.0	G

Table 8. Summary of All Calibrated Scribe Spectra Available at AFGL (Cont.)

Name	Minutes After Launch	Altitude Above Sea Level (km)	Zenith Angle (deg)	Tangent Height (km msl)	Radiosonde Temp. at Altitude (K)	667 cm^{-1} Brightness Temp. (K)	800 cm^{-1} Brightness Temp. (K)	800 cm^{-1} Radiance ($W/(cm^2\ sr\ cm^{-1}) \times 10^{-6}$)	Comments
Spectra from the October 23, 1983 Flight Processed by U. Mass (cont.)									
SP83044	156.3	29.62	95.4		231	222	268	9.2	G
SP83045	156.7	29.61	95.4		230	223	271	9.7	G
SP83046	157.1	29.59	95.4		230	223	272	9.7	G
SP83047	157.5	29.58	95.4		230	222	273	9.9	G
SP83095	173.7	28.04	82.5		227	220	-	0.2	
SP83096*	174.1	27.96	82.5	(up)	227	218	-	0.2	
SP83097	174.5	27.88	82.5		227	219	-	0.3	
SP830P1	176.0	27.81	82.5		227	220	-	0.1	B
SP830P3	176.8	27.77	180.0		227	243	304	-	A
SP830Q1	180.0	27.44	180.0		226	228	284	-	
Spectra from the July 5, 1984 Flight Processed by U. Denver									
SC841*	-	31.3	180.0	(grnd)	230	247	315	16.5	A,C
SC842*	-	31.3	93.7	16.90	230	225	-	1.0	
SC843*	-	31.3	93.2	20.40	230	223	-	0.8	
SC844*	-	31.3	88.1	(up)	230	222	-	0.3	

Notes:
1. Spectra marked with an asterisk (*) after the name are analyzed in some detail in this report
2. Under Tangent Height, (grnd) means that the optical path intersects the ground, and (up) means the path is above the horizon. Tangent Height is given only for spectra with an marked with a *.
3. 800 cm^{-1} brightness temperatures are give only for spectra whose paths intersect the ground.
4. The 1984 spectra represent co-adds of from 10 to 13 individual spectra. Times for these spectra are not available.

Comment key:
A. Brightness Temperatures are too high or too low when compared with radiosonde data.
B. Contains negative radiance values.
C. Envelope of downlooking spectra does not match that of the blackbody curve.
D. Apparently good data but inconsistent with spectra at the same viewing angle.
E. Spectrum shows modulation (channel spectra and/or spikes).
F. Shape completely inconsistant with expected values.
G. The 800 cm-1 brightness temperature of these spectra increases 20 K in 8 minutes.

one spectrum chosen for each zenith angle. The names of these spectra are marked with an asterisk in Table 8. Low resolution plots of these spectra both in radiance and brightness temperature are shown in Figures 10 through 14 and in Figures 17 through 20. The smooth curve on the radiance plot is the blackbody curve for the maximum brightness temperature seen between 600 and 900 cm^{-1}.

4.1 Spectra from the 1983 Flight

Figure 10 shows the spectrum for a downlooking case. The radiance in the window region closely follows the shape of a blackbody curve as expected and the observed brightness temperature at 800 cm^{-1} of 272 K is not unreasonable for a desert surface near dawn. The CO_2 bands around 667 cm^{-1} and the O_3 bands around 1040 cm^{-1} appear as predicted in Figure 1. The brightness temperature at 667 cm^{-1} is 8 K less that of the nominal air temperature at the balloon altitude, but considering the uncertainties in the radiosonde profile, this difference is acceptable.

Figures 11 through 13 show limb spectra with tangent heights decreasing from 30.47 km to 22.02 km to nominally just striking the ground. Figure 11 show the CO_2 and O_3 bands in emission as expected with very little radiance in the windows. In Figure 12 these bands appear broader due to the larger optical path and,in addition, the HNO_3 band between 850 and 950 appears. Figure 13 looks somewhat like the downward looking spectrum in Figure 11. Note that due

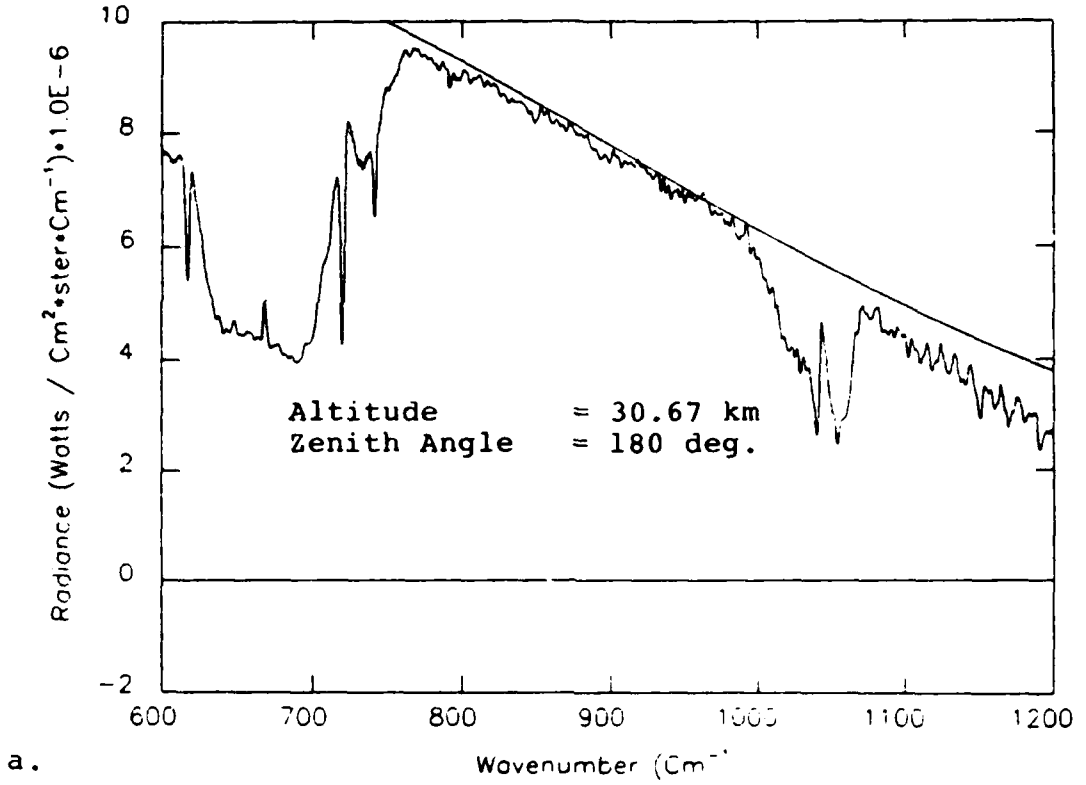

a.

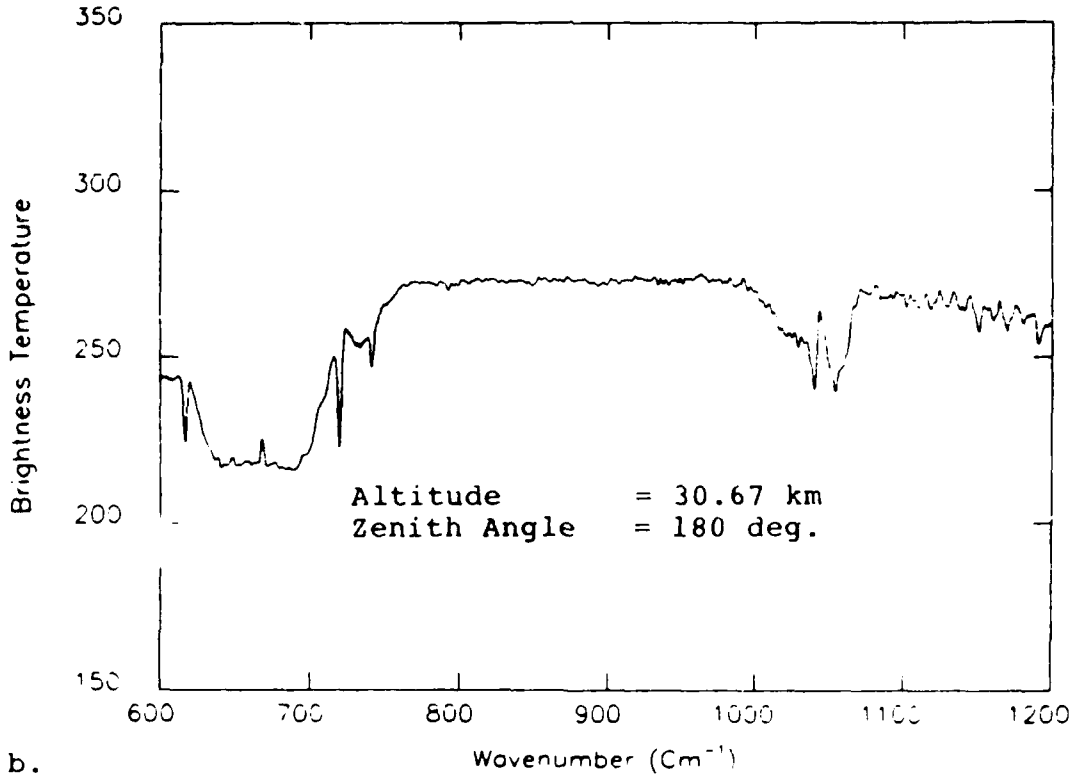

b.

Figure 10. Spectrum **SP830W1** from 600 cm^{-1} to 1200 cm^{-1} Degraded to 1.0 cm^{-1} Resolution: a. Radiance, b. Brightness Temperature. Spectrum was processed by the University of Massachusetts

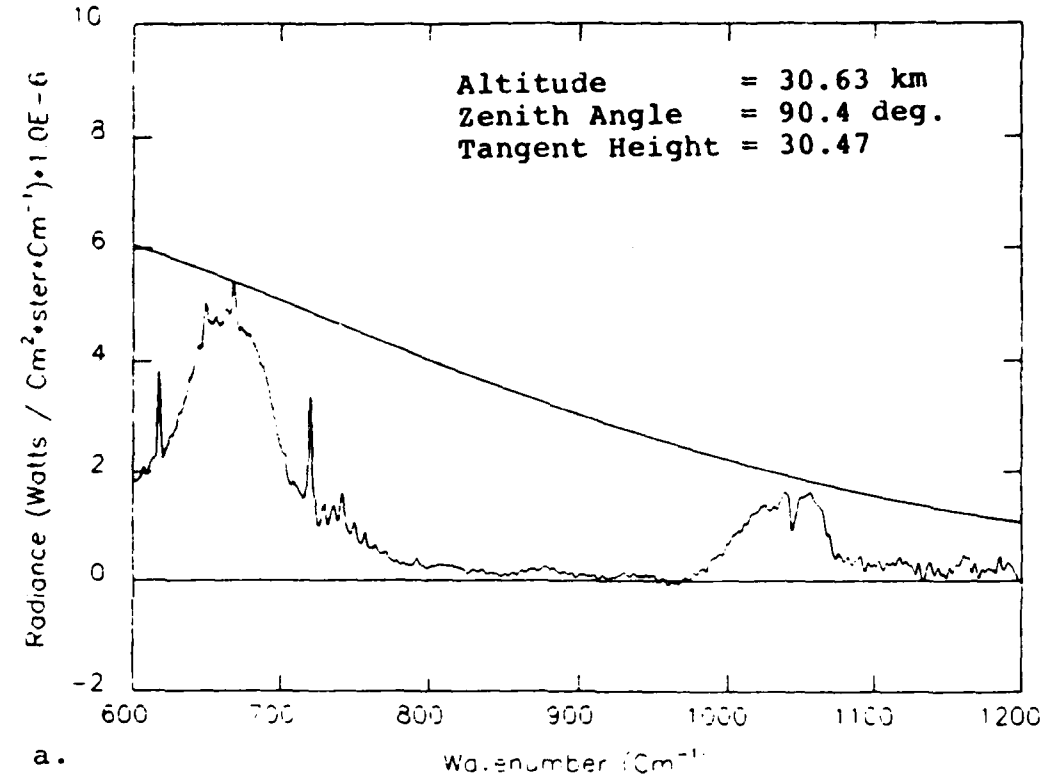

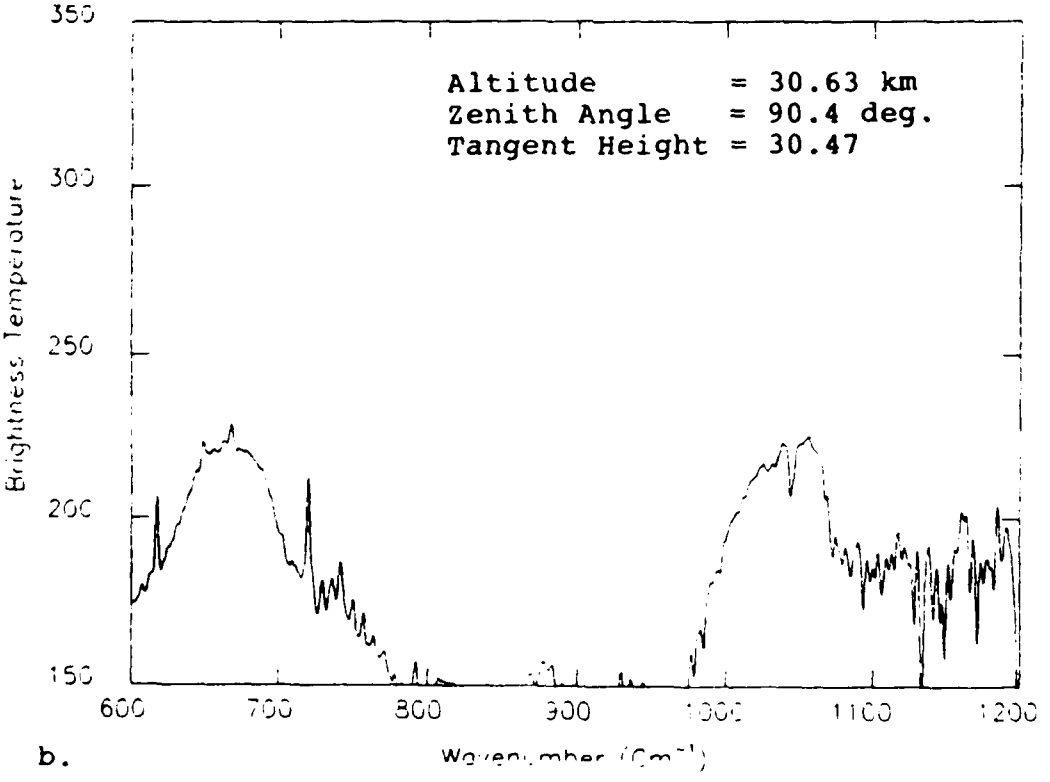

Figure 11. Spectrum SP830E1 from 600 cm^{-1} to 1200 cm^{-1} Degraded to 1.0 cm^{-1} Resolution: a. Radiance, b. Brightness Temperature. Spectrum was processed by the University of Massachusetts

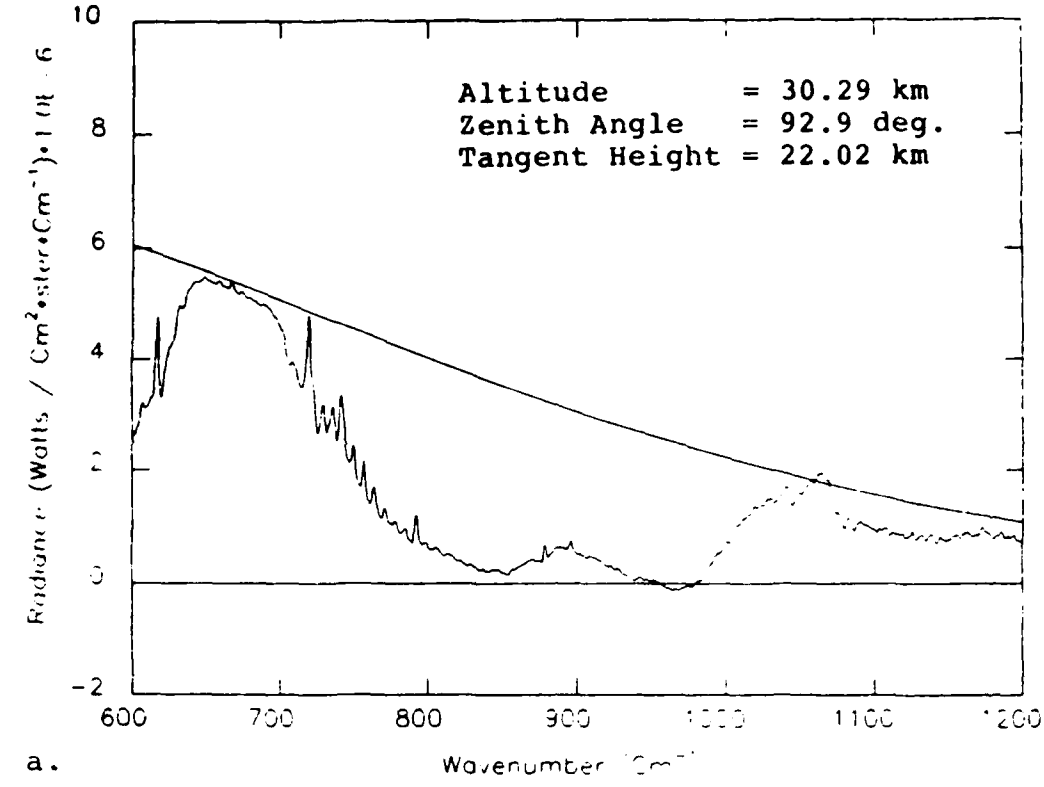

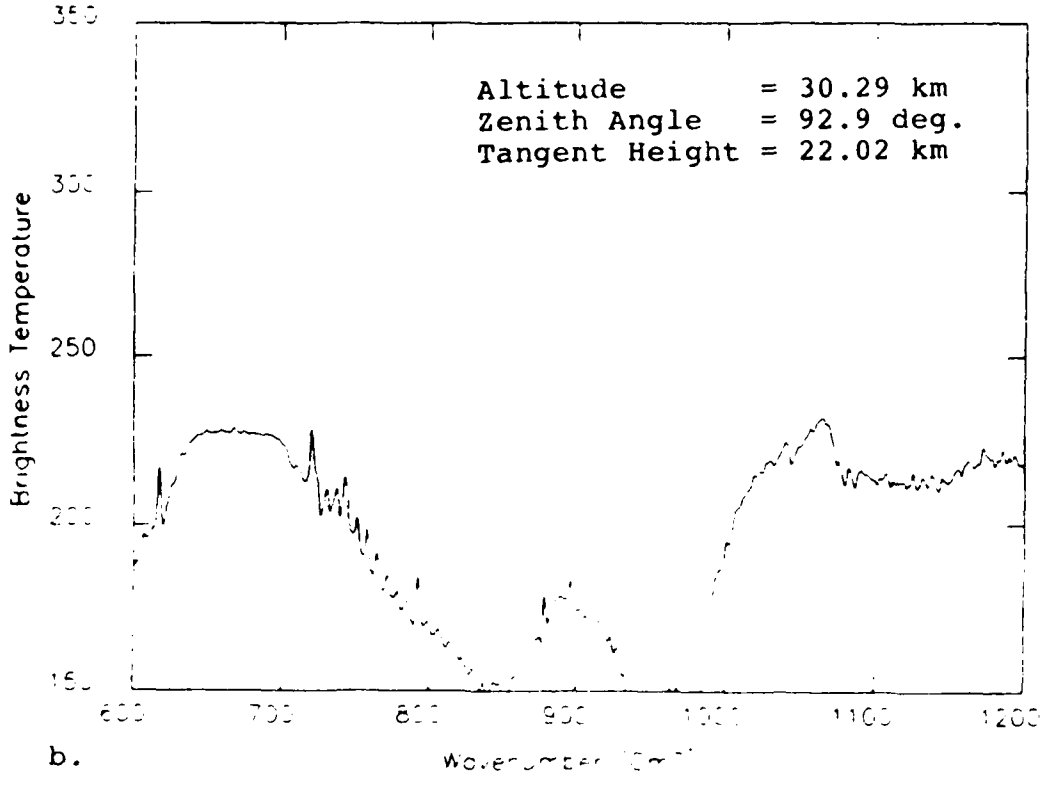

Figure 12. Spectrum SP830I2 from 600 cm^{-1} to 1200 cm^{-1} Degraded to 1.0 cm^{-1} Resolution: a. Radiance, b. Brightness Temperature. Spectrum was processed by the University of Massachusetts

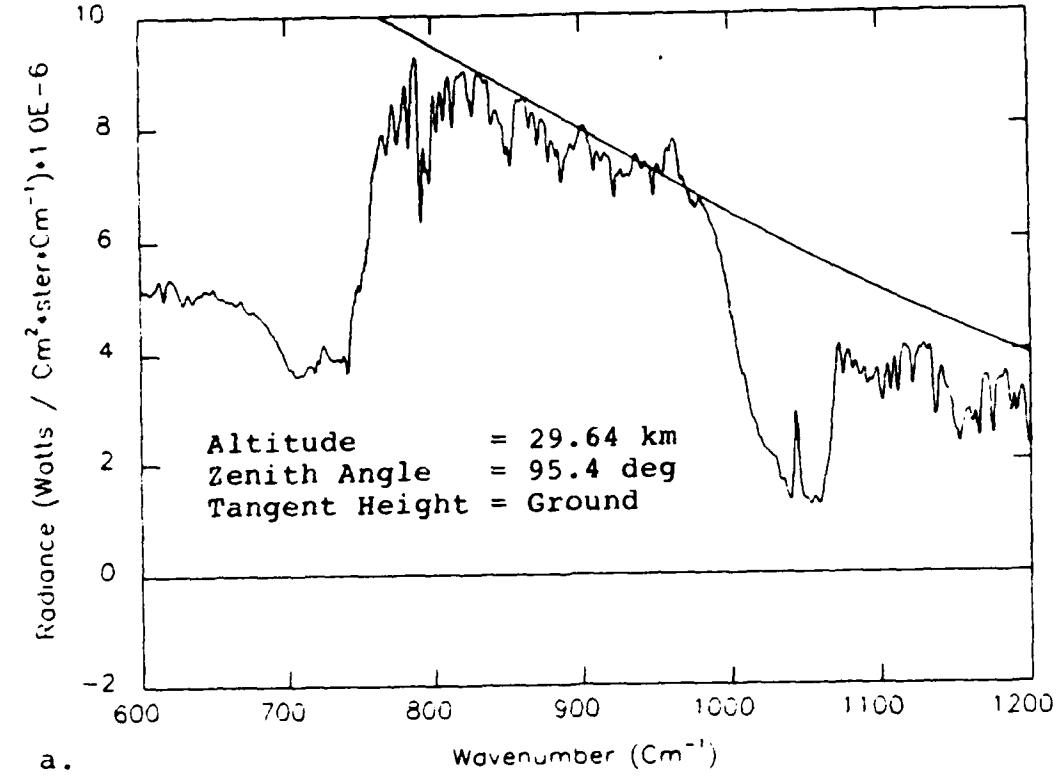

a.

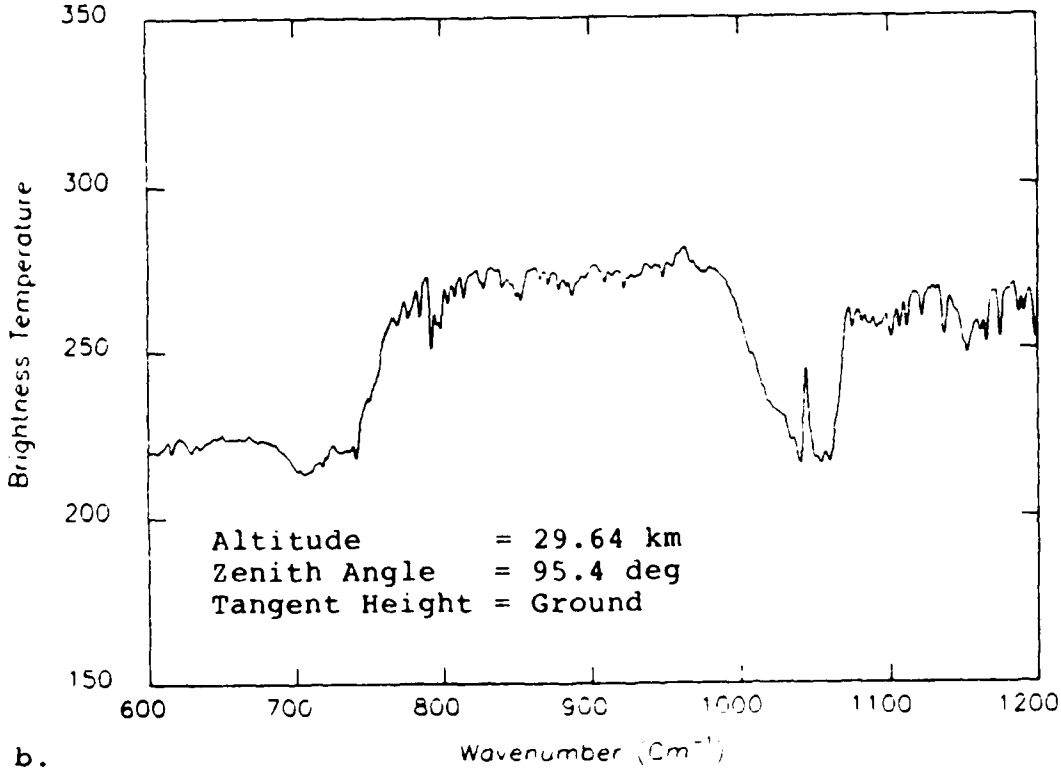

b.

Figure 13. Spectrum SP83043 from 600 cm^{-1} to 1200 cm^{-1} Degraded to 1.0 cm^{-1} Resolution: a. Radiance, b. Brightness Temperature. Spectrum was processed by the University of Massachusetts

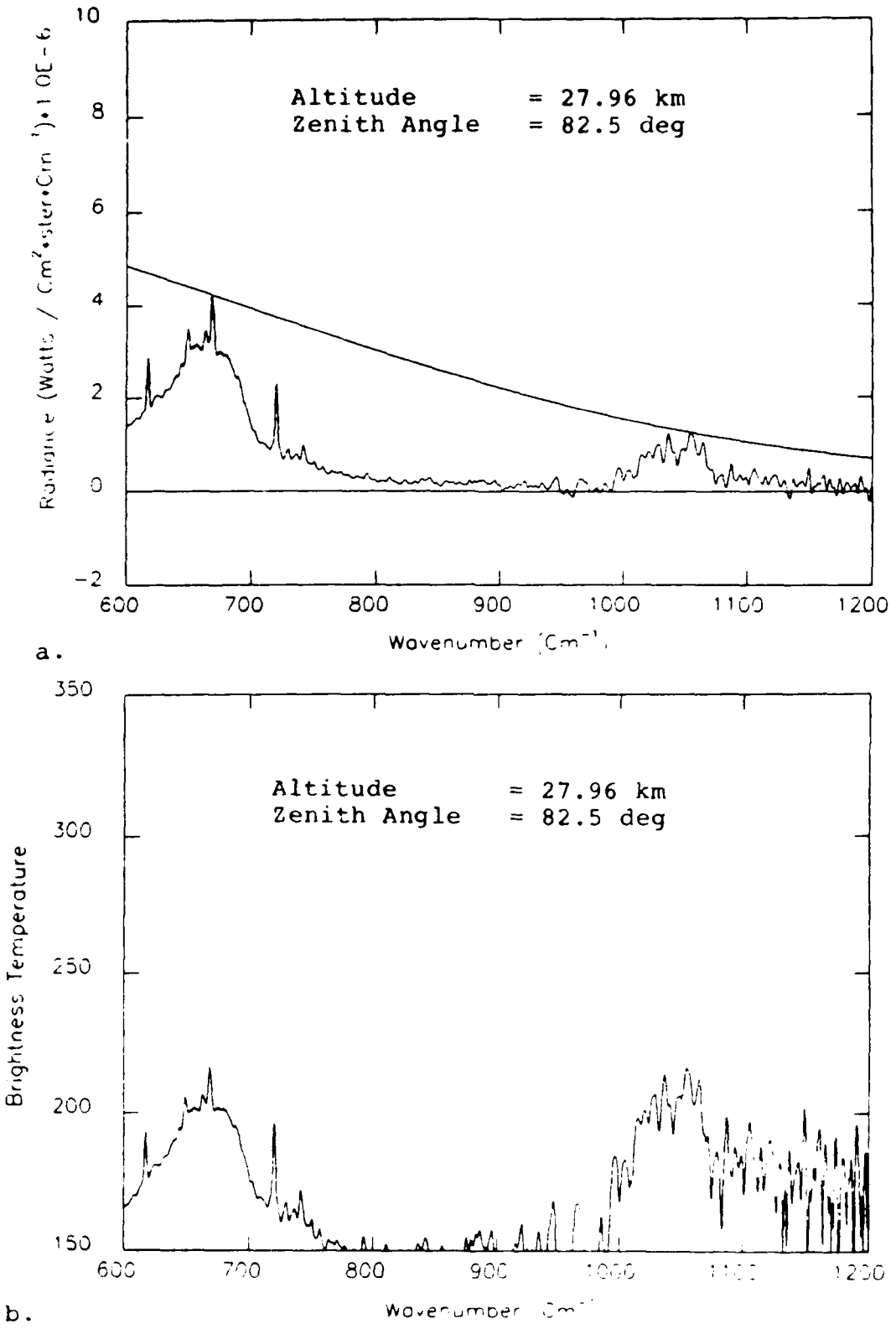

Figure 14. Spectrum SP83096 from 600 cm^{-1} to 1200 cm^{-1} Degraded to 1.0 cm^{-1} Resolution: a. Radiance, b. Brightness Temperature. Spectrum was processed by the University of Massachusetts

to the finite field-of-view effect, the ground only partially fills the field-of-view and that part of the radiance comes from a long limb path almost tangent to the earth. The brightness temperatures at 667 cm^{-1} are between 4 and 7 K less than the nominal air temperature.

Finally, Figure 14 shows an upward looking spectra. The temperature at 667 cm^{-1} is 9 K less than the nominal air temperature at float which is a relatively large difference but not completely unreasonable.

However, most of the spectra from the 1983 flight which are listed in Table 8 showed inconsistencies in the radiance levels or obvious flaws in their shape. The first two spectra showed brightness temperatures at 667 cm^{-1} of about 300 K, which is far higher than any temperature seen in the atmosphere. The next spectrum showed significantly negative radiance values in the window regions. The whole series of downward looking spectra from **SP830B1** to **SP830D1** shows a pronounced slope in the brightness temperature between 800 and 1000 cm^{-1} and a brightness temperature at 667 cm^{-1} which is far below a reasonable level. An example of one of these spectra is shown in Figure 15. The problem appears to be caused by the fact that the detector bias was improperly set high for these spectra, resulting in the saturation of the detector near zero point crossing. Distorting the interferogram near the zero point crossing would result in a low spatial frequency distortion in the spectrum, such as a linear trend.

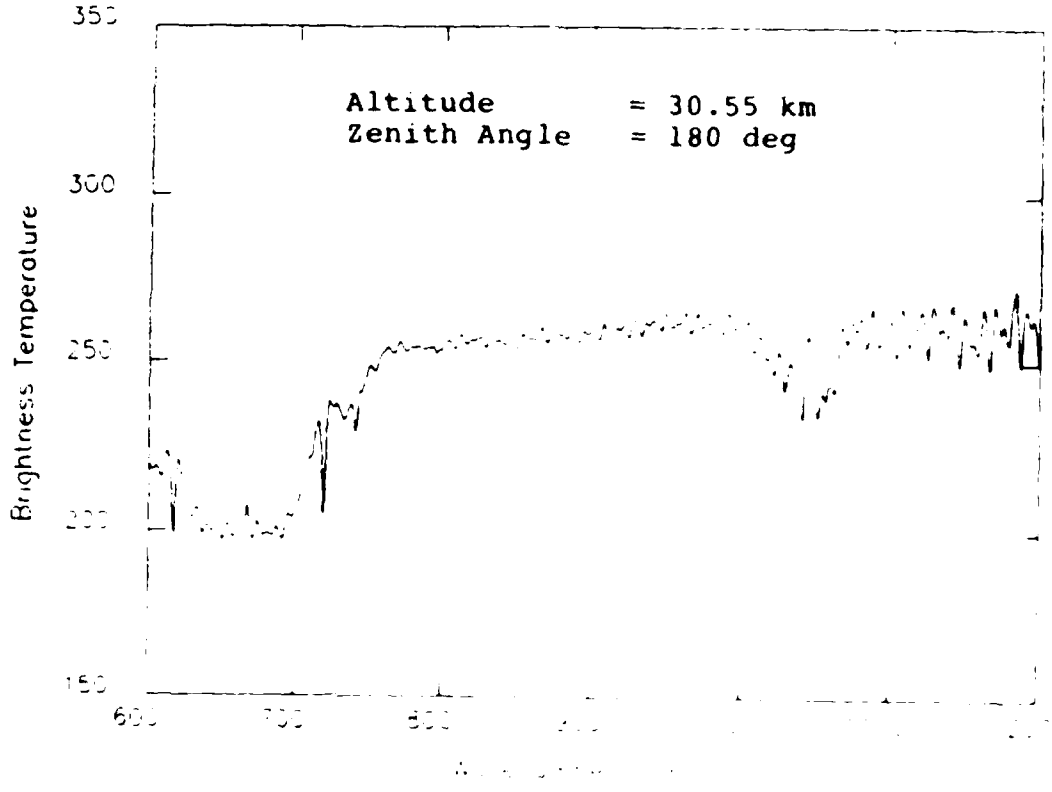

Figure 15. Spectrum SP830B2: an Example of Bad Calibration due to Improper Gain Setting. Note the Upward Slope of the Brightness Temperature in the Window Region. Spectrum was processed by the University of Massachusetts

Other spectra, such as **SP830P6** and **SP830G1**, exhibit no particular problem but show large differences in shape even though they have the same nominal altitude and look angle. Severe modulation due either to channel spectra or to spikes in the interferogram are seen in several spectra one of which is shown in Figure 16. The series of spectra from **SP830K7** to **SP83047** are otherwise acceptable but show an increase in the brightness temperature at 800 cm^{-1} of 20 K in 8 minutes. While such a change might possibly be caused by the sensor passing rapidly over terrain of greatly differing temperature, this appears unlikely.

4.2 Spectra from the 1984 Flight

The four spectra from the 1984 flight are shown in Figures 17 through 20. The large scale features in the downward looking spectrum in Figure 17 appear normal except for a slight, but definite downward trend in the window region. Note also in Table 8 that the brightness temperature at 667 cm^{-1} for this spectrum is 3 K above the nominal air temperature while the corresponding temperatures for the other three spectra are 6 to 8 K below. The brightness temperature at 667 cm^{-1} should be independent of viewing angle. This difference of up to 11 K between the downward looking spectrum and the limb viewing spectra is a serious problem. The brightness temperature at [illegible] high even for a desert surface [illegible]

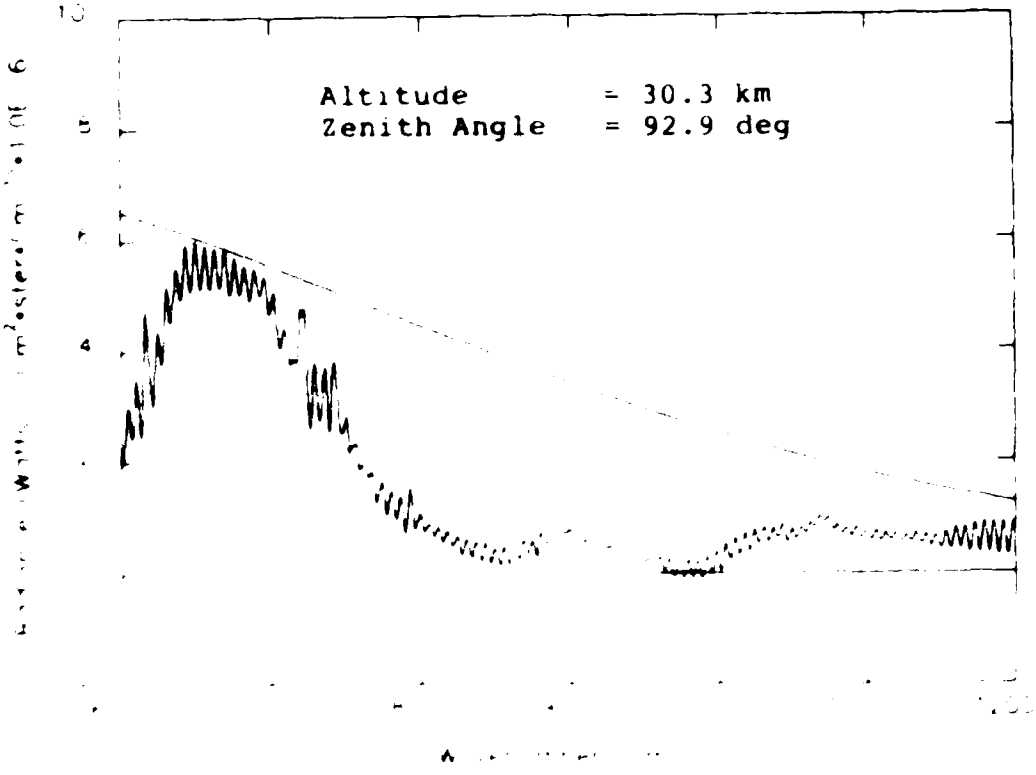

[illegible] spectrum SPB3011. An example of Severe [illegible] Anomalous Spike in the Interferogram. [illegible] was processed [illegible] University of Massachusetts

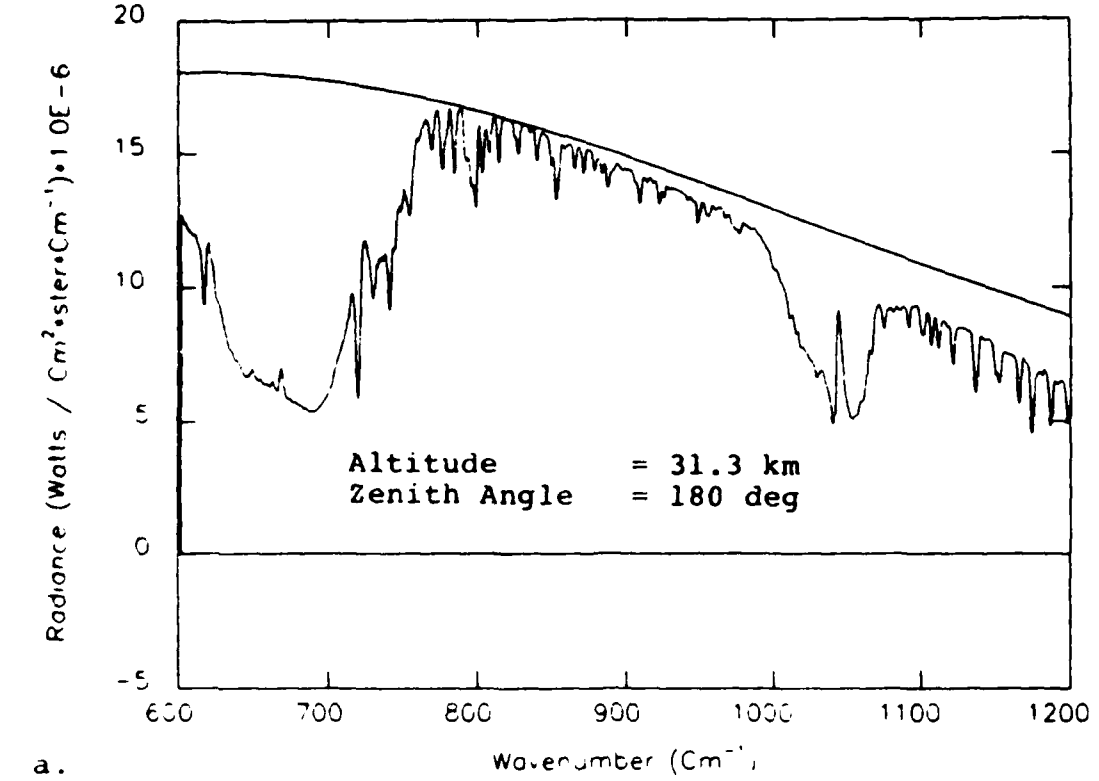

a.

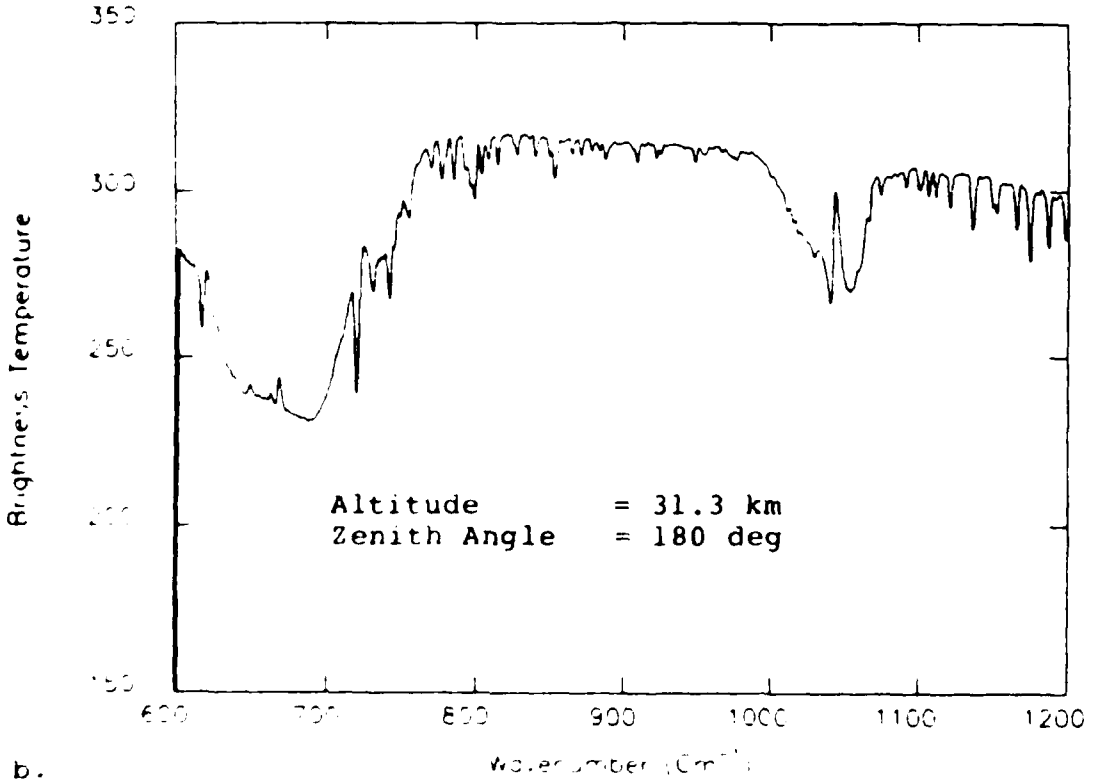

b.

Figure 17. Spectrum SC841 from 600 cm^{-1} to 1200 cm^{-1} Degraded to 1.0 cm^{-1} Resolution: a. Radiance, b. Brightness Temperature. Spectrum was processed by the University of Denver

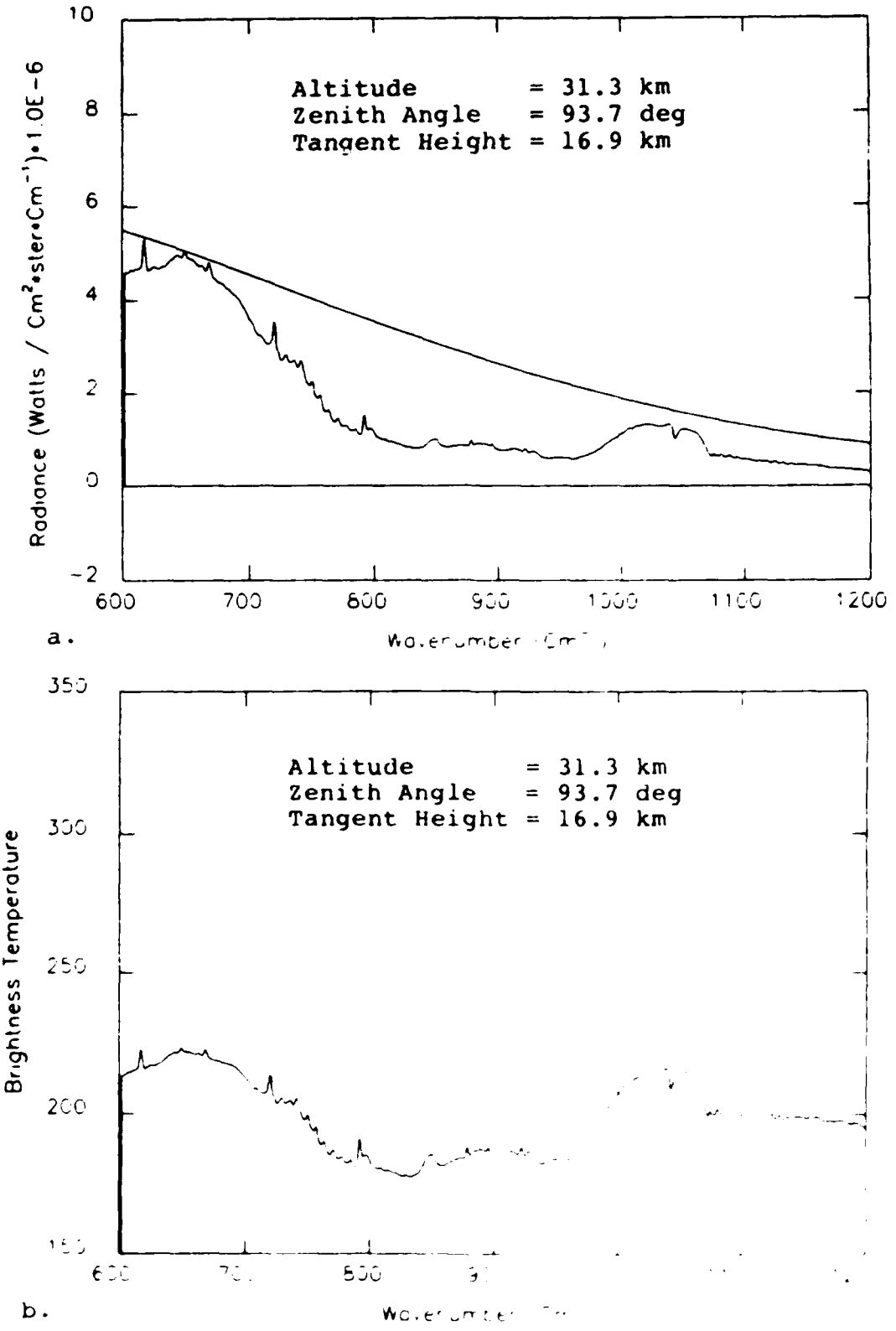

Figure 18. Spectrum SC842 from 600 cm^{-1} to 1200 cm^{-1} Degraded to 1.0 cm^{-1} Resolution: a. Radiance, b. Brightness Temperature. Spectrum was processed by the University of Denver

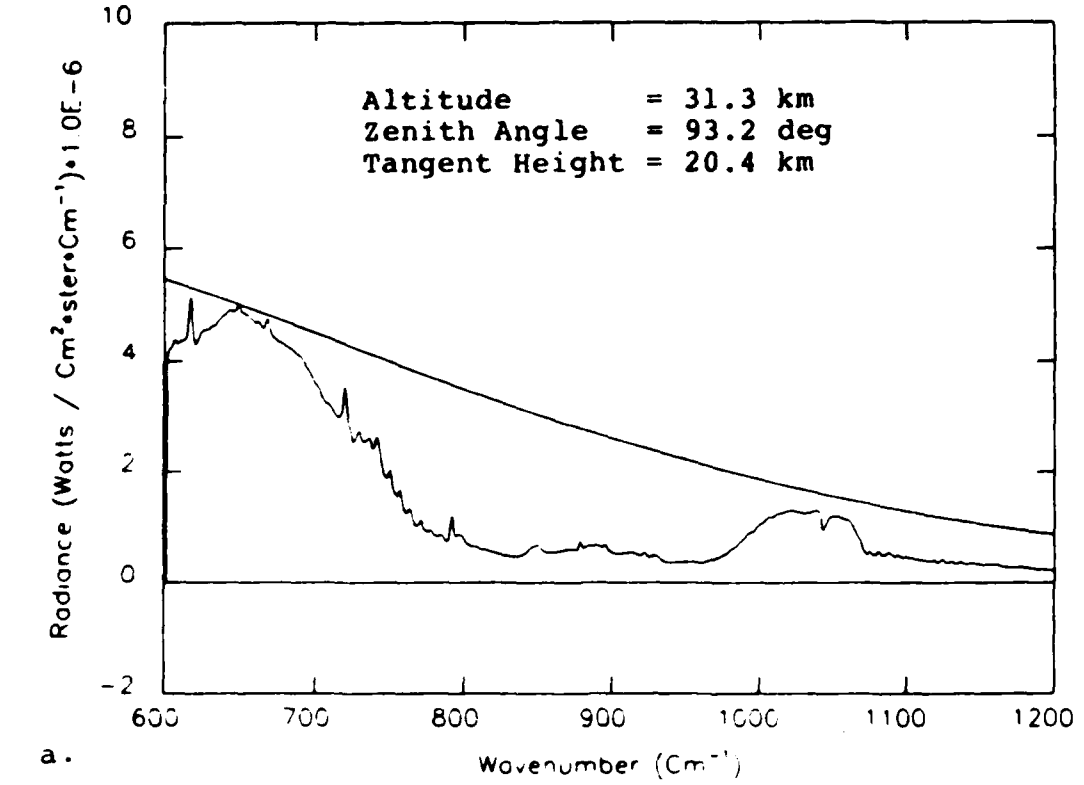

a.

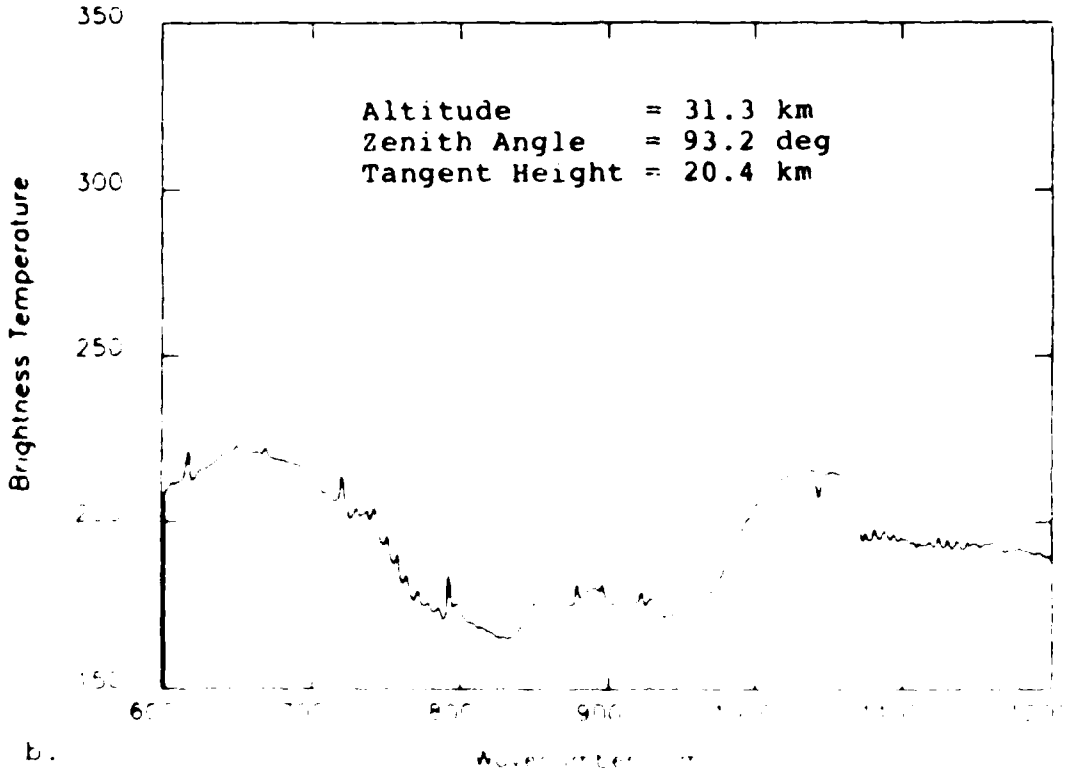

b.

Figure 19. Spectrum SC843 from 600 cm^{-1} to 1200 cm^{-1} Degraded to 1.0 cm^{-1} Resolution: a. Radiance, b. Brightness Temperature. Spectrum was processed by the University of Denver

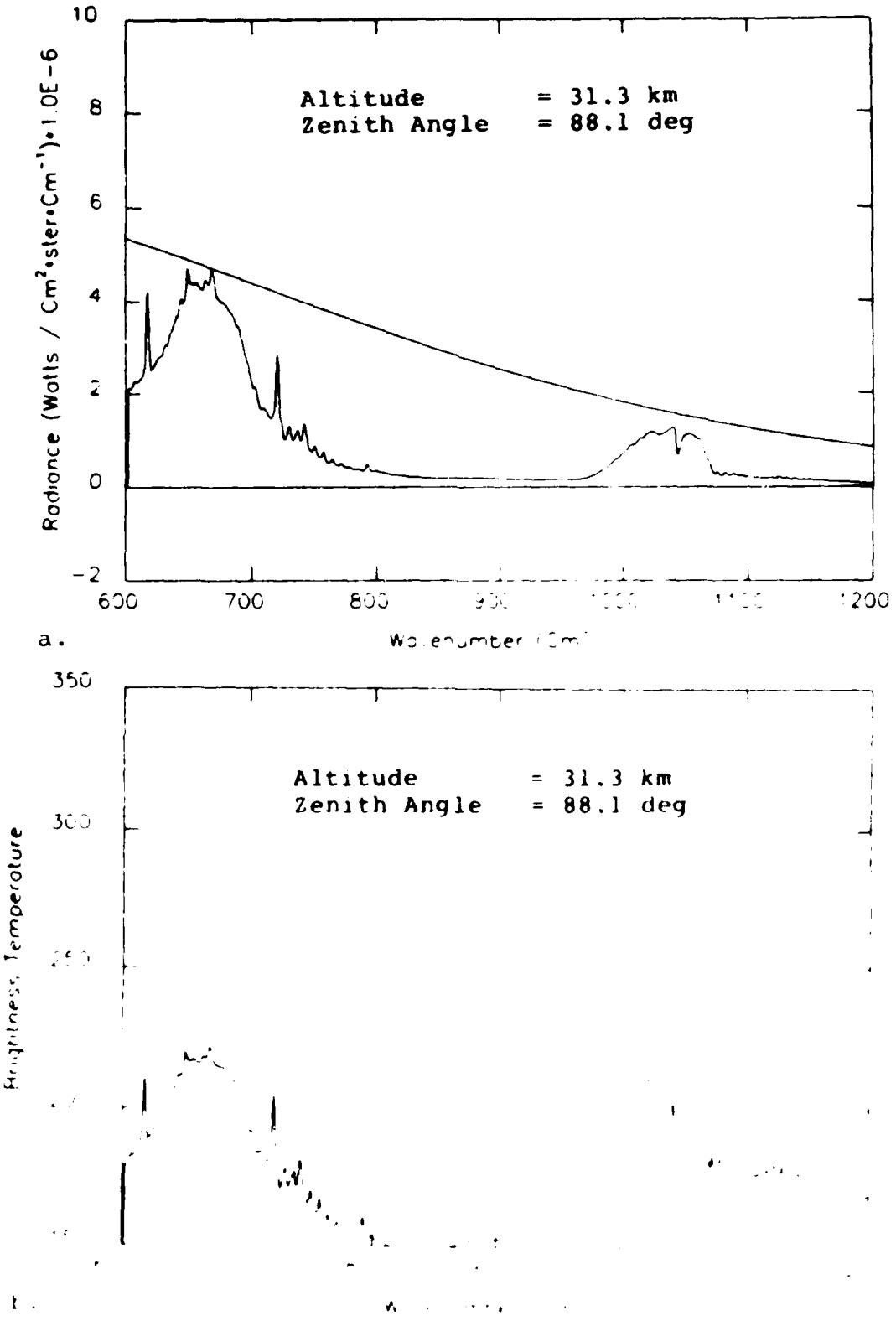

Figure 20. Spectrum SC844 from 600 cm⁻¹ to 1200 cm⁻¹ Degraded to 1.0 cm⁻¹ Resolution a. Radiance, b. Brightness Temperature. Spectrum was processed by the Air Force Denver

these three discrepancies suggest a significant error in the calibration of this spectrum. The trend in the window region recalls the appearance of the spectrum in Figure 15. In spite of these discrepancies, this spectrum was selected for further analysis since it is the only downward looking spectrum for this flight.

The large scale features for the other three spectra in Figures 18 through 20 appear normal. The two limb spectra in Figures 18 and 19 clearly show the HNO_3 bands around 900 cm^{-1} but this feature is hardly seen at all in the upward looking spectrum in Figure 20. The brightness temperatures at 667 cm^{-1} differ by only 3 K and are about 7 K less than the ambient air temperature.

It is interesting to compare the upward looking spectrum from the 1983 flight in Figure 14 to the one from the 1984 flight in Figure 20. While the main features are similar in the two spectra, Figure 20 shows much less variance and (presumably) noise. This is reasonable since Figure 20 represents a co-added spectrum of 13 spectra, while Figure 14 is not co-added.

5. COMPARISON OF SELECTED SPECTRA WITH FASCODE

Nine spectra which had no identifiable errors were chosen from Table 8 for further evaluation by comparing them with spectra calculated by FASCODE. The chosen spectra are identified in Table 8 by an asterisk. As discussed in Section 3.2, three figures were prepared for each case. The first figure at 1.0 cm^{-1} resolution covered 600 to 1200 cm^{-1} while the other two at full resolution covered the regions 665 to 675 cm^{-1} and 800 to 820 cm^{-1}. These three sets of plots are discussed separately here.

5.1 600 to 1200 cm^{-1} Region (1 cm^{-1} Resolution)

The comparisons between the measured spectra and the FASCODE calculations for the 600 to 1200 cm^{-1} region at 1 cm^{-1} resolution are shown in Figures 21 through 29. Figure 21 shows the comparison for the downward looking spectrum from the 1983 flight. The agreement between the measured and the calculated radiance is excellent within the 15 micrometer CO_2 band, but it worsens at the edges of the band. In particular, the calculated radiance at 600 cm^{-1} is 20 percent greater than the measured. The agreement within the O_3 band around 1040 cm^{-1} is surprisingly good considering that only an average O_3 profile was used in the calculation.

Within the window region between 800 and 970 cm^{-1} the calculation is systematically 3 K higher in brightness

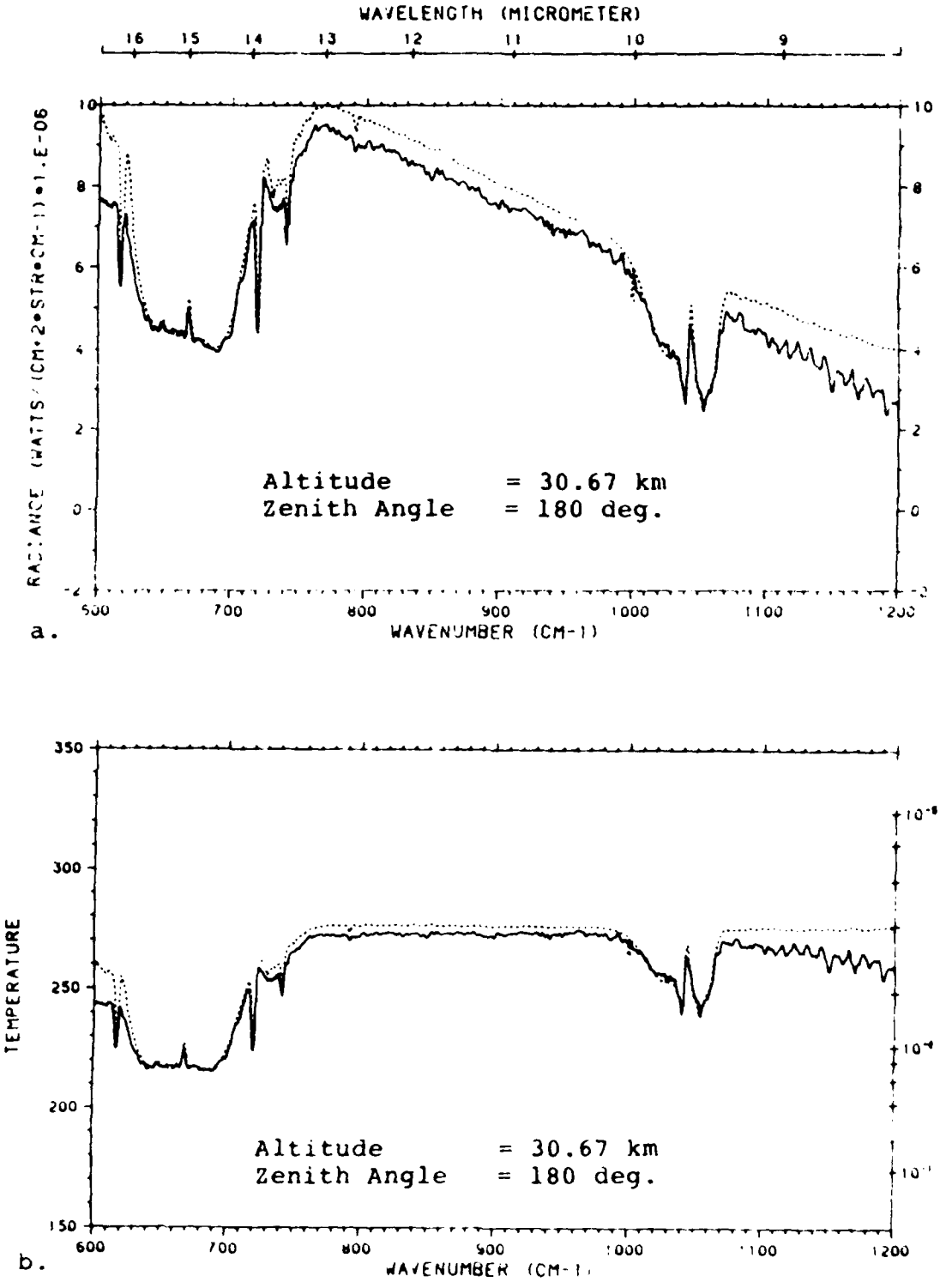

Figure 21. Comparison Between Spectrum SP830W1 (solid line) and FASCODE (dashed line) for the Region 600 to 1200 cm^{-1} at 1.0 cm^{-1} Resolution: a. Radiance, b. Brightness Temperature. Spectrum was processed by the University of Massachusetts

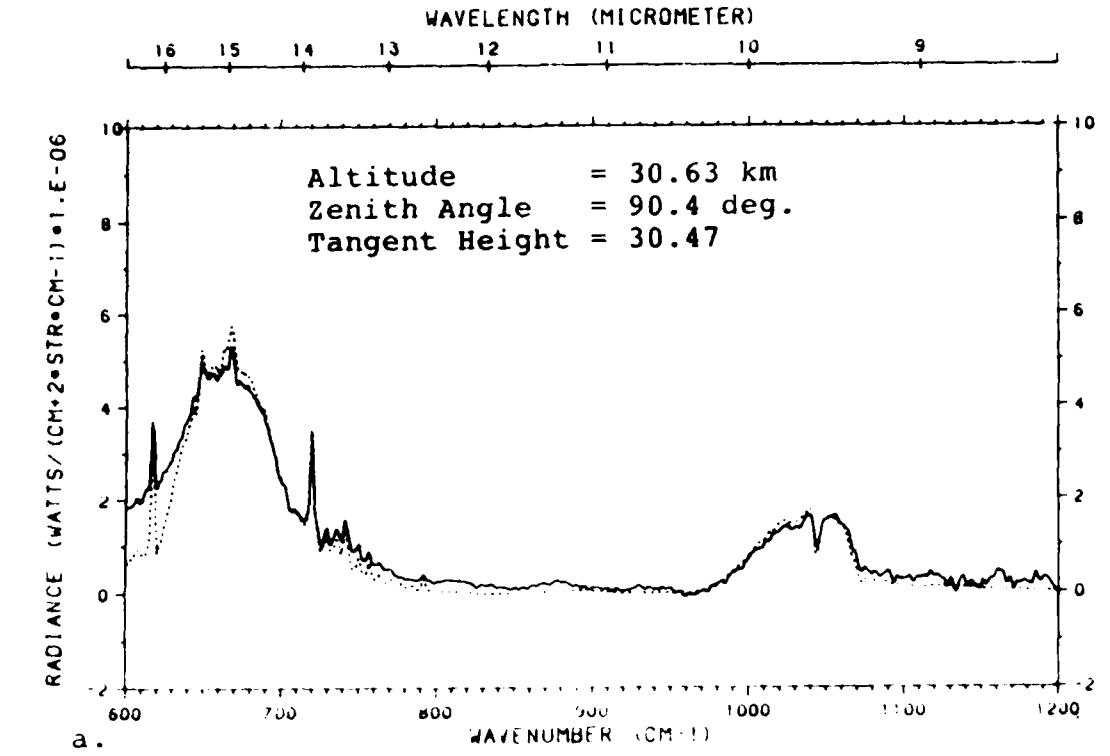

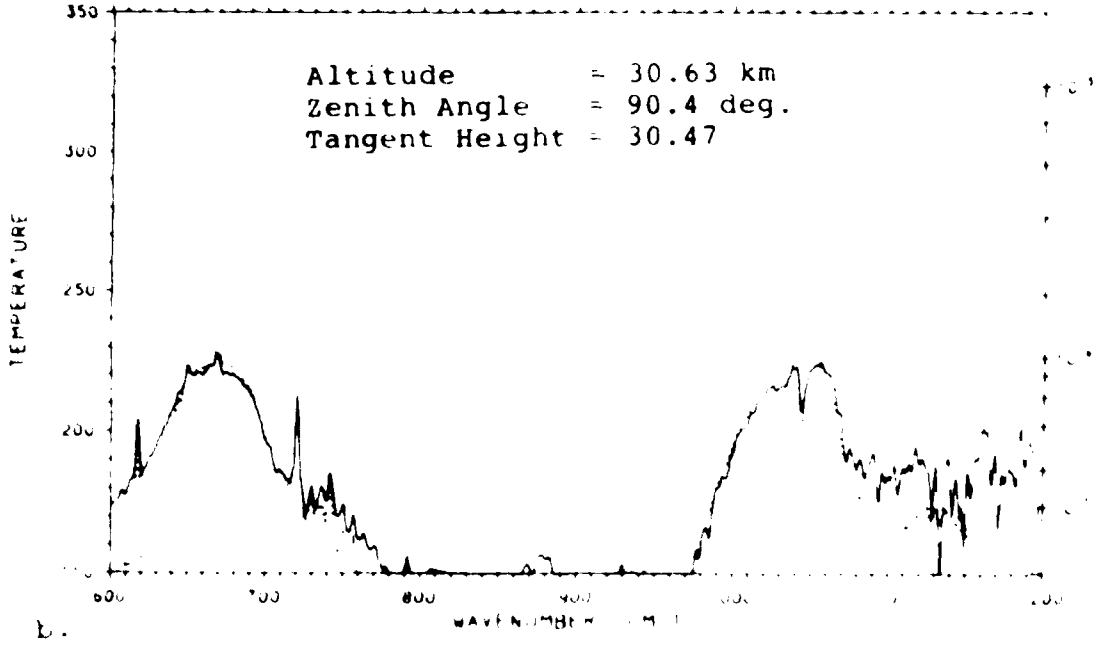

Figure 22. Comparison Between Spectrum SP830E1 (solid line) and FASCODE (dashed line) for the Region 600 to 1200 cm^{-1} at 1.0 cm^{-1} Resolution: a. Radiance, b. Brightness Temperature. Spectrum was processed by the University of Massachusetts

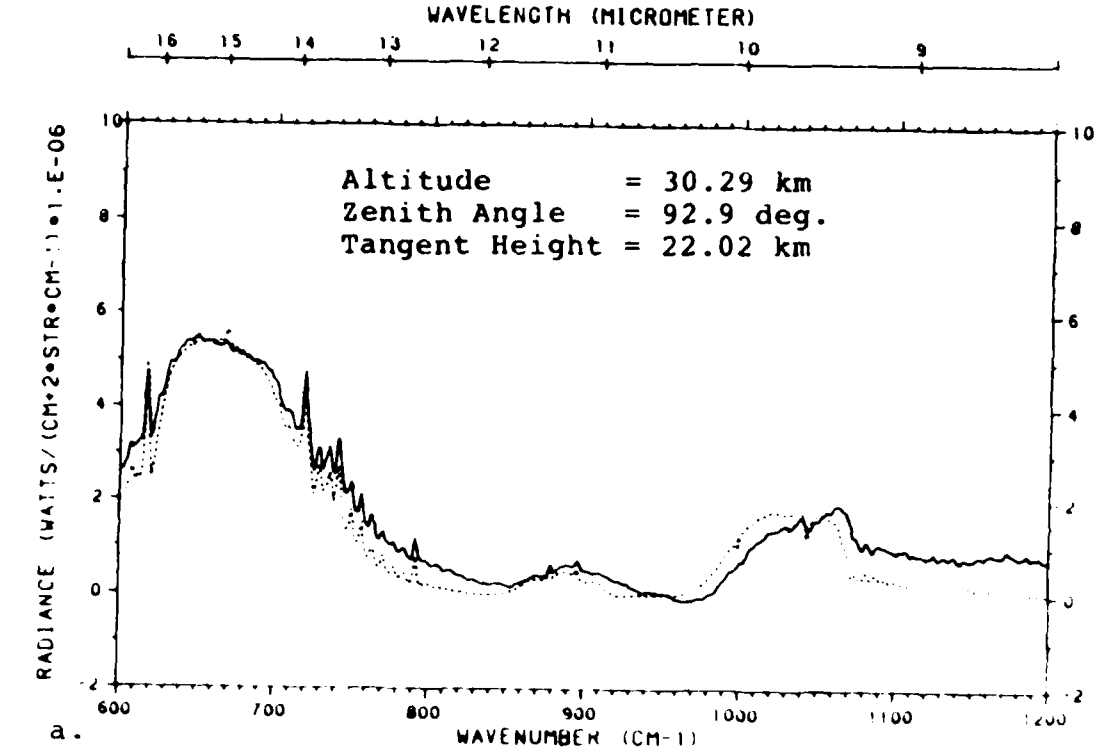

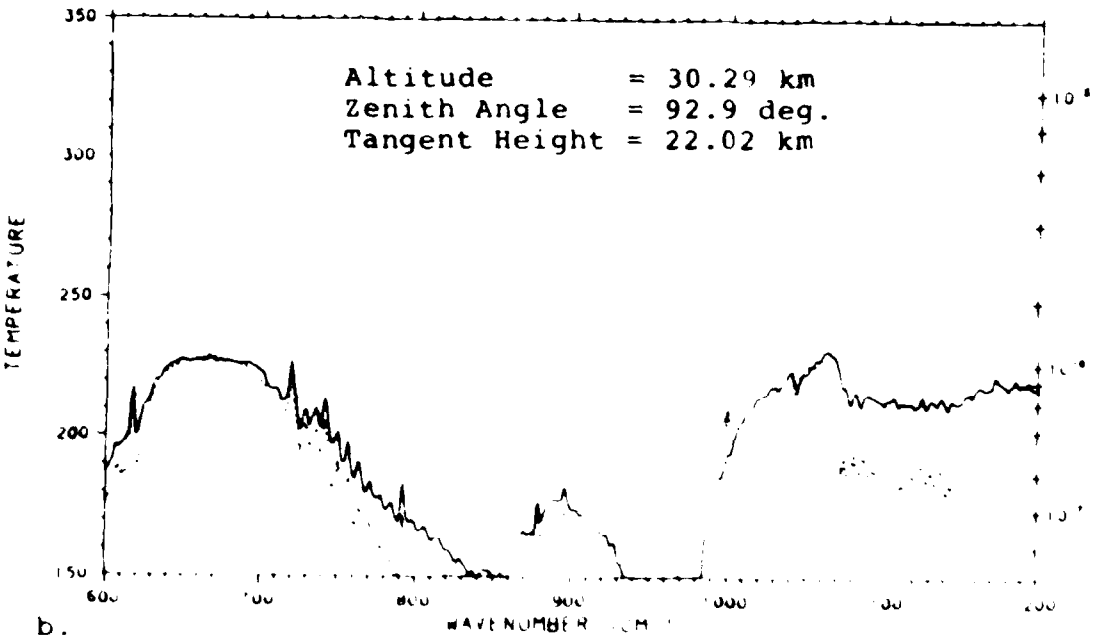

Figure 23. Comparison Between Spectrum SP830I2 (solid line) and FASCODE (dashed line) for the Region 600 to 1200 cm^{-1} at 1.0 cm^{-1} Resolution: a. Radiance, b. Brightness Temperature. Spectrum was processed by the University of Massachusetts

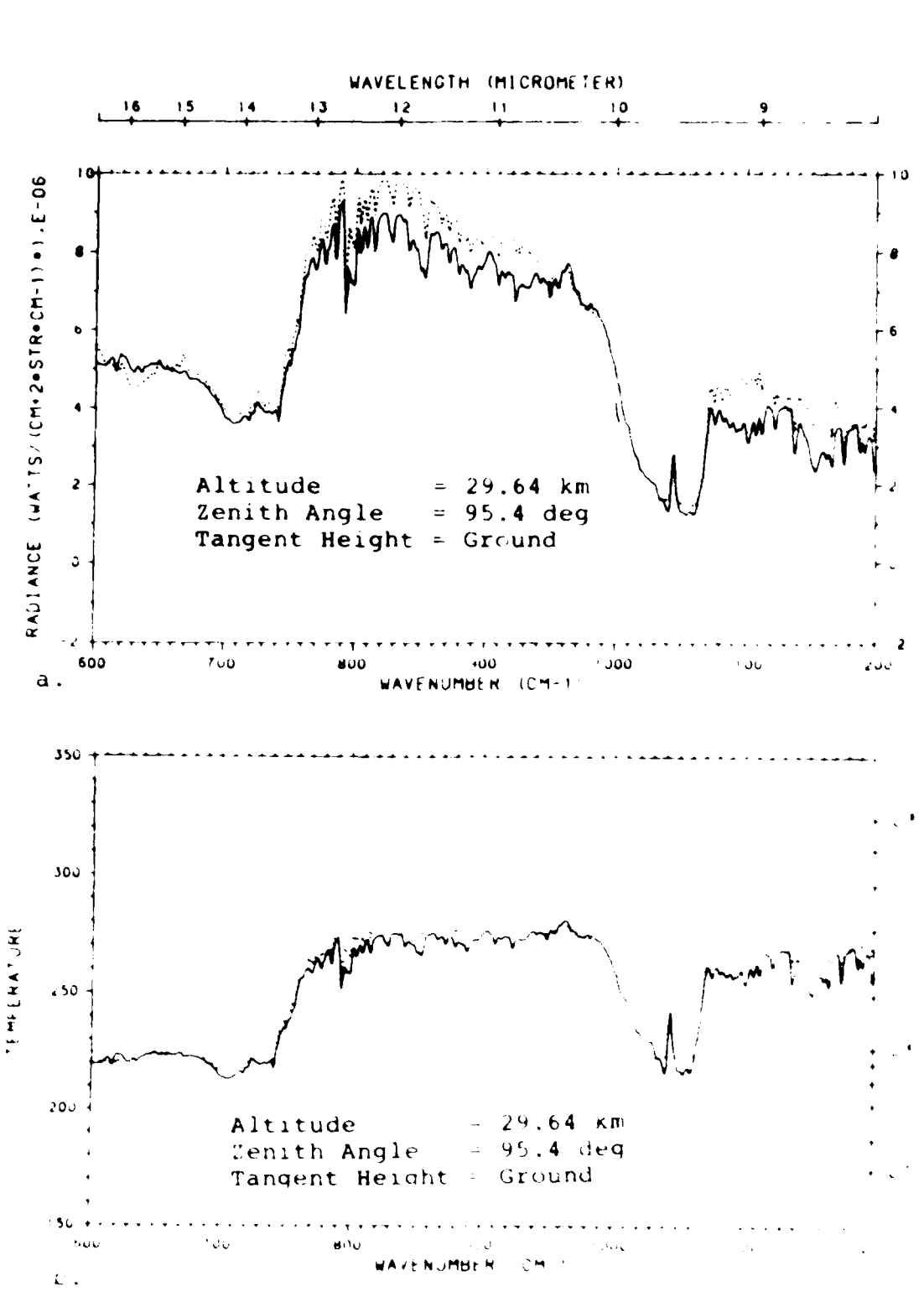

Figure 24. Comparison Between Spectrum SP83043 [illegible] and FASCODE (dashed line) for the Region 600 to 1200 cm^{-1} Resolution: a. Radiance, b. Brightness Temperature. Spectrum was processed by the University of Massachusetts

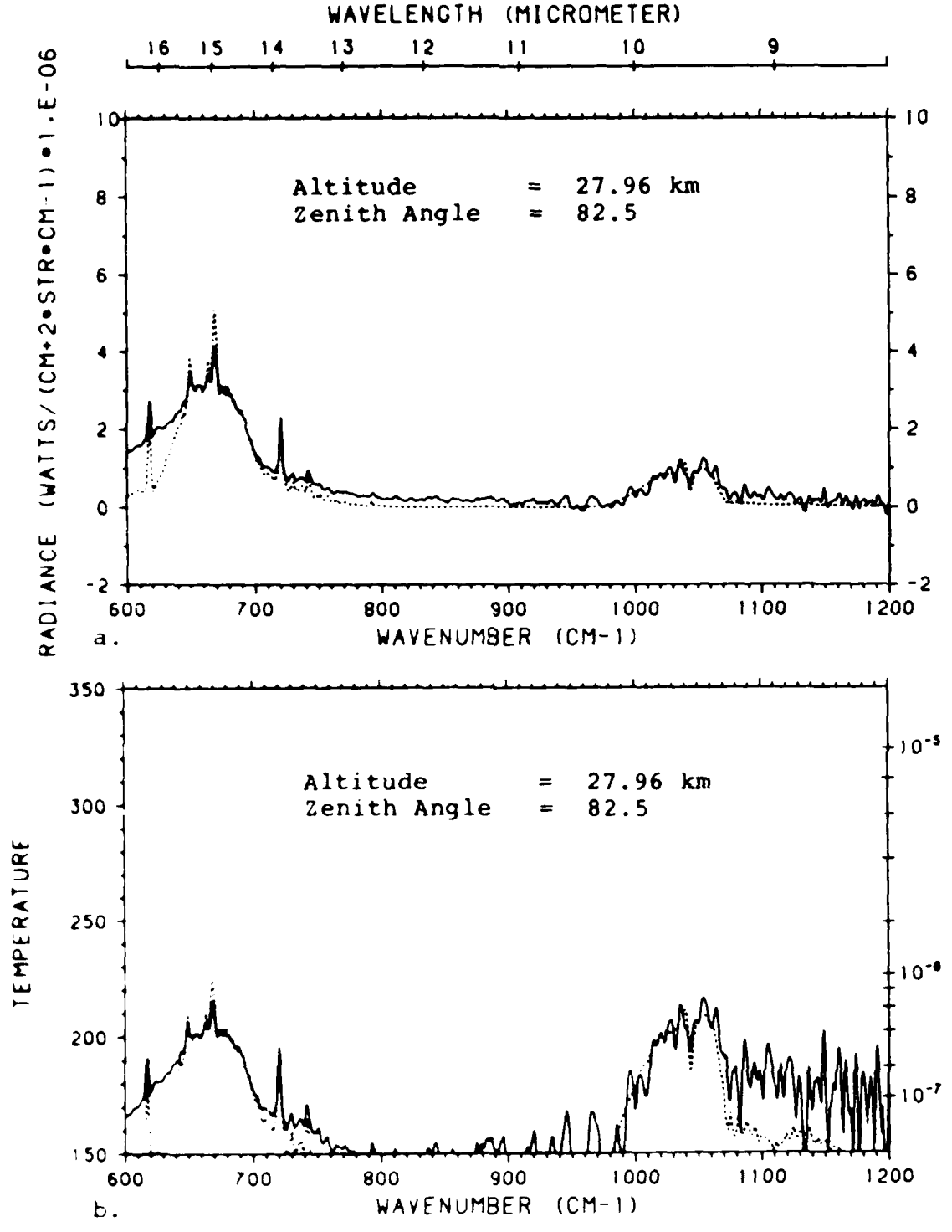

Figure 25. Comparison Between Spectrum SP83096 (solid line) and FASCODE (dashed line) for the Region 600 to 1200 cm^{-1} at 1.0 cm^{-1} Resolution: a. Radiance, b. Brightness Temperature. Spectrum was processed by the University of Massachusetts

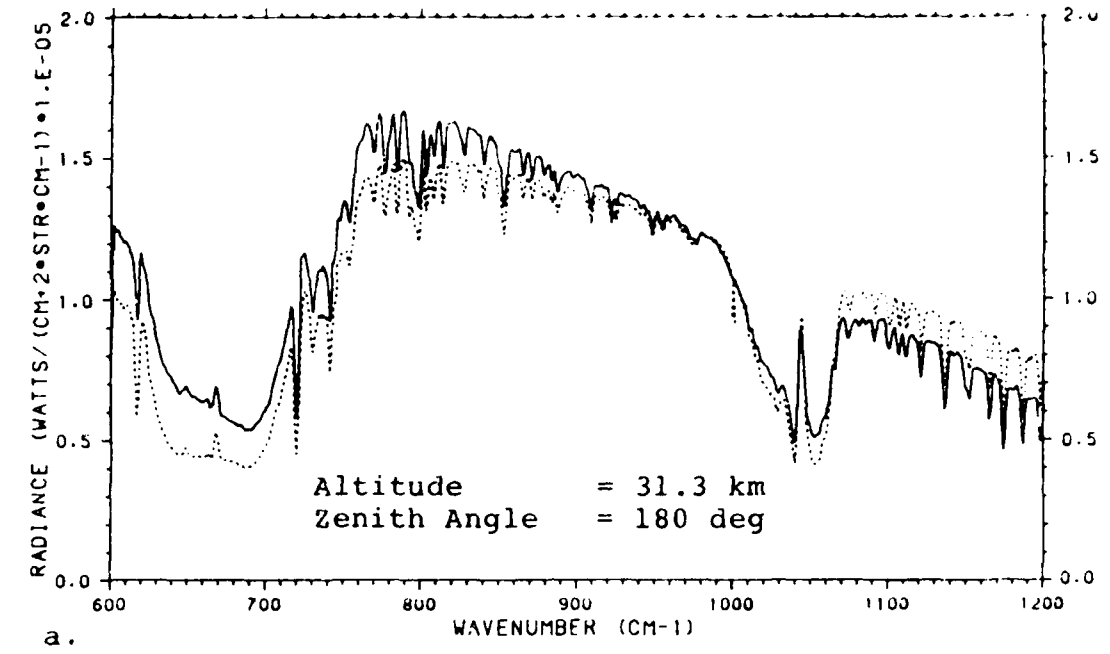

a.

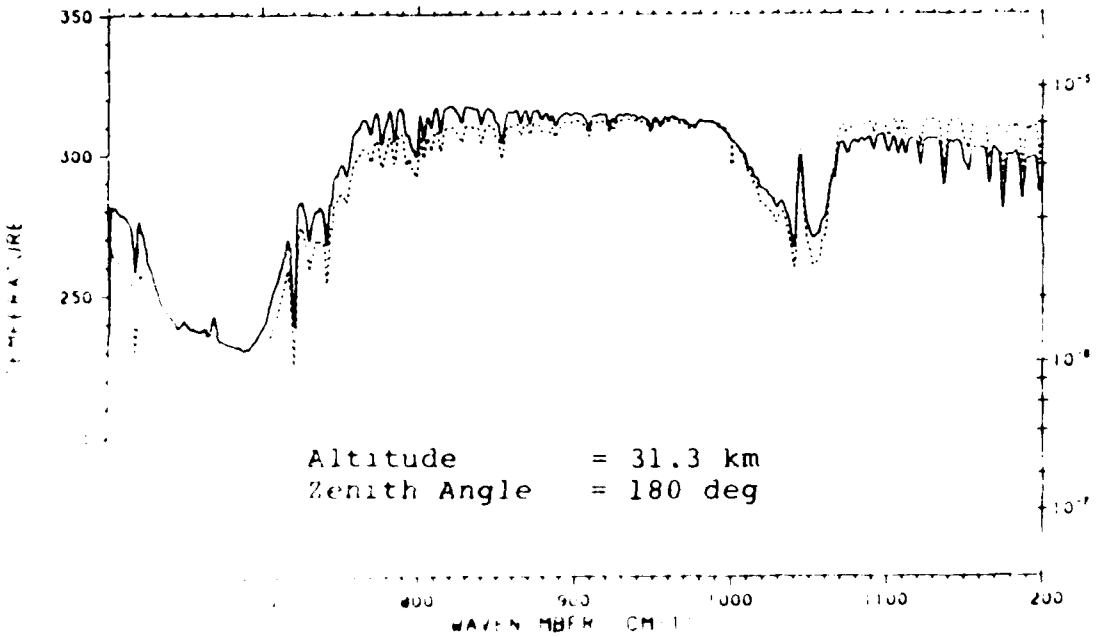

Between Spectrum SC841 (solid line) ... 600 to 1200 cm^{-1} at ... Brightness Temperature. ... Denver

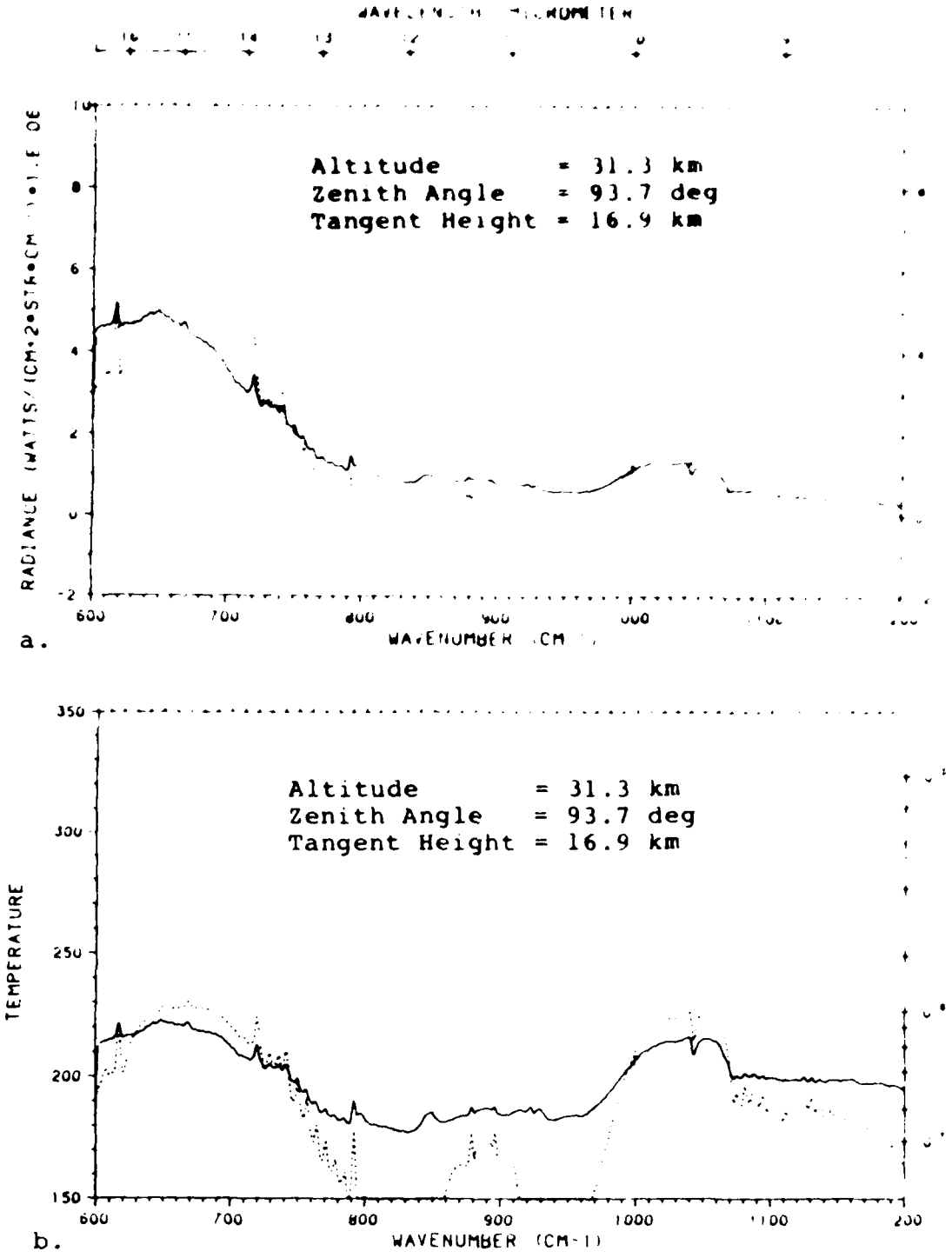

Figure 27. Comparison Between Spectrum SC842 (solid line) and FASCODE (dashed line) for the Region 600 to 1200 cm^{-1} at 1.0 cm^{-1} Resolution: a. Radiance, b. Brightness Temperature. Spectrum was processed by the University of Denver

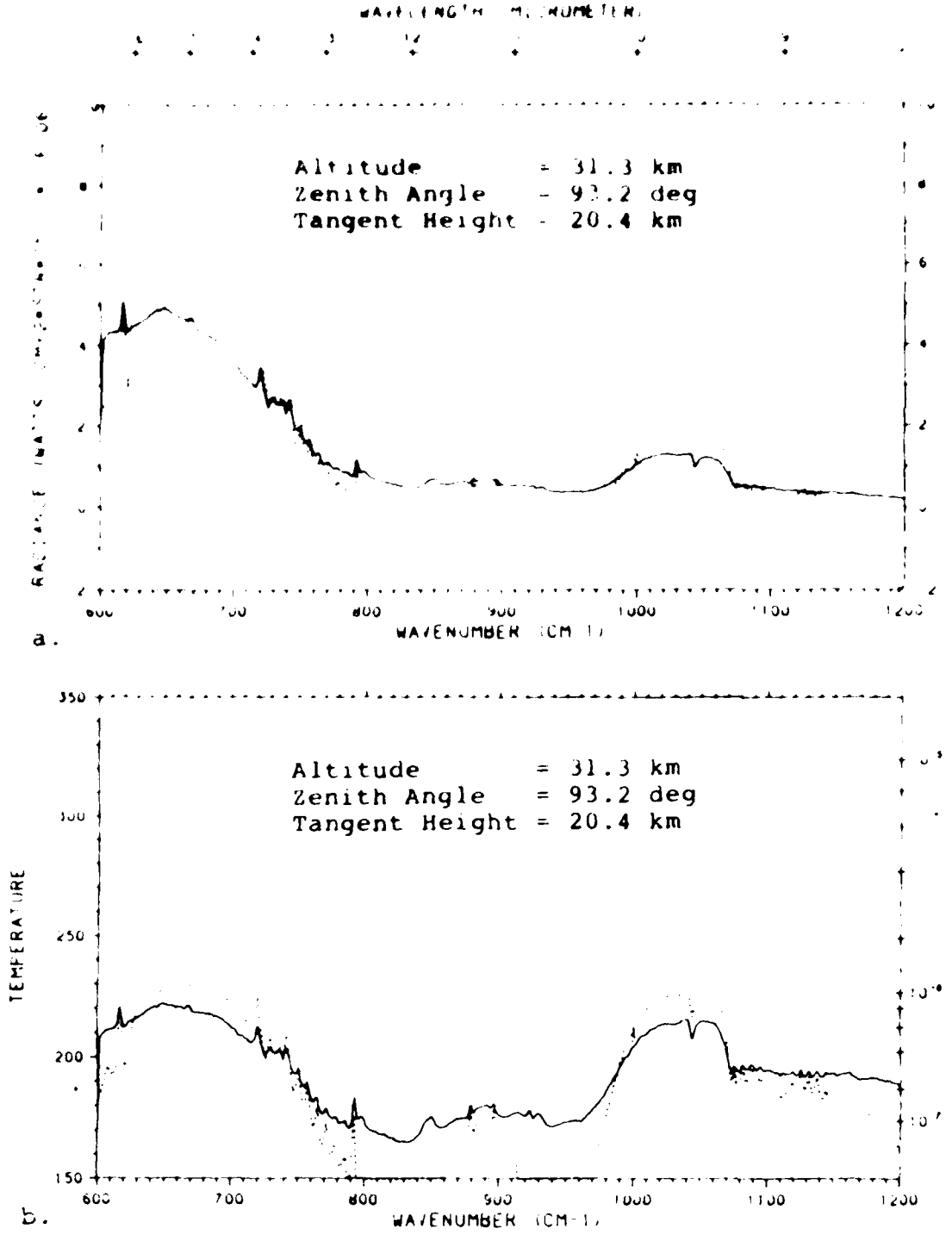

Figure 28. Comparison Between Spectrum SC843 (solid line) and FASCODE (dashed line) for the Region 600 to 1200 cm^{-1} at 1.0 cm^{-1} Resolution: a. Radiance, b. Brightness Temperature. Spectrum was processed by the University of Denver

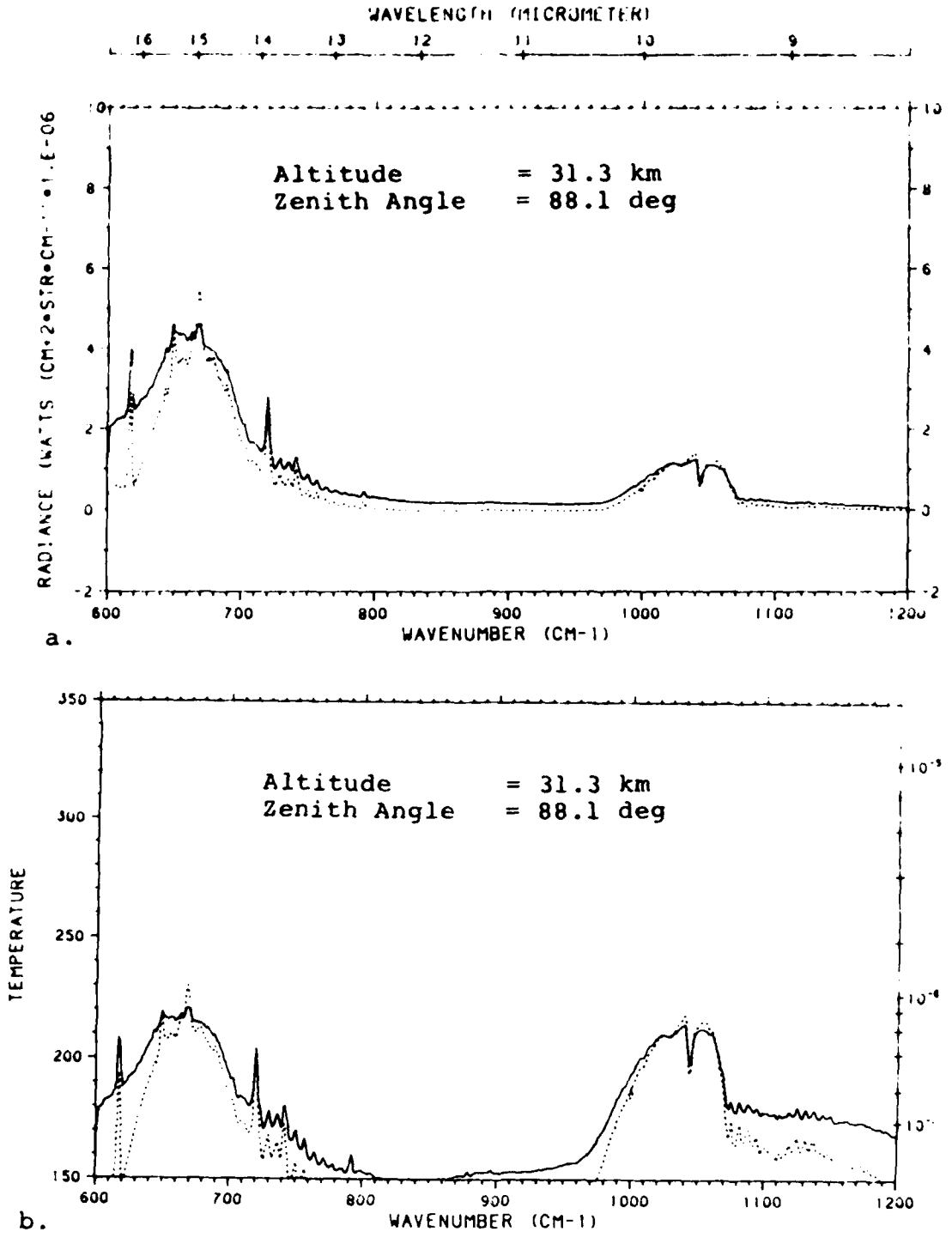

Figure 29. Comparison Between Spectrum SC844 (solid line) and FASCODE (dashed line) for the Region 600 to 1200 cm^{-1} at 1.0 cm^{-1} Resolution: a. Radiance, b. Brightness Temperature. Spectrum was processed by the University of Denver

temperature than the measurement. Recall from Section 5.1 that the measured brightness temperature around 800 cm^{-1} was used as the ground temperature in the calculation. It may seem surprising then that the calculated brightness temperature at 800 cm^{-1} is greater than the ground temperature. Note however from the temperature profile in Figure 7 that there is a strong inversion at the ground. It is the calculated emission from this warm layer just above the ground which makes the calculated brightness temperature in the window greater than the ground temperature. This inversion at the ground may very well not be characteristic of the actual profile at the time of this measurement, so the difference in the radiance in the window region should not be considered significant.

In the window region beyond 1070 cm^{-1}, the calculation and the measurement start to diverge and the measurement shows much more structure than the calculation.

The comparison for the near horizontal viewing spectrum shown in Figure 22 again shows good agreement within the 15 micrometer CO_2 band and the O_3 band, and a large discrepancy at 600 cm^{-1}. In the window regions the measured radiance is small but is several times larger than the calculated radiance. Figure 23 for the limb viewing case with a 22 km tangent height shows similar characteristics. The agreement within the HNO_3 band around 900 cm^{-1} is fair, but like O_3 the profile for HNO_3 is an average.

Figure 24 shows the comparison for a long slant path which nominally just hits the earth. From the discussion in Section 3.3.1 it can be seen that the field-of-view actually encompasses a range of paths, including paths which are tangent above the ground. Therefore the disagreement in the window regions is not surprising. It is noteworthy that the disagreement at 600 cm^{-1} seen in the previous figures has disappeared.

Unlike the previous spectra, the upward looking spectrum shown in Figure 25 shows a large disagreement within the 15 micrometer CO_2 band, with the measured radiance significantly lower than the calculated radiance. In the window regions, the measured radiance is small but significant while the calculated radiance is negligible.

The comparison for the downward looking spectrum from the 1984 flight shown in Figure 26 shows significant discrepancies, as expected from the discussion in Section 4.2. There appears to be an error in the measured radiance which is a nearly linear function of wavenumber.

The comparisons for the limb viewing spectra shown in Figures 27 and 28 are not as good as the one shown in Figure 22 for 1983, primarily due to the difference in brightness temperatures at 667 cm^{-1}. In the window region, the measured spectra show significantly more emission than the calculation but this difference may be caused (at least partly), by the field-of-view effect.

The comparison for the upward looking spectrum shown in Figure 29 shows that the calculated emission on the low wavenumber side of the 15 micrometer CO_2 band is much less than the measured. This discrepancy has been seen in all the previous limb and upward viewing spectra but is most pronounced here. Also, the shape at the center of the band does not match. At 667 cm^{-1} the calculated radiance is too large, while at 650 cm^{-1}, it is too small.

In the window region, the measured radiance is again small but significant, and is larger than the calculated. The magnitude of the measured radiance is somewhat surprising since as part of the calibration process, the Denver group assumed that the emission in the window region for upward viewing spectra was negligible. They then used the measured emission in the window region to estimate and to correct for the radiance introduced by the ZeSe window. According to this scheme, the corrected spectra for upward viewing geometry should have negligible radiance in the window.

5.2 655 to 675 cm^{-1} Region (0.06 cm^{-1} Resolution)

The comparisons between the measurements and the calculations in the 665 to 675 cm^{-1} region are shown in Figures 30 through 38. The radiometric comparisons in Figures 30 through 33 is excellent, particularly in Figure 31 where the the measurement and the calculation match almost exactly at both the peaks and the valleys. Note

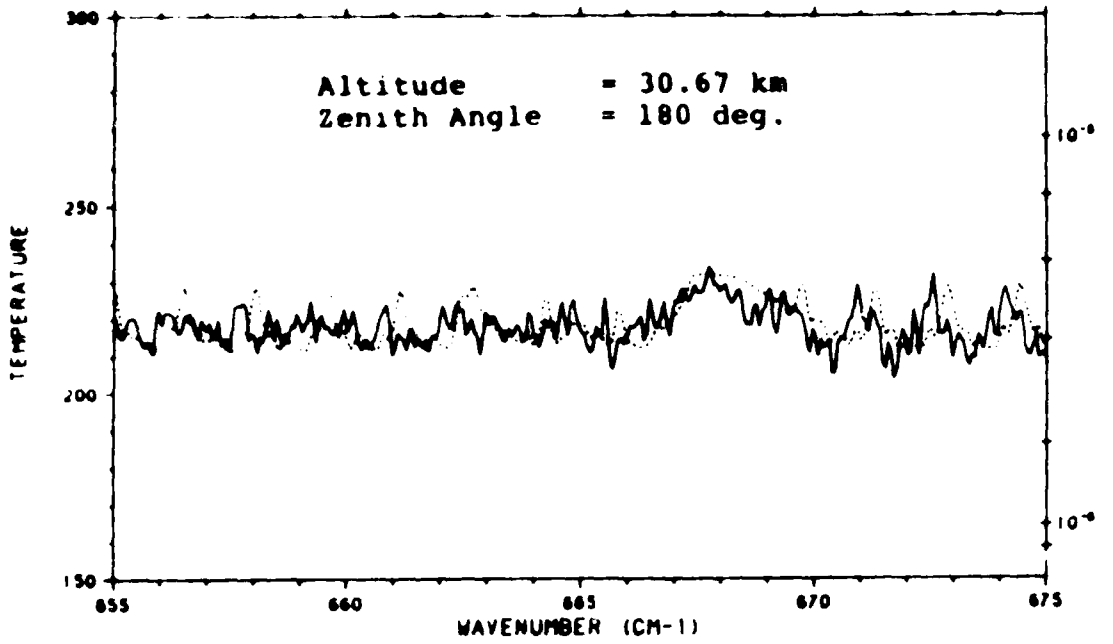

Figure 30. Comparison Between Spectrum SP830W1 (solid line) and FASCODE (dashed line) for the Region 655 to 675 cm^{-1} at 0.06 cm^{-1} Resolution. Spectrum was processed by the University of Massachusetts

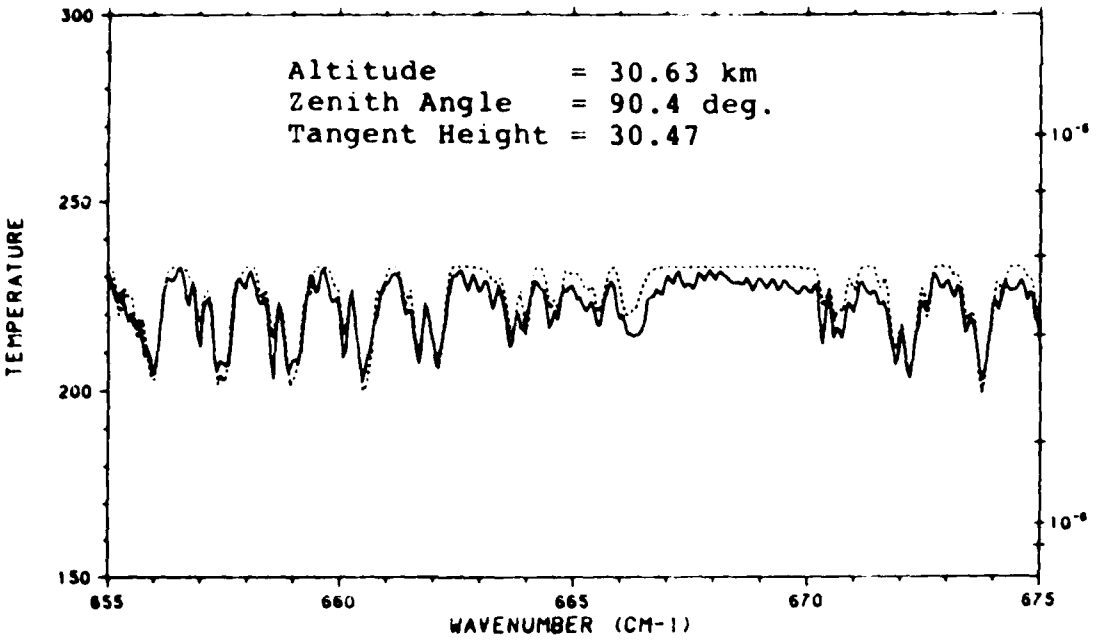

Figure 31. Comparison Between Spectrum SP830E1 (solid line) and FASCODE (dashed line) for the Region 655 to 675 cm^{-1} at 0.06 cm^{-1} Resolution. Spectrum was processed by the University of Massachusetts

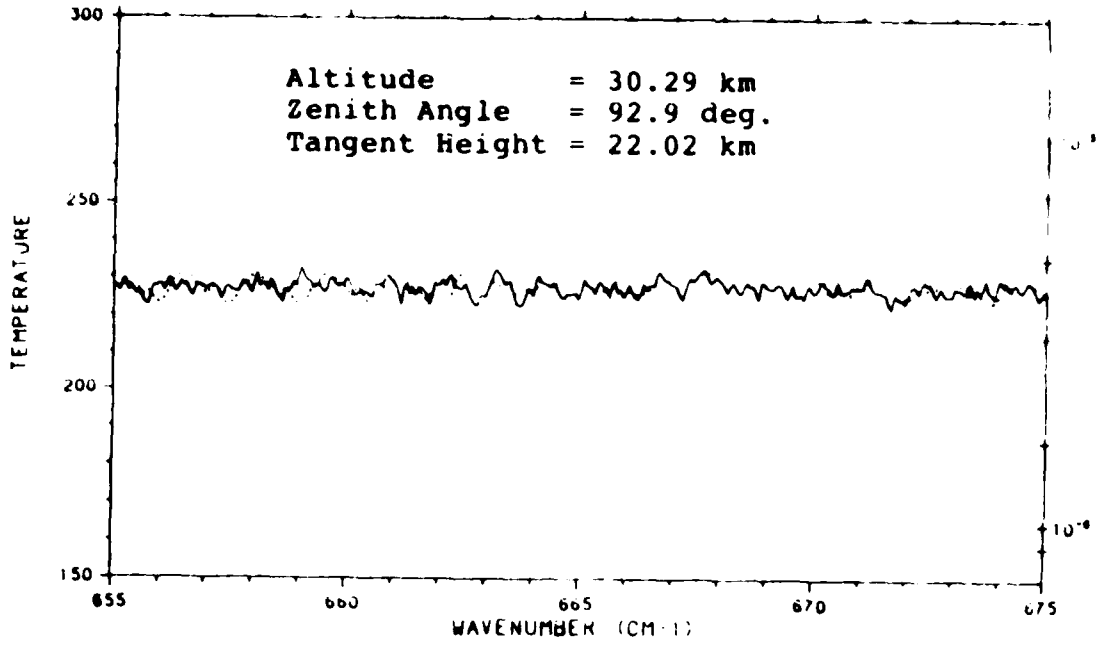

Figure 32. Comparison Between Spectrum SP8301I2 (solid line) and FASCODE (dashed line) for the Region 655 to 675 cm^{-1} at 0.06 cm^{-1} Resolution. Spectrum was processed by the University of Massachusetts

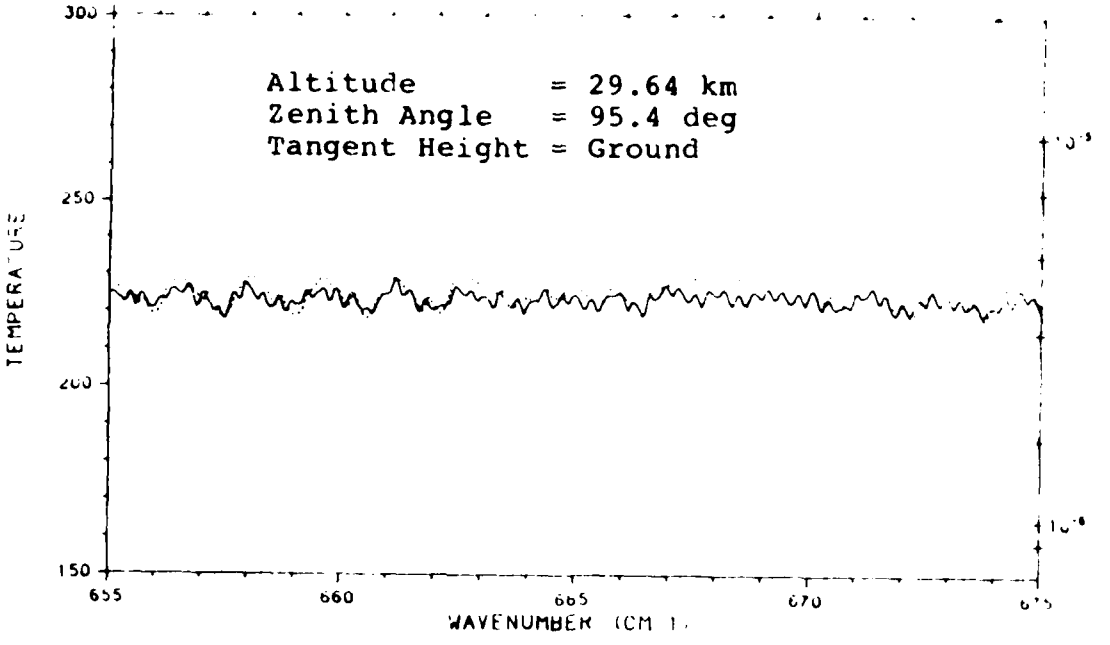

Figure 33. Comparison Between Spectrum SP83043 (solid line) and FASCODE (dashed line) for the Region 655 to 675 cm^{-1} at 0.06 cm^{-1} Resolution. Spectrum was processed by the University of Massachusetts

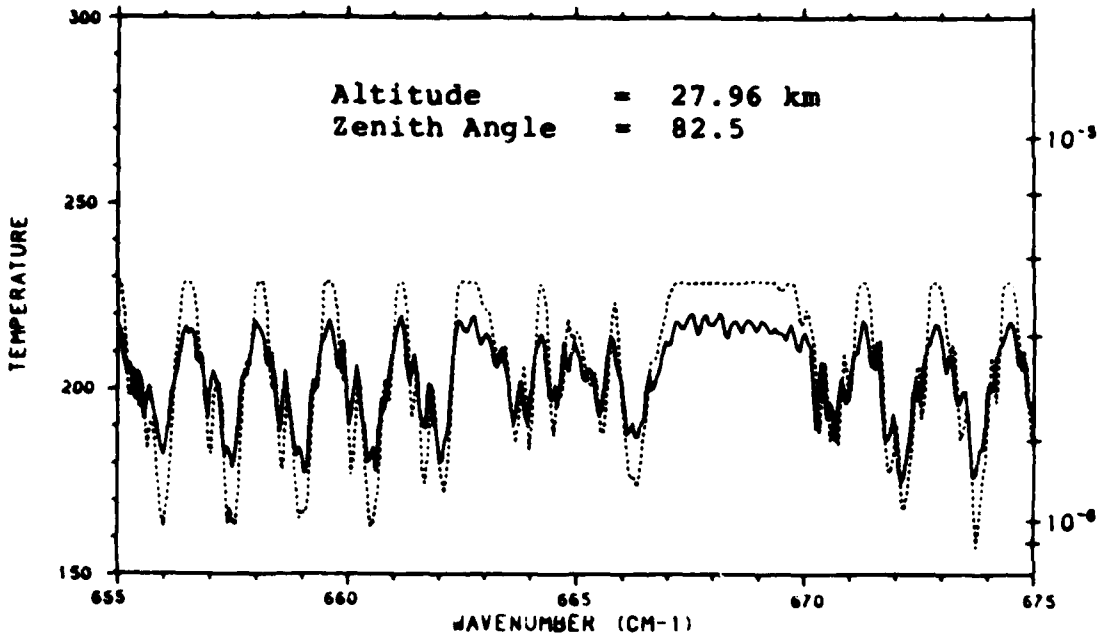

Figure 34. Comparison Between Spectrum SP83096 (solid line) and FASCODE (dashed line) for the Region 655 to 675 cm^{-1} at 0.06 cm^{-1} Resolution. Spectrum was processed by the University of Massachusetts

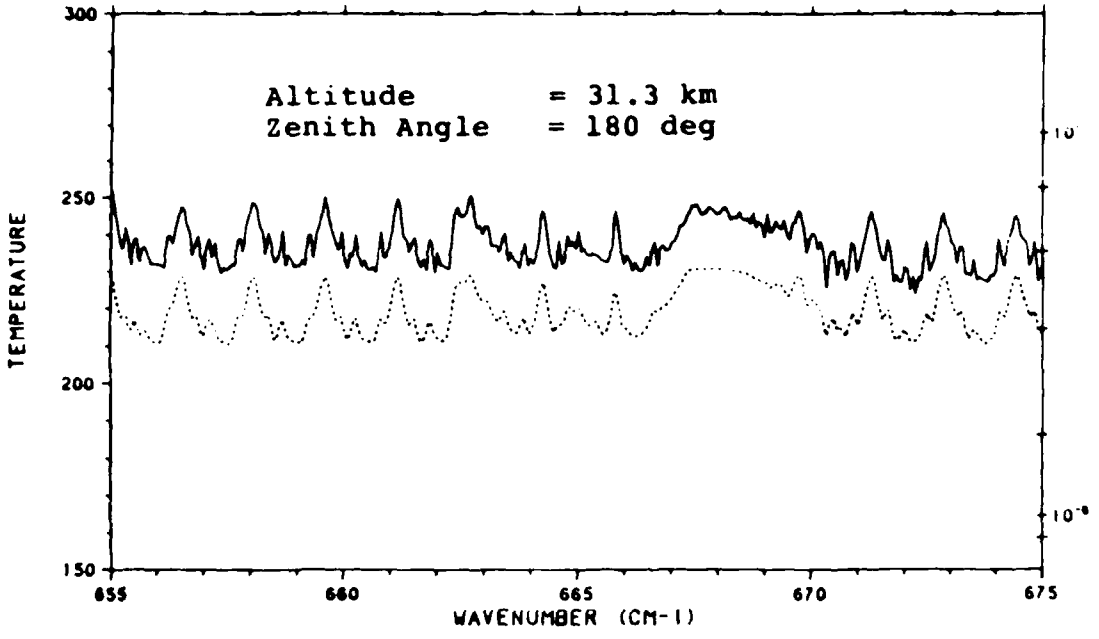

Figure 35. Comparison Between Spectrum SC841 (solid line) and FASCODE (dashed line) for the Region 655 to 675 cm^{-1} at 0.06 cm^{-1} Resolution. Spectrum was processed by the University of Denver

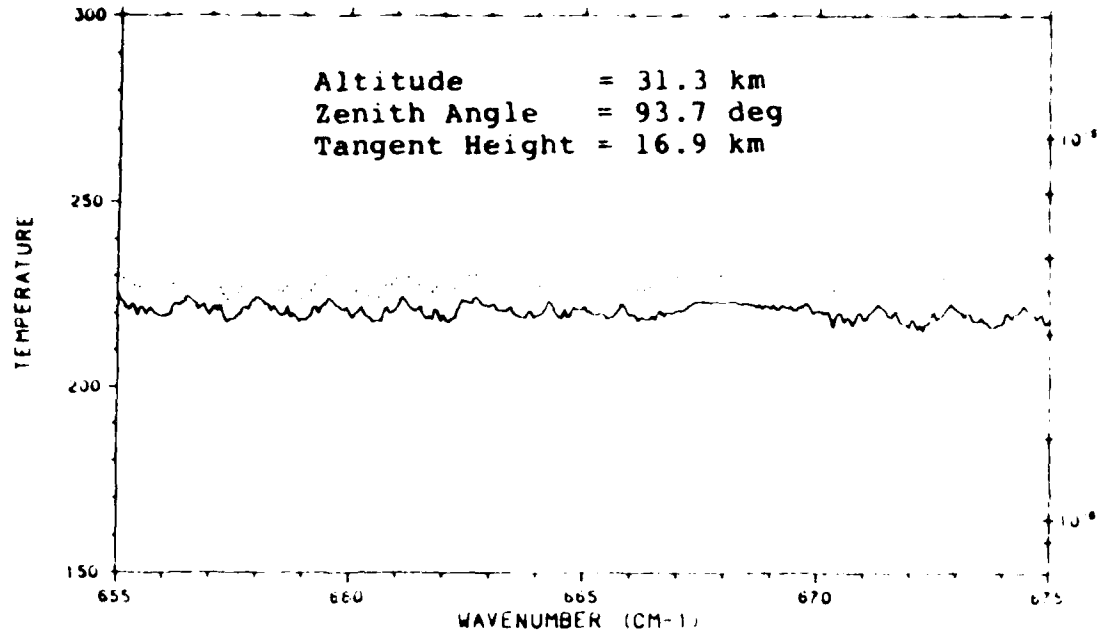

Figure 36. Comparison Between Spectrum SC842 (solid line) and FASCODE (dashed line) for the Region 655 to 675 cm^{-1} at 0.06 cm^{-1} Resolution. Spectrum was processed by the University of Denver

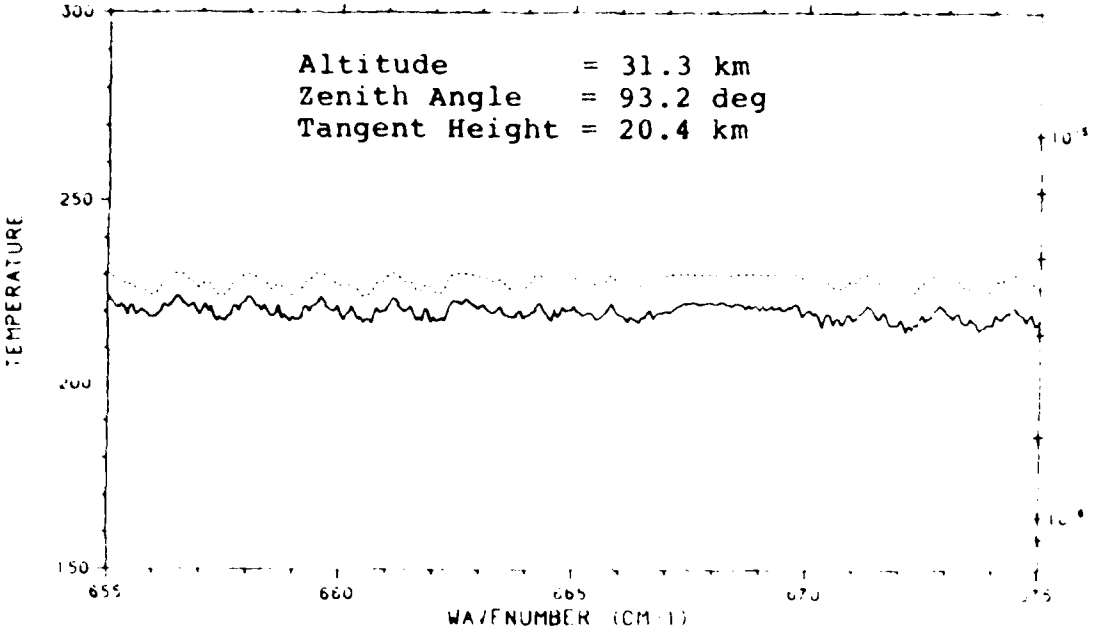

Figure 37. Comparison Between Spectrum SC843 (solid line) and FASCODE (dashed line) for the Region 655 to 675 cm^{-1} at 0.06 cm^{-1} Resolution. Spectrum was processed by the University of Denver

however in Figure 30 the frequency shift of about 0.3 cm^{-1} between the peaks of the measured and the calculated lines. Since the positions of these lines are known to better than 0.001 cm^{-1}, the error is in the measured spectrum. None of the other spectra (except possible Figure 32) show a frequency shift. The source of this frequency shift is unknown.

In Figure 34 for the upward viewing case for the 1983 flight, the brightness temperature in the Q branch and at the centers of the strong lines is systematically greater for the calculated spectrum than for the measured as noted in the previous section. The depth of the valleys between the peaks is less for the calculation than for the measurement. This is contrasted sharply by Figure 38 (also for an upward viewing case but for the 1984 flight), where the depths of the valleys are twice as great for the calculation as for the measurement.

The comparisons for the rest of the 1984 spectra seen in Figures 35 through 37 show good agreement apart from a systematic offset which could be caused by the uncertainty in the measured temperature profile.

5.3 800 to 820 cm^{-1} Region (0.06 cm^{-1} Resolution)

The comparisons for the 800 to 820 cm^{-1} region are shown in Figures 39 through 47. Figures 39 and 44 for the downlooking cases from the two flights show sharply different characteristics. In Figure 44, the strong lines of water vapor stand out clearly in absorption but cannot be

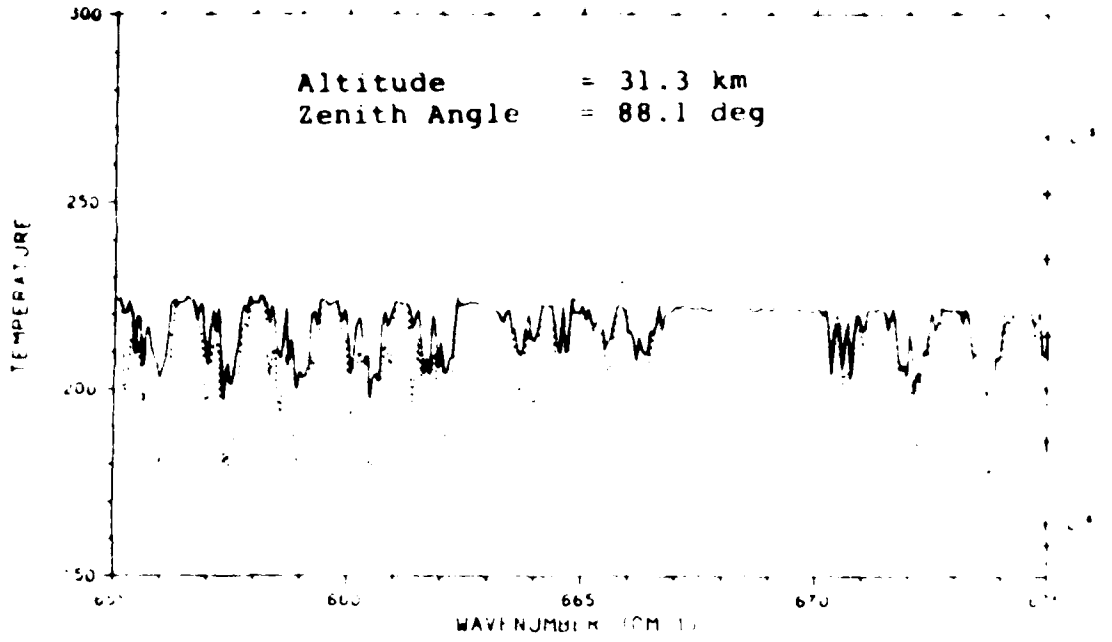

Figure 38. Comparison Between Spectrum SC844 (solid line) and FASCODE (dashed line) for the Region 655 to 675 cm^{-1} at 0.06 cm^{-1} Resolution. Spectrum was processed by the University of Denver

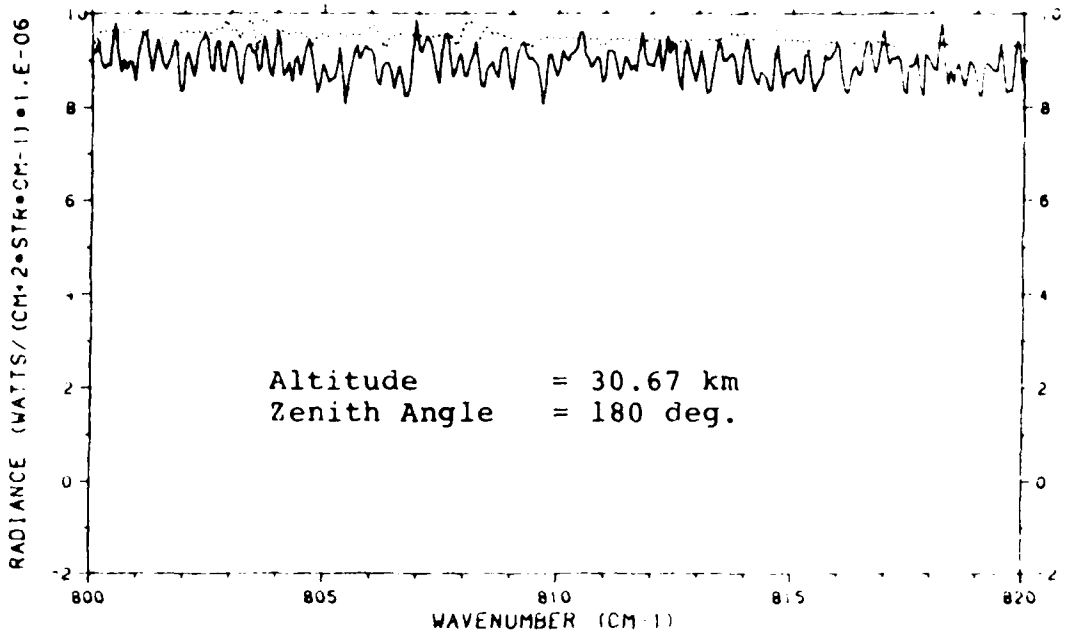

Figure 39. Comparison Between Spectrum SP830W1 (solid line) and FASCODE (dashed line) for the Region 800 to 820 cm^{-1} at 0.06 cm^{-1} Resolution. Spectrum was processed by the University of Massachusetts

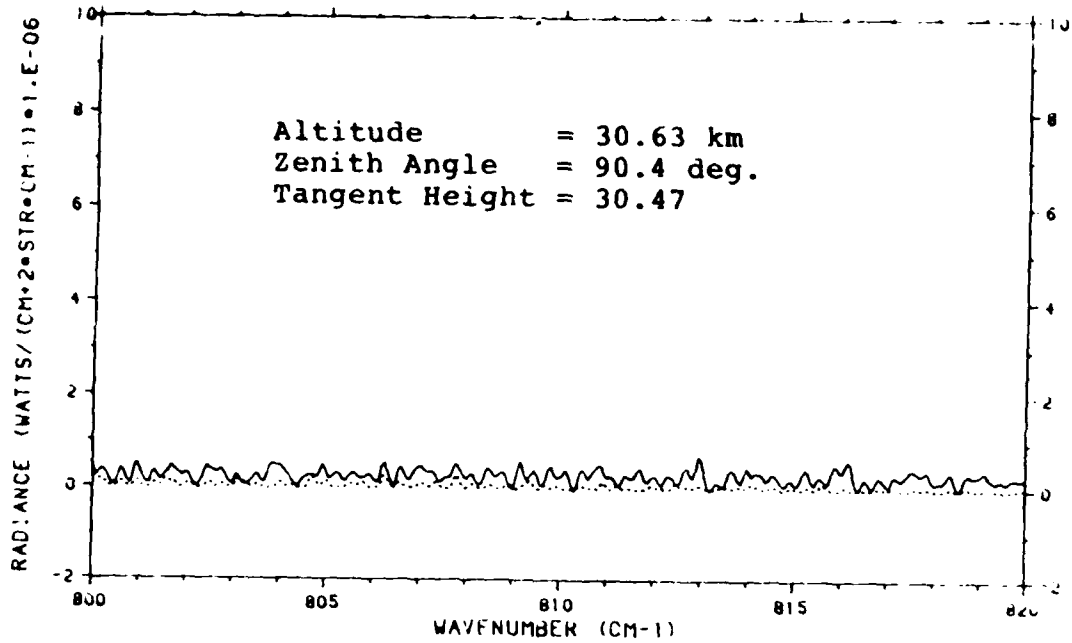

Figure 40. Comparison Between Spectrum SP830E1 (solid line) and FASCODE (dashed line) for the Region 800 to 820 cm^{-1} at 0.06 cm^{-1} Resolution. Spectrum was processed by the University of Massachusetts

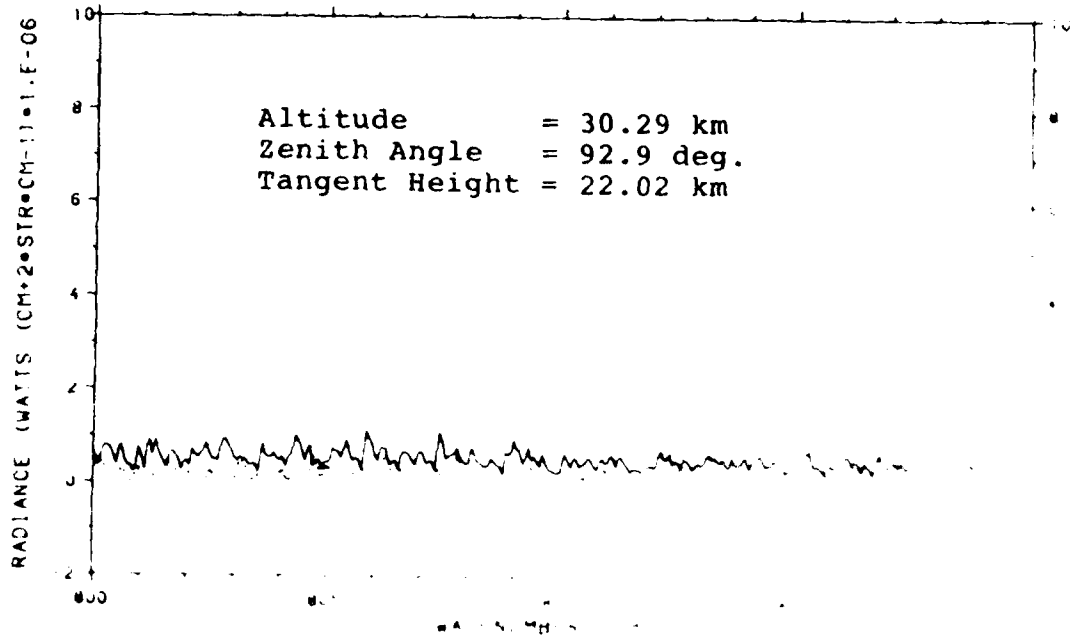

Figure 41. Comparison Between Spectrum [illegible] and FASCODE (dashed line) for the Region [illegible] at 0.06 cm^{-1} Resolution. Spectrum was processed by the University of Massachusetts

AD-A183 538 SCRIBE (STRATOSPHERIC CRYOGENIC INTERFEROMETER BALOON EXPERIMENT) DATA SU..(U) OPTIMETRICS INC BURLINGTON MA W O GALLERY ET AL. 16 FEB 87 OMI-201 AFGL-TR-87-0061 2/2

UNCLASSIFIED F19628-86-C-0102 F/G 4/1 NL

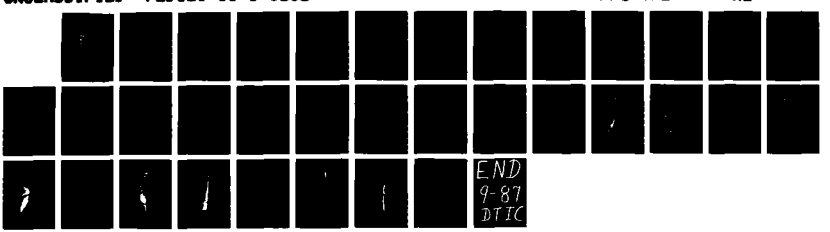

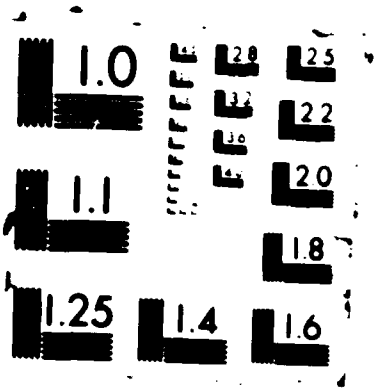
1.0
1.1
1.25
1.4
1.6
1.8
2.0
2.2
2.5

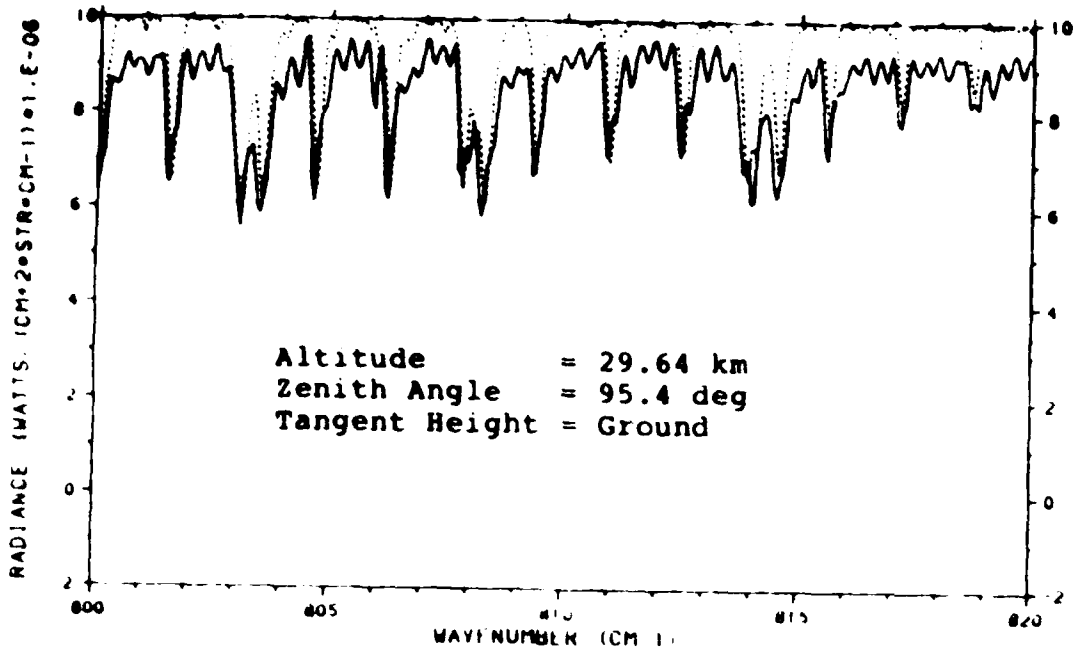

Figure 42. Comparison Between Spectrum SP83043 (solid line) and FASCODE (dashed line) for the Region 800 to 820 cm^{-1} at 0.06 cm^{-1} Resolution. Spectrum was processed by the University of Massachusetts

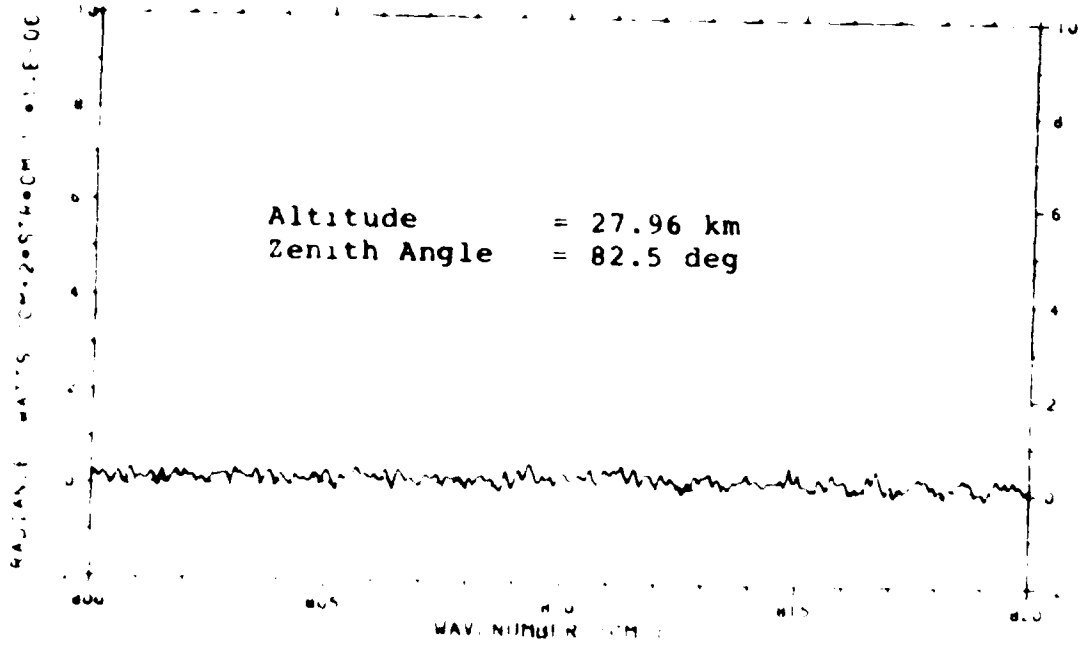

Figure 43. Comparison Between Spectrum SP83096 (solid line) and FASCODE (dashed line) for the Region 800 to 820 cm^{-1} at 0.06 cm^{-1} Resolution. Spectrum was processed by the University of Massachusetts

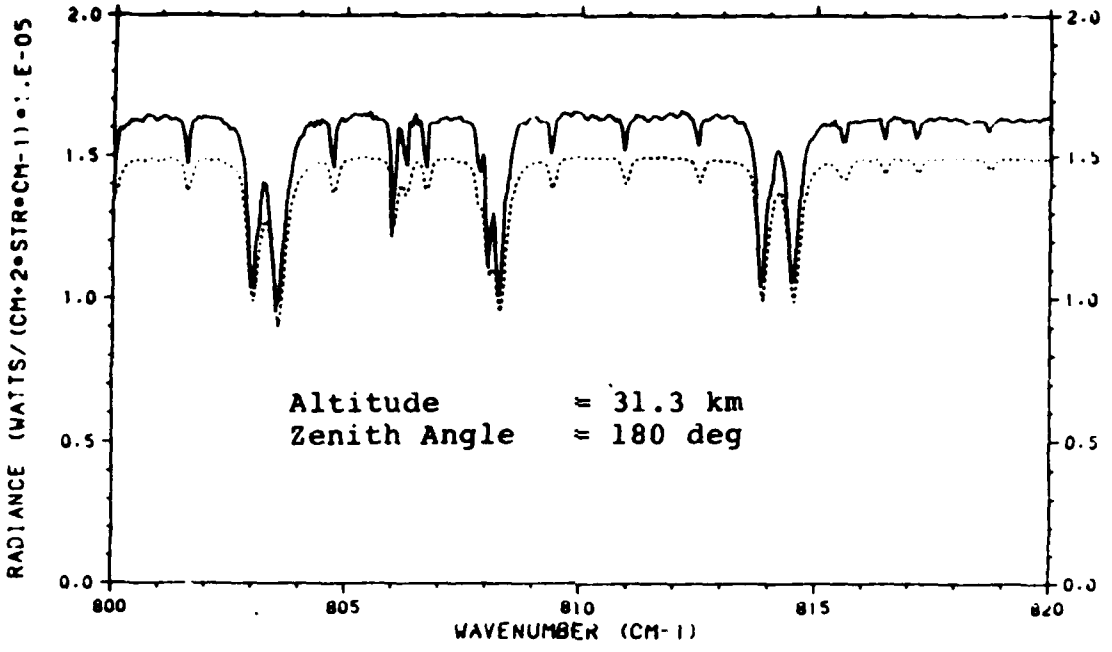

Figure 44. Comparison Between Spectrum SC841 (solid line) and FASCODE (dashed line) for the Region 800 to 820 cm^{-1} at 0.06 cm^{-1} Resolution. Spectrum was processed by the University of Denver

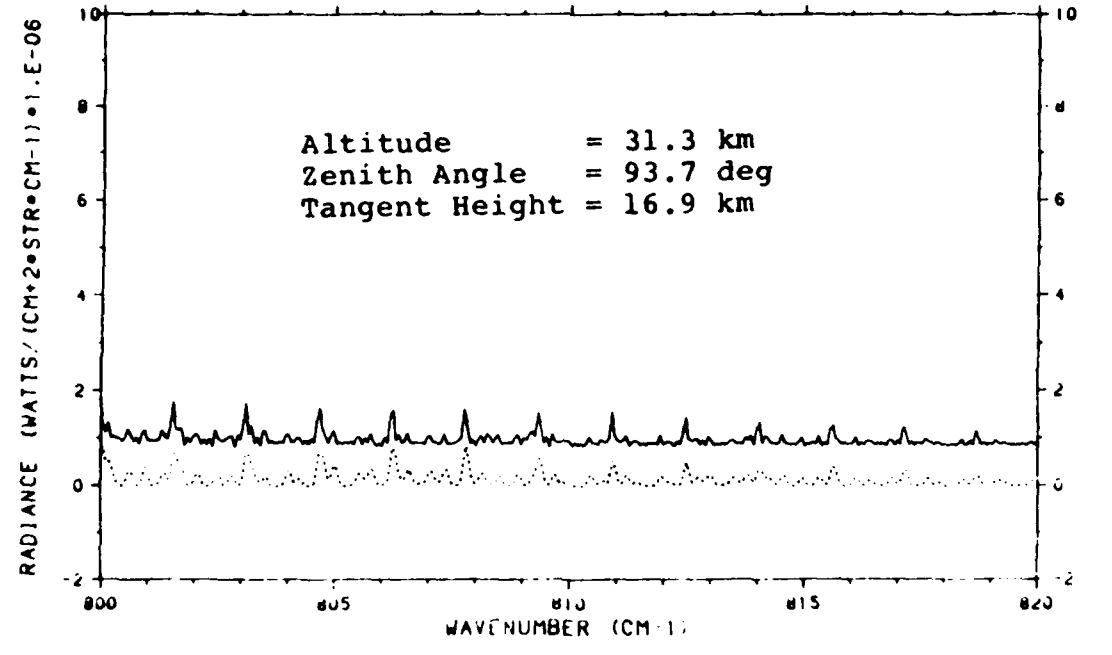

Figure 45. Comparison Between Spectrum SC842 (solid line) and FASCODE (dashed line) for the Region 800 to 820 cm^{-1} at 0.06 cm^{-1} Resolution. Spectrum was processed by the University of Denver

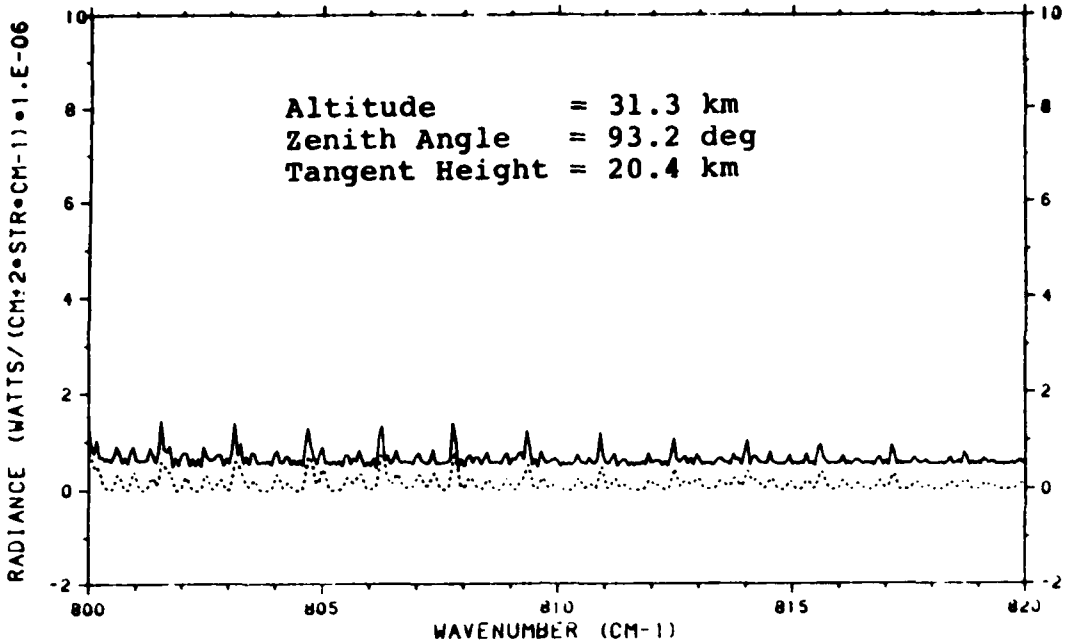

Figure 46. Comparison Between Spectrum SC843 (solid line) and FASCODE (dashed line) for the Region 800 to 820 cm^{-1} at 0.06 cm^{-1} Resolution. Spectrum was processed by the University of Denver

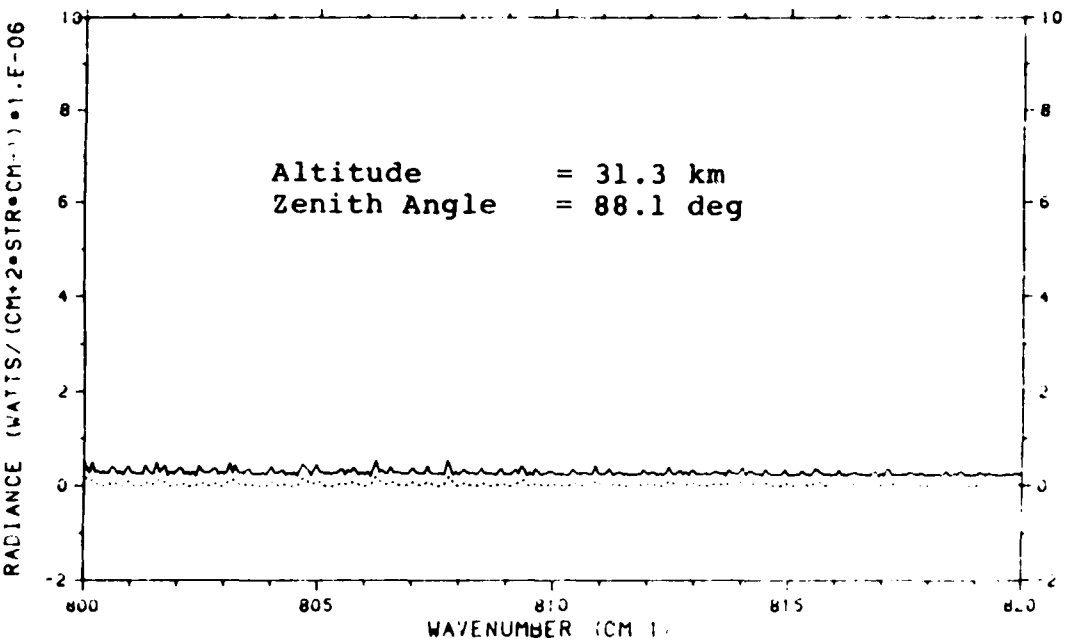

Figure 47. Comparison Between Spectrum SC844 (solid line) and FASCODE (dashed line) for the Region 800 to 820 cm^{-1} at 0.06 cm^{-1} Resolution. Spectrum was processed by the University of Denver

seen at all in the noise in Figure 39. The cause of the effect seen in Figure 39 is the temperature inversion near the ground seen in Figure 7. The water vapor in this warm layer near the ground radiates at the same or at a higher temperature than the ground so that the thermal contrast between the water vapor and the ground is lost. Note that in the calculated spectrum some of the water lines stand out above the ground temperature.

The depth of the water lines in Figure 44 is less in the calculated spectrum than in the measured. The opposite effect is seen in Figure 42 for the case of a long slant path to the ground. These discrepancies could easily be accounted for by uncertainties in the water vapor profiles or, in the case of Figure 42, by the effect of the finite field-of-view.

The radiance between the lines for the upward looking spectra is always greater in the measured spectra than in the calculated, and the differences are larger in the 1984 spectra. In particular, the calculated radiance between the lines in Figure 45 is negligible, while the measured radiance is 1×10^{-6} Watt/(cm^2 sr cm^{-1}). The discrepancy could be caused by an error in the calibration or by neglecting to include in the calculation a source of continuum emission such as aerosol emission or scattering. The fact that the measured radiance is always greater suggests the latter cause.

The noise in these spectra can be estimated from the limb and upward viewing spectra where the total radiance is small and there are few strong features. The noise in the 1983 spectra from Figures 40, 41 and 43 appears to be about 2×10^{-7} Watts/(cm^2 sr cm^{-1}). The noise in the 1984 spectra in Figures 45, 46, and 47 is too small to estimate accurately, but is several times less than the 1983 value. This difference is expected since the 1984 spectra are co-adds of about 12 individual spectra, while the 1983 spectra shown here have not been co-added.

5.4 Summary

The results of this section can be summarized as follows:

1. There is generally very good agreement between the measured and the calculated spectra at the center of the 15 micrometer CO_2 band except for upward looking spectra.

2. There is poorer agreement at the edges of this band, particularly between 600 and 630 cm^{-1}.

3. For limb and upward viewing spectra, the background emission in the window regions is greater in the measured spectra than in the calculated, suggesting that the calculation is neglecting a source of continuum emission.

4. The comparison brightness temperature in the window regions for downward looking spectra is not significant since the measured brightness temperature is used in the calculation as the ground temperature.

5. The comparison between the measured and the calculated spectra for long slant path low in the atmosphere is obscured by the effect of the finite field-of-view of the instrument which receives the emission from a broad range of paths.

6. CONCLUSIONS AND RECOMMENDATIONS

This report has surveyed the available spectra from the SCRIBE project. It has evaluated them critically in terms of radiometric and spectral calibration by comparing them with physical constraints imposed by the state of the atmosphere and with model calculations. The result of this evaluation has been to identify a set of spectra which appear well calibrated and can be analyzed further for scientific content.

In the course of the evaluation many of the spectra were shown be exhibit one or more anomalies. These included severe modulation caused by spikes and/or channel spectra in the interferogram, radiance values outside the limits imposed by the state of the atmosphere, significantly negative radiance values, and a trend or slope in the envelope of the spectrum which is inconsistent with model calculations and with other spectra for similar conditions. Some of these anomalies are only apparent when the spectra are examined at low resolution. At high resolution they are overwhelmed by the fine detail in the spectra.

One conclusion drawn from this study is that reducing the interferograms and calibrating the spectra is a difficult and tedious process. The interferograms and spectra must be individually examined at each step to ensure that the final calibrated spectra are free from errors. This examination must include comparisons between the

measured spectra and atmospheric parameters and the models in order to uncover inconsistencies not apparent in the spectra alone.

The comparisons presented here between the measured spectra and the spectra calculated with FASCODE has revealed several discrepancies which represent interesting areas for further investigation. These are:

1. The large difference between the measured and the calculated radiance between 600 and 630 cm^{-1}, with the measured radiance being larger,

2. The difference in the depth of the valleys between the strong lines around 667 cm^{-1} for upward looking spectra, and

3. The much greater measured radiance in the window region between 800 and 970 cm^{-1} for limb and upward viewing geometries.

Some of the evidence suggests that these differences are most likely due to deficiencies in the model and as such represent an important result from the data.

The results of this study lead to a number of recommendations for the future SCRIBE flights. These are:

1. There should be higher quality and more frequent meteorological support. Several radiosonde ascents should be made in the course of the flight and these should be closer to the actual flight path. An attempt should be made to measure the O_3 using an ozonesonde.

2. An attempt should be made to independently measure the ground temperature either in situ or remotely using a radiometer either from an aircraft, on the SCRIBE package itself, or from a satellite.

3. The narrower field-of-view in the current configuration of SCRIBE 99 should be retained. With the wide field-of-view in the previous configuration, interpretation of data from spectra

with low nominal tangent heights was difficult due to the spread in actual tangent height.

4. Black body calibration spectra should be made several times during the flight to verify the stability of the instrument response.

References

1. Murcray, F. H., F. J. Murcray , D. G. Murcray, and W. J. Williams (1981) Stratospheric Cryogenic Infrared Balloon Experiment, Air Force Geophysics Laboratory, Hanscom AFB, MA, AFGL-TR-81-0186, AD-A104 168.

2. Sakai, H. and G. A. Vanasse (1983) Atmospheric Infrared Emission Observed at Altitude of 27000 to 28000 m, SPIE Publ. 366, p165-172, AD-A133 472.

3. Sakai, H., T. C. Li, J. Pritchard, F. J. Murcray, F. H. Murcray, J. Williams, and G. A. Vanasse (1981) Measurement of Atmospheric Emission using a Balloon - Borne Cryogenic Fourier Spectrometer SPIE Publ. 289, p196-198, AD-A111 343.

4. Sakai, H., W. Barowy, S. Pulchtopek, J. Pritchard, F. J. Murcray, F. H. Murcray, and G. A. Vanasse (1982) Study of Atmospheric Infrared Emission Using a Balloon-Borne Cryogenic Fourier Spectrometer, SPIE Publ. 364, p38-45.

5. Vanasse, G. A. (1981) Stratospheric Cryogenic Interferometer Balloon Experiment (SCRIBE), Air Force Geophysics Laboratory, Hanscom AFB, MA, AFGL-TR-81-0048, AD-A100 218.

6. Sakai, H. (1981) SCRIBE I DATA ANALYSIS Air Force Geophysics Laboratory, Hanscom AFB, MA, AFGL-TR-81-0129, AD-A102 262.

7. Murcray, F.H., F. J. Murcray, D. G. Murcray, J. Prichard, G. A. Vanasse, and H. Sakai (1984) Liquid Nitrogen Cooled Fourier Transform Spectrometer System for Measuring Atmospheric Emission At High Altitudes, J. Atm. and Oceanic Tech., 1., p351-357, AD-A152 450.

8. Murcray, F.H., F. J. Murcray, D. G. Murcray, and A. Goldman (1986) Measurement of Atmospheric Emission Spectra at High Altitudes, Air Force Geophysics Laboratory, Hanscom AFB, MA, AFGL-TR-86-0061, AD-A170 143.

9. Vanasse, G. A. and H. Sakai (1967) "Fourier Spectroscopy" in ,Progress in Optics (E. Wolf ed.), Vol VI, North Holland Publishing Co., Amsterdam.

10. Rothman, L. S. (1986) HITRAN, The Molecular Absorption Database, in the Sixth Conference on Atmospheric Radiation, Williamsburg, Virginia, May 13-16, 1986, p137-140.

11. A. Goldman, private communication.

12. Sakai, H., and G. A. Vanasse (1982) SCRIBE II DATA ANALYSIS, Air Force Geophysics Laboratory, Hanscom AFB, MA, AFGL-TR-82-0150, AD-A116 250.

13. Sakai, H., anD G. A. Vanasse (1983) SCRIBE Data of October 23, 1983, Air Force Geophysics Laboratory, Hanscom AFB, Ma., AFGL-TR-84-0208, AD-A154 862.

14. Sakai, H., G. A. Vanasse, F. H.Murcray, and F. J. Murcray, (1984) Detector-Nose-Limited Sensitivity of Fourier Spectroscopy Plus Stratospheric Emission Measurements and Observed Trace Gas Spectra, Proceedings of the 13th Congress of the International Commission for Optics, p550-551.

15. Sakai, H., (1985) Processing of Scribe Data, Air Force Geophysics Laboratory, Hanscom AFB, MA, AFGL-TR-85-0279, AD-A165 226.

16. Murcray, D. G., F. H. Murcray, F. J. Murcray and G. A. Vanasse (1985) Measurements of Atmospheric Emission at High Spectral Resolution, J. of Met. Soc. Japan, 63, p320-324, AD-A159 338.

17. Goldman, A. (1986) Atmospheric Radiance in the 8.6 - 13.6 Micrometer Region-an Update, Scientific Report, Dept of Physics, U. of Denver, Denver CO.

18. Goldman, A. (1985) Cold Interferometer July 5 1984 Flight Scientific Report, Dept. of Physics, U. of Denver, Denver, CO.

19. Goldman, A. (1985) Preliminary Qualitative Comparison of Calculated and Experimental Cold Interferometer Spectra, Scientific Report, Dept of Physics, U. of Denver, Denver CO.

20. Clough, S. A., F. X. Kneizys, E. P. Shettle, and G. P. Anderson (1986) Atmospheric Radiance and Transmittance: FASCODE 2, in the Sixth Conference on Atmospheric Radiation, Williamsburg, Virginia, May 13-16, 1986

21. Anderson, G. P. , S. A. Clough, F. X. Kneizys, J. H. Chetwynd, and E. P. Shettle (1986) AFGL Atmospheric Constituent Profiles (0-120km), AFGL-TR-86-0110, AD-A175 173.

22. Gallery, W. O. , J. L. Manning, and D. Tucker (1987) Enhancements to the Atmospheric Transmittance/Radiance Program FASCODE, OptiMetrics Inc, OMI 200.

23. F. J. Murcray, private communication.

24. A. Goldman, private communication.

25. Nestler, M. S. (1983) A Comparative Study of Measurements from Radiosondes, Rocketsondes, and Satellites, NASA Contractor Report 168343, April 1983

Appendix A Flight Details

This appendix includes the details of the flights of October 23, 1983 and July 5, 1984. Included are listings of the radiosonde profiles in Tables A-1 and A-2 and of the flight track from the ground radars given in Tables in A-3 and A-4. The flight track data is shown graphically in Figures A-1 through A-4 in plots of altitude vs time and of the ground track. Plots of the temperature profiles were shown previously in Figures 7 and 8.

Table A-1. Radiosonde Profile for October 23, 1983 at 0700 MST for Holloman AFB, NM. The Station is at 32.889 Deg West Latitude and 106.100 Deg North Longitude with an Altitude of 1.258 km MSL. The Levels Marked with an Asterisk under Dew Point are Extrapolated as Discussed in the Text

Altitude (km MSL)	Pressure (mb)	Temperature (°C)	Dew Point (°C)
1.258	878.9	7.2	4.0
1.430	861.1	15.1	3.8
1.740	830.2	15.9	3.9
2.331	774.0	11.0	-0.2
2.486	759.8	11.2	-7.2
3.906	639.1	2.4	-18.3
4.258	611.8	0.1	-20.2
4.415	599.9	-0.1	-22.9
4.740	576.0	-1.6	-24.1
6.896	435.5	-19.2	-35.9
7.750	387.7	-26.4	-41.6
7.869	381.4	-26.2	-41.5
9.143	318.8	-36.2	-50.5
9.565	300.0	-38.3	-51.6
9.625	297.4	-39.1	-52.3
10.80	250.0	-45.8	-87.8
11.33	231.0	-50.0	
11.96	209.5	-53.1	
12.26	200.0	-54.0	
12.61	189.6	-55.6	
12.83	183.2	-55.4	
13.46	165.8	-59.1	
14.09	150.0	-60.5	
14.34	144.1	-62.3	
14.95	130.5	-61.9	
15.47	120.0	-64.3	
15.73	115.1	-63.9	
16.09	108.6	-65.7	
16.59	100.0	-66.5	
16.91	94.8	-67.5	
17.65	84.0	-64.9	
18.05	78.7	-66.9	
18.76	70.0	-65.5	
19.35	63.6	-63.9	
19.64	60.7	-64.9	
20.03	57.0	-62.5	
20.84	50.0	-63.6	
21.22	47.0	-62.6	
21.58	44.4	-59.4	

Table A-1. (Cont.)

Altitude (km MSL)	Pressure (mb)	Temperature (°C)	Dew Point (°C)
21.99	41.6	-60.1	
22.38	39.1	-58.6	
24.08	30.0	-52.7	
24.92	26.4	-52.7	
26.11	22.0	-51.5	
26.73	20.0	-48.3	
27.82	17.0	-46.4	
28.67	15.0	-44.5	*
31.45	10.0	-38.3	*
36.19	5.0	-27.7	*
47.20	1.0	-3.2	*

Table A-2. Radiosonde Profile for July 5, 1984 at 0700 MST for White Sands Missile Range. The Station is at 32.400 Deg West Latitude and 106.370 Deg North Longitude with an Altitude of 1.216 km MSL. The Levels Marked with an Asterisk under Dew Point are Extrapolated as Discussed in the Text

Altitude (km MSL)	Pressure (mb)	Temperature (°C)	Dew Point (°C)
1.216	879.7	22.3	12.0
1.338	867.4	22.1	12.1
1.515	850.0	22.7	12.3
2.532	755.5	15.9	8.9
2.844	728.3	14.9	4.0
3.053	710.5	12.8	6.8
3.179	700.0	12.6	3.6
3.479	675.4	11.1	-1.0
3.915	640.3	7.0	-3.2
4.473	599.0	2.9	-8.4
5.033	558.4	-1.3	-9.6
5.414	532.2	-5.3	-11.0
5.730	511.2	-7.3	-27.5
5.909	500.0	-7.4	-28.8
6.203	481.1	-8.1	-30.1
6.690	451.7	-12.0	-28.8
7.065	430.1	-13.8	-30.1
7.163	400.0	-18.3	-35.2
8.603	349.8	-25.5	-41.3
9.701	300.0	-34.3	-48.5
10.31	274.1	-39.4	-52.5
10.53	266.3	-41.5	
10.95	250.0	-43.8	
12.43	200.0	-53.3	
13.37	172.3	-60.9	
14.23	150.0	-64.5	
15.18	128.3	-68.3	
15.59	120.0	-66.4	
16.26	107.4	-70.9	
16.68	100.0	-73.7	
17.24	91.0	-74.4	
17.77	83.4	-67.4	
18.64	70.0	-64.5	
19.36	64.4	-64.4	
20.93	50.0	-64.9	
24.22	30.0	-61.	
26.89	20.0	-48.7	
27.86	17.3	-46.4	
28.80	15.1	-45.7	

Table A-2. (Cont.)

Altitude (km MSL)	Pressure (mb)	Temperature (°C)	Dew Point (°C)
31.28	10.5	-42.2	
31.61	10.0	-41.3	*
32.33	9.0	-39.4	*
33.14	8.0	-37.4	*
34.05	7.0	-34.9	*
35.10	6.0	-32.2	*
36.34	5.0	-28.9	*
37.87	4.0	-24.9	*
39.83	3.0	-19.7	*
42.60	2.0	-12.4	*
47.33	1.0	0.0	*

Table A-3. Flight Path for the SCRIBE Flight of October 23, 1983. The Columns X and Y are the Distances from the Launch Point = Holloman AFB, NM. Launch Time was 1210 GMT or 0510 MST

Time (hr GMT)	Minutes After Launch	Distance from Launch X (km)	Y (km)	Altitude (km MSL)
12.200	2	-1.147	-0.547	1.859
12.283	7	-0.392	-1.116	3.816
12.367	12	2.389	-2.273	5.619
12.450	17	5.761	-2.986	7.489
12.533	22	13.162	-3.447	9.384
12.617	27	23.144	-3.900	11.241
12.700	32	32.716	-4.365	13.049
12.783	37	38.433	-5.402	14.755
12.867	42	41.840	-6.377	16.231
12.950	47	42.918	-8.069	17.592
13.033	52	42.845	-8.921	18.697
13.117	57	42.778	-10.985	19.787
13.200	62	41.867	-11.868	21.151
13.283	67	41.547	-13.236	22.327
13.367	72	40.879	-13.394	23.609
13.450	77	41.653	-14.243	24.986
13.533	82	42.983	-13.393	26.399
13.617	87	45.966	-12.523	27.387
13.700	92	49.758	-12.140	28.329
13.783	97	53.285	-10.839	29.288
13.867	102	58.110	-9.064	30.381
13.950	107	63.941	-6.863	30.357
14.033	112	69.841	-4.727	30.286
14.117	117	75.577	-2.462	30.070
14.200	122	81.253	-0.078	30.133
14.283	127	86.769	2.567	30.033
14.367	132	92.225	5.220	29.845
14.450	137	97.630	7.115	29.662
14.533	142	101.902	8.128	29.463
14.617	147	107.701	10.158	29.186
14.700	152	111.929	12.172	28.941
14.783	157	115.670	13.753	28.519
14.867	162	118.809	14.989	28.049
14.950	167	122.050	15.520	27.574
15.033	172	125.857	16.815	27.041
15.117	177	129.086	18.063	26.366
15.200	182	131.529	20.090	25.843
15.283	187	133.456	22.341	25.300
15.367	192	135.758	23.250	24.896

Table A-3. (Cont.)

Time (hr GMT)	Minutes After Launch	Distance from Launch X (km)	Y (km)	Altitude (km MSL)
15.450	197	137.792	24.366	24.406
15.533	202	138.797	26.003	23.918
15.617	207	138.662	26.626	23.290
15.700	212	138.509	25.870	22.625
15.783	217	139.381	24.832	21.728
15.867	222	138.147	24.911	20.720
15.950	227	137.238	23.037	19.727
16.033	232	137.165	22.361	18.479
16.117	237	136.399	20.781	17.070
16.200	242	137.006	19.950	15.329
16.283	247	139.294	18.463	12.559
16.367	252	145.357	17.160	9.266
16.450	257	153.102	15.823	6.372
16.533	262	156.662	14.830	4.156

Table A-4. Flight Path for the SCRIBE Flight of July 5, 1984. The Columns X and Y are the Distances from the Launch Point = Roswell, NM. Launch Time was 1210 GMT or 0451 MST

Time (hr GMT)	Minutes After Launch	Distance from Launch X (km)	Y (km)	Altitude (km MSL)
12.810	57.6	124.941	18.991	16.836
12.893	62.6	121.884	18.218	17.973
12.977	67.6	119.748	17.653	19.185
13.060	72.6	116.856	17.087	20.490
13.143	77.6	113.178	17.111	21.681
13.227	82.6	109.471	16.356	22.882
13.310	87.6	105.333	15.133	24.147
13.393	92.6	99.858	14.741	25.453
13.477	97.6	95.416	14.853	26.787
13.560	102.6	90.799	15.597	28.036
13.643	107.6	85.593	16.131	29.455
13.727	112.6	78.669	16.832	30.213
13.810	117.6	71.711	16.631	30.196
13.893	122.6	64.828	16.223	30.216
13.977	127.6	58.313	15.899	30.279
14.060	132.6	52.022	15.785	30.417
14.143	137.6	45.265	15.447	30.460
14.227	142.6	38.379	15.176	30.591
14.310	147.6	31.650	15.003	30.625
14.393	152.6	25.285	14.806	30.601
14.477	157.6	18.689	14.266	30.712
14.560	162.6	12.029	13.382	30.601
14.643	167.6	5.430	12.101	30.677
14.727	172.6	-0.831	11.041	30.593
14.810	177.6	-6.844	9.897	30.696
14.893	182.6	-13.282	8.375	30.730
14.977	187.6	-19.813	6.535	30.695
15.060	192.6	-26.174	4.799	30.662
15.143	197.6	-32.230	3.290	30.660
15.227	202.6	-38.383	1.757	30.662
15.310	207.6	-44.721	0.249	30.600
15.393	212.6	-51.183	-1.042	30.608
15.477	217.6	-57.838	-2.969	30.499
15.560	222.6	-64.464	-4.480	30.495
15.643	227.6	-70.313	-5.273	30.220
15.727	232.6	-75.778	-5.783	30.009
15.810	237.6	-81.835	-5.333	29.760

Table A-4. (Cont.)

Time (hr GMT)	Minutes After Launch	Distance from Launch X (km)	Y (km)	Altitude (km MSL)
15.893	242.6	-88.055	-4.886	29.417
15.977	247.6	-92.953	-3.750	29.081
16.060	252.6	-99.194	-2.610	28.760
16.143	257.6	-103.798	-1.839	22.755
16.227	262.6	-106.525	-1.288	16.932
16.310	267.6	-108.474	-2.827	13.084
16.393	272.6	-110.678	-5.501	9.942
16.477	277.6	-114.426	-8.059	7.268
16.560	282.6	-117.819	-7.991	4.852
16.643	287.6	-120.118	-8.004	2.802

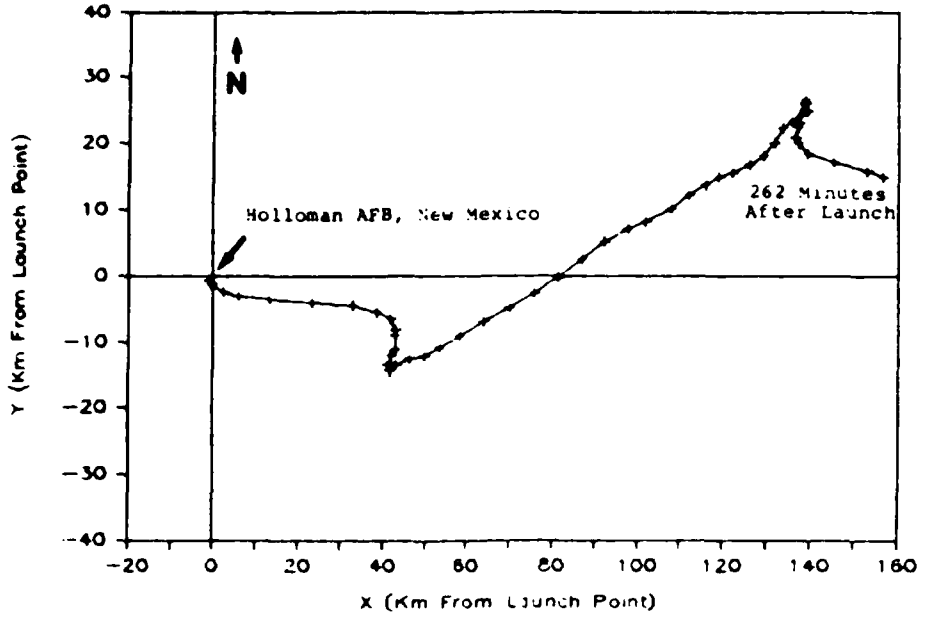

Figure A-1. Ground Track of the October 23, 1983 Flight. The Symbols Denote 5 Minute Intervals.

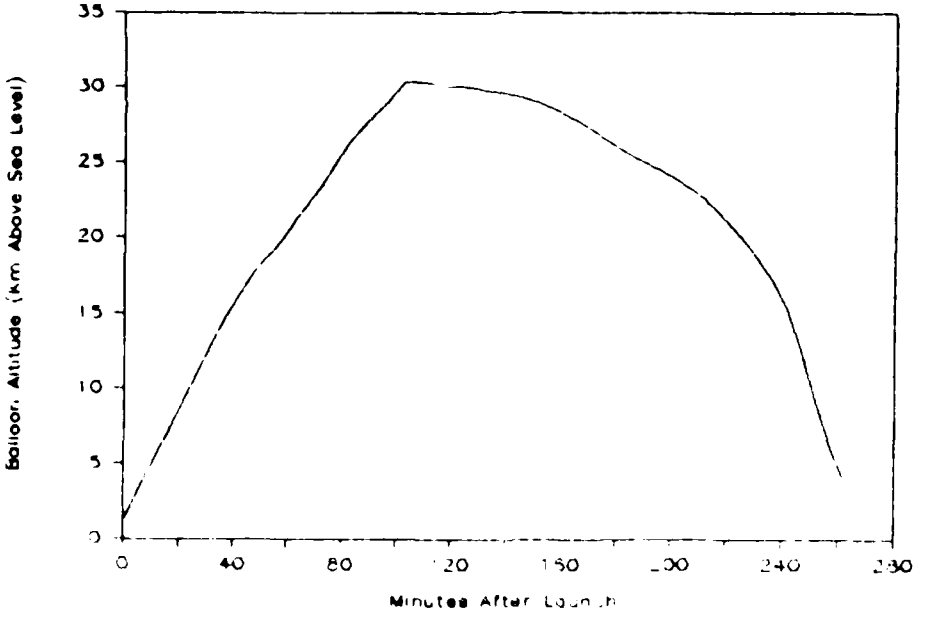

Figure A-2. Balloon Altitude as a Function of Time for the October 23, 1983 Flight.

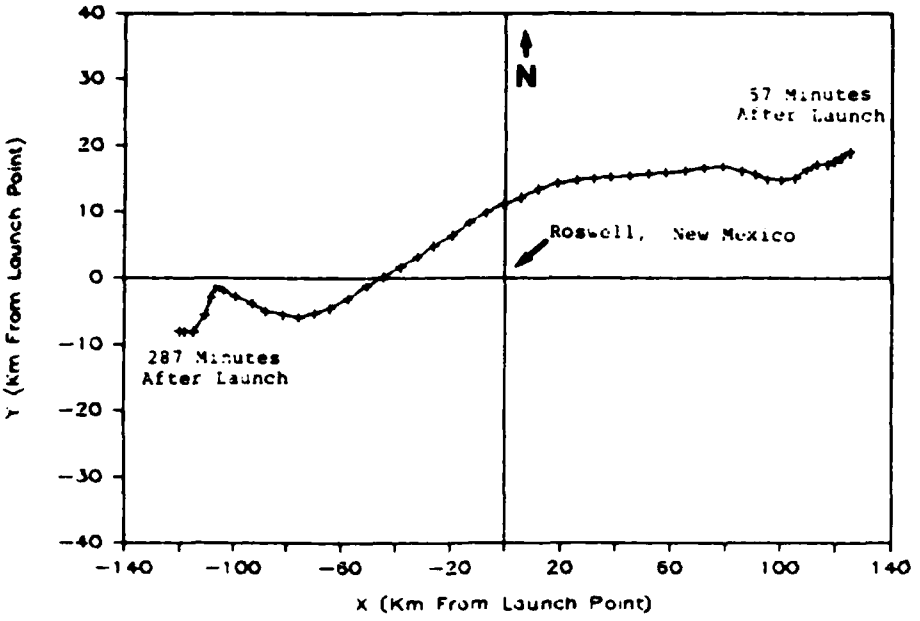

Figure A-3. A Partial Ground Track of the July 5, 1984 Flight. The Symbols Denote 5 Minute Intervals.

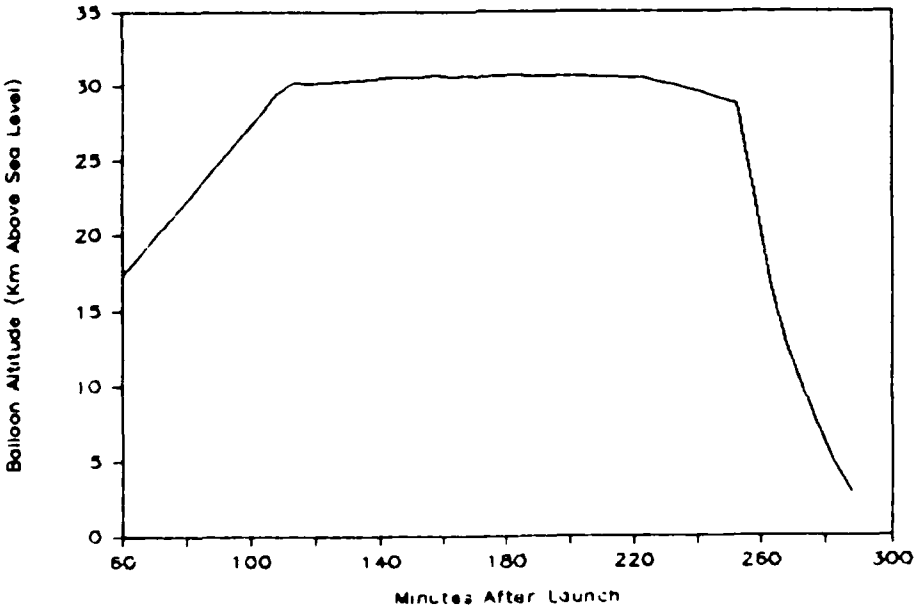

Figure A-4. Balloon Altitude as a Function of Time for the July 5, 1984 Flight.

Appendix B. Spectra SC841 and SC843

In the body of the report, the measured spectra were shown at full resolution only over the limited intervals of 665 to 675 cm^{-1} and 800 to 820 cm^{-1}. As a useful reference, two of the spectra are shown here at full resolution over the range 600 to 1200 cm^{-1}. The spectra selected are SC841 and SC844 which are from the July 5, 1984 flight and were processed by the Denver group. These spectra correspond to zenith angles of 180 deg and 88.1 deg respectively and both are taken from an altitude of 31.3 km msl. These spectra were chosen because they represent the extremes of a downward looking and an upward looking spectrum and because they have a high signal-to-noise ratio compared to the 1983 spectra.

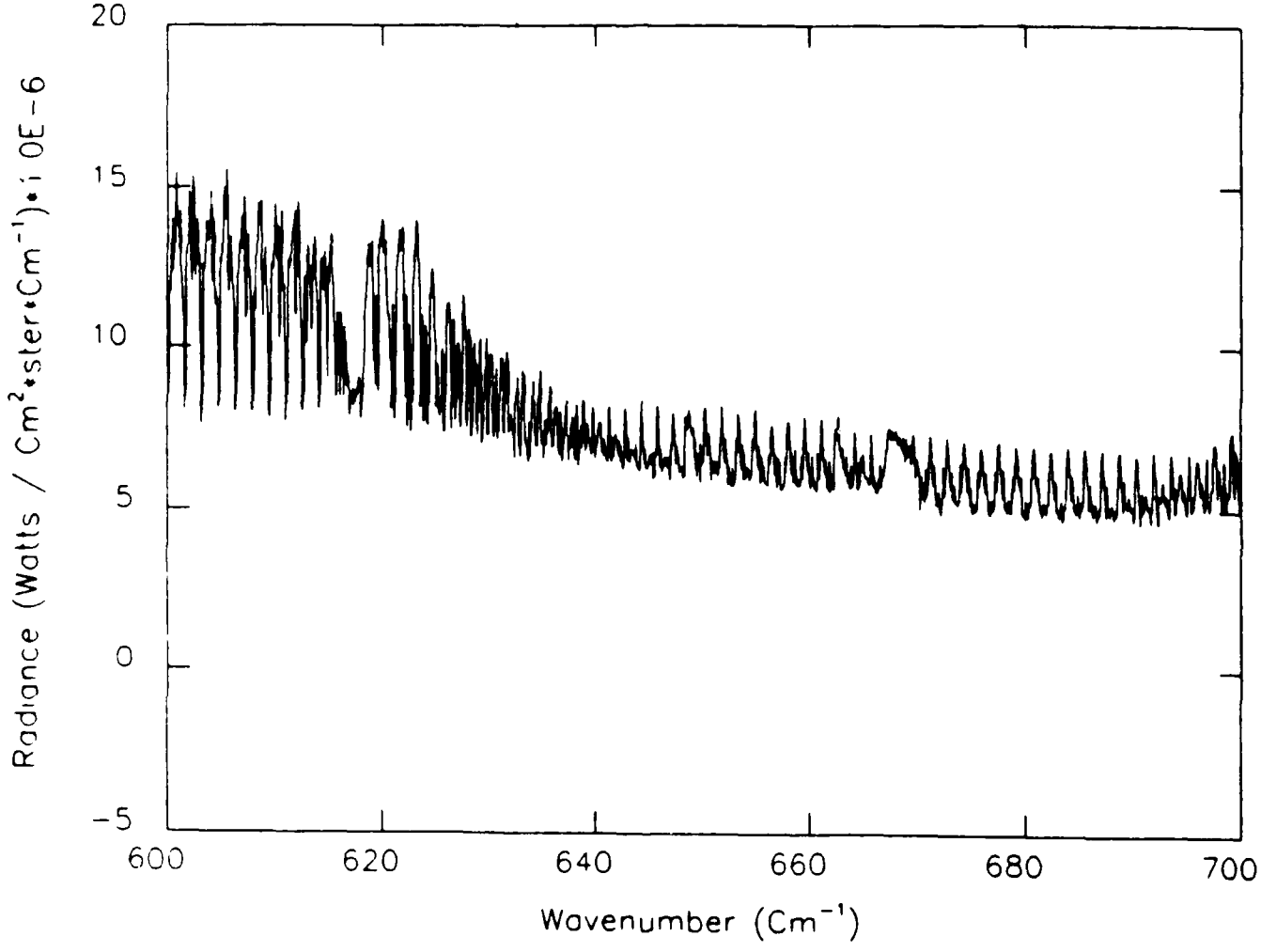

Figure B-1a. Spectrum SC841 from 600 to 700 cm^{-1}.

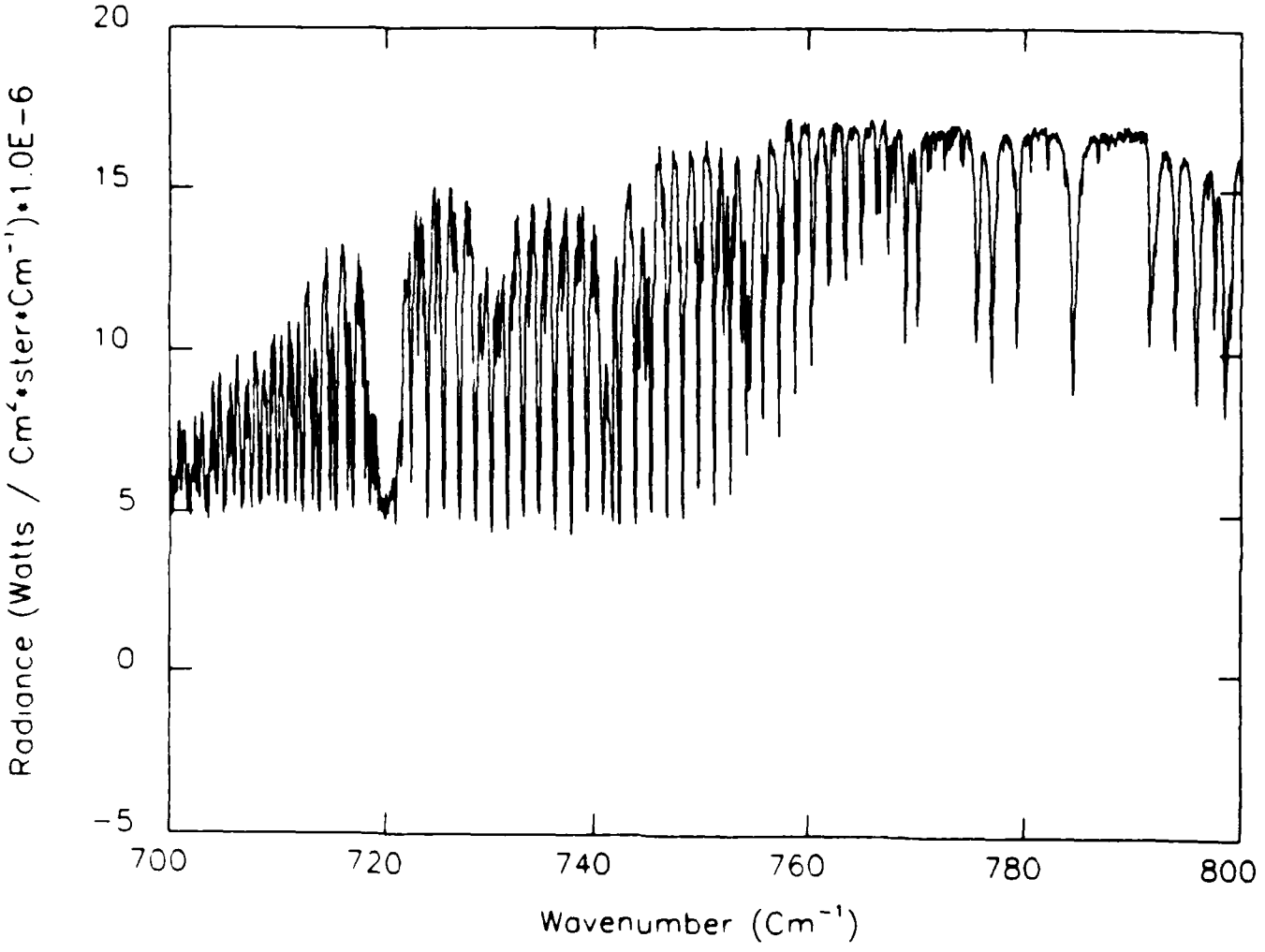

Figure B-1b. Spectrum **SC841** from 700 to 800 cm^{-1}.

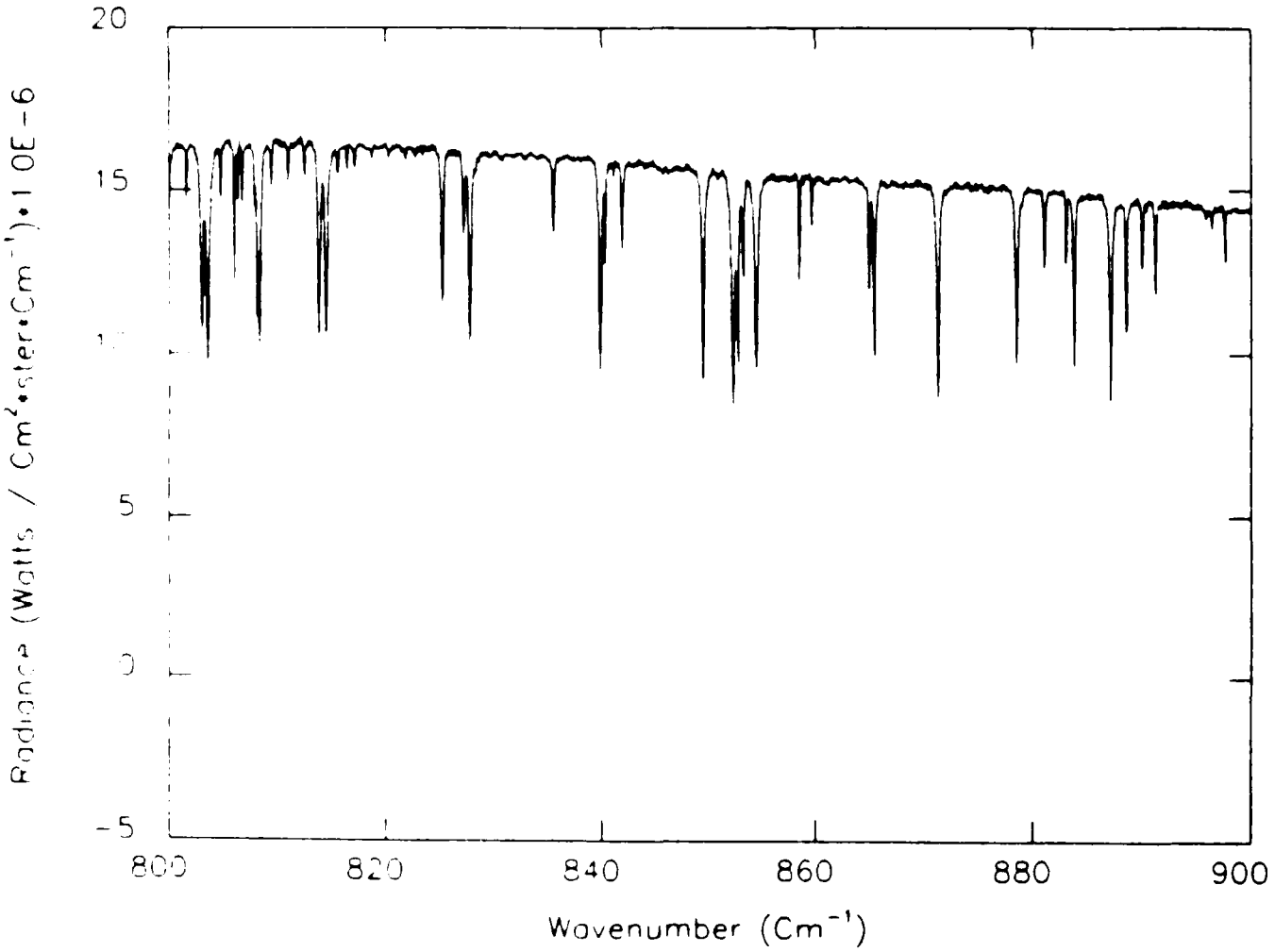

Figure B-1c. Spectrum SC841 from 800 to 900 cm^{-1}.

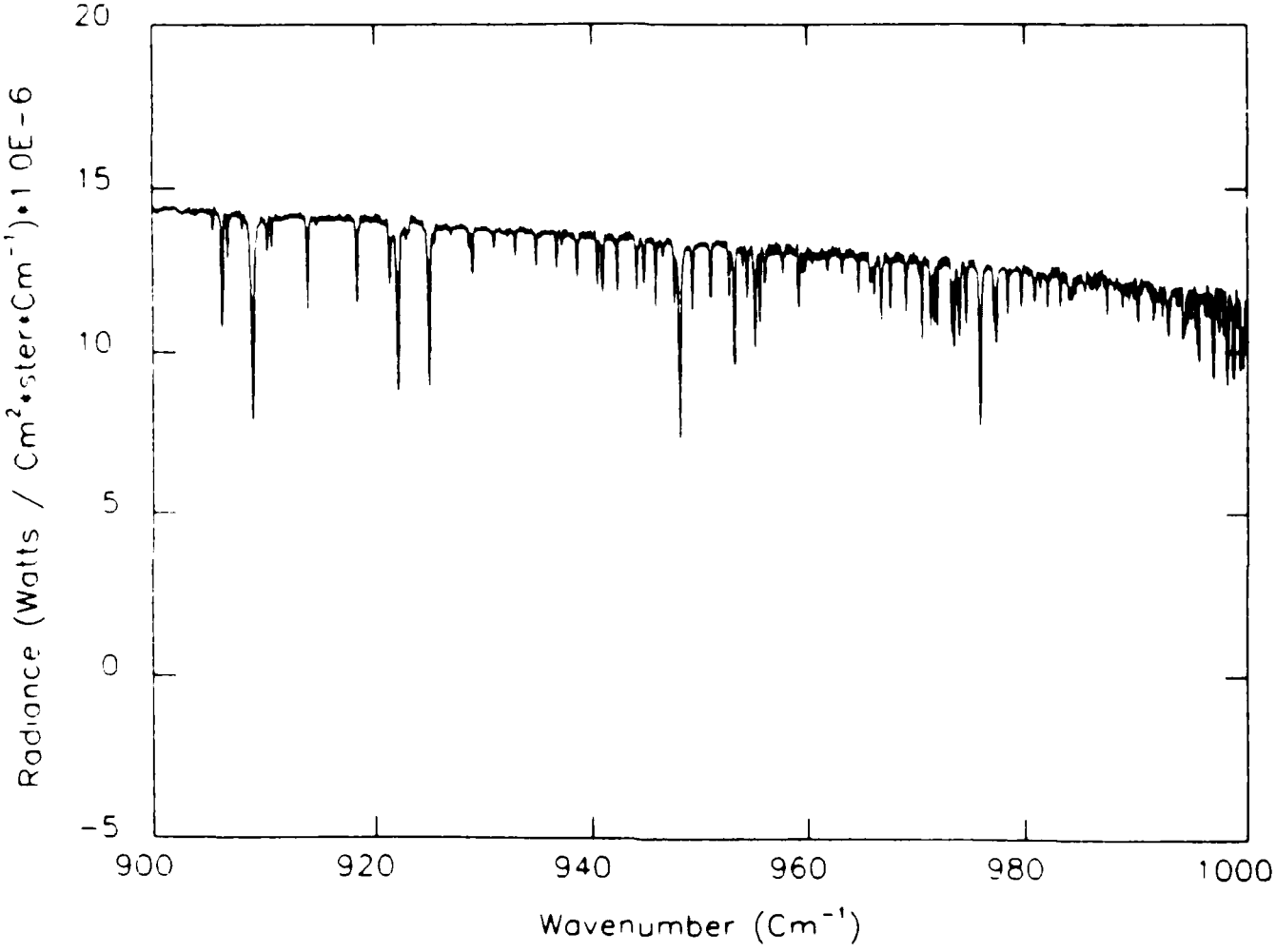

Figure B-1d. Spectrum SC841 from 900 to 1000 cm^{-1}.

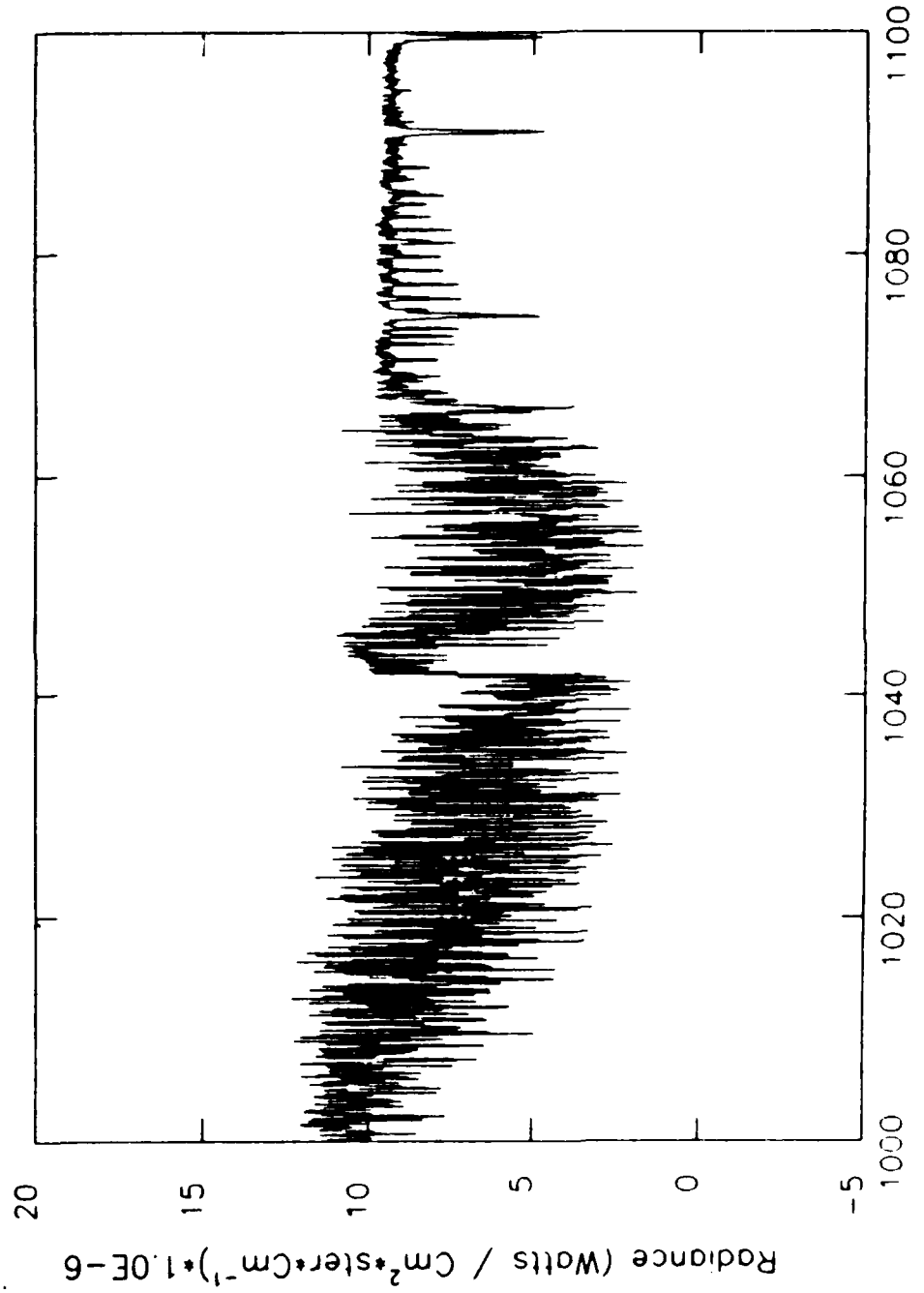

Figure B-1e. Spectrum SC841 from 1000 to 1100 cm^{-1}.

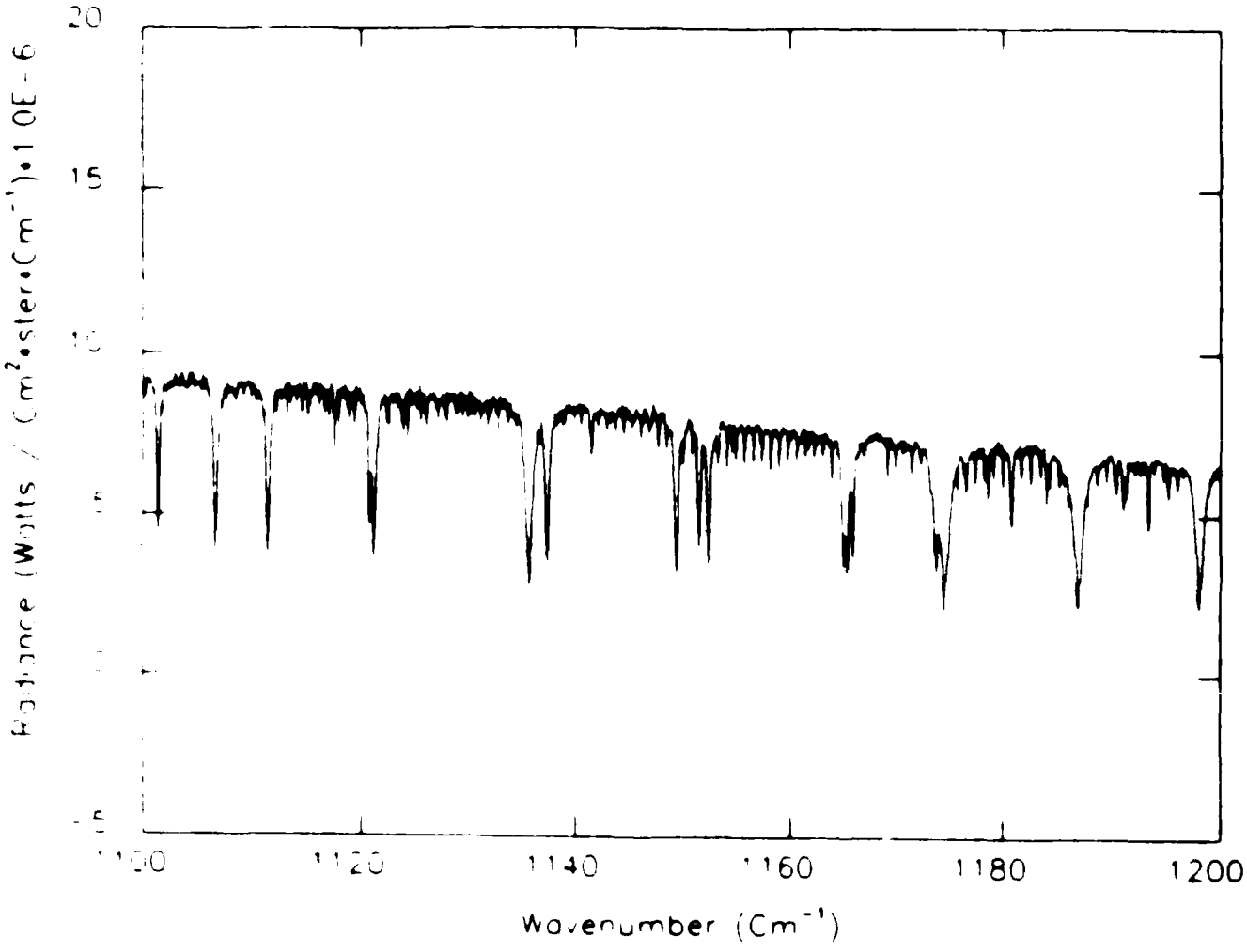

Figure B-1f. Spectrum SC841 from 1100 to 1200 cm^{-1}.

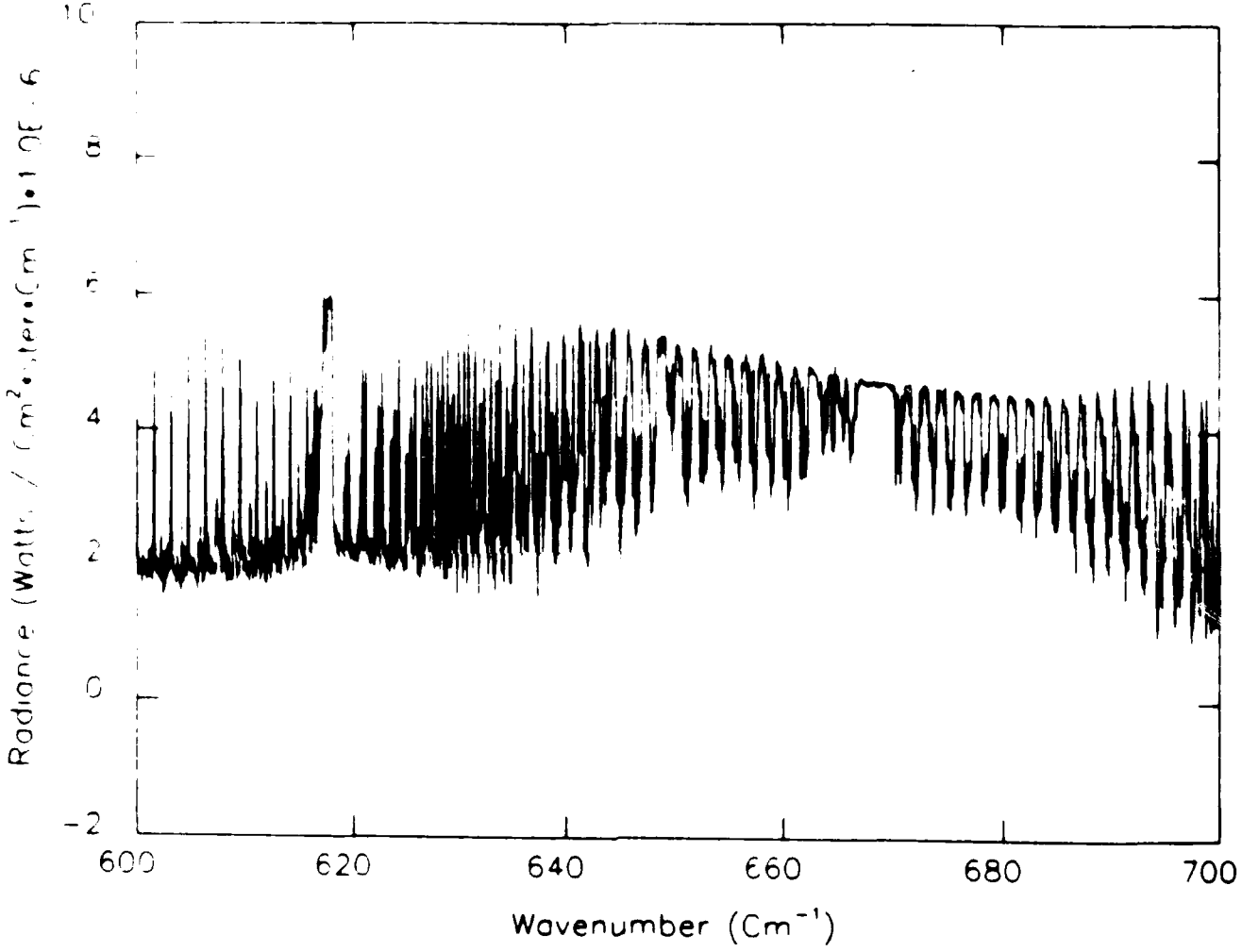

Figure B-2a. Spectrum **SC844** from 600 to 700 cm^{-1}.

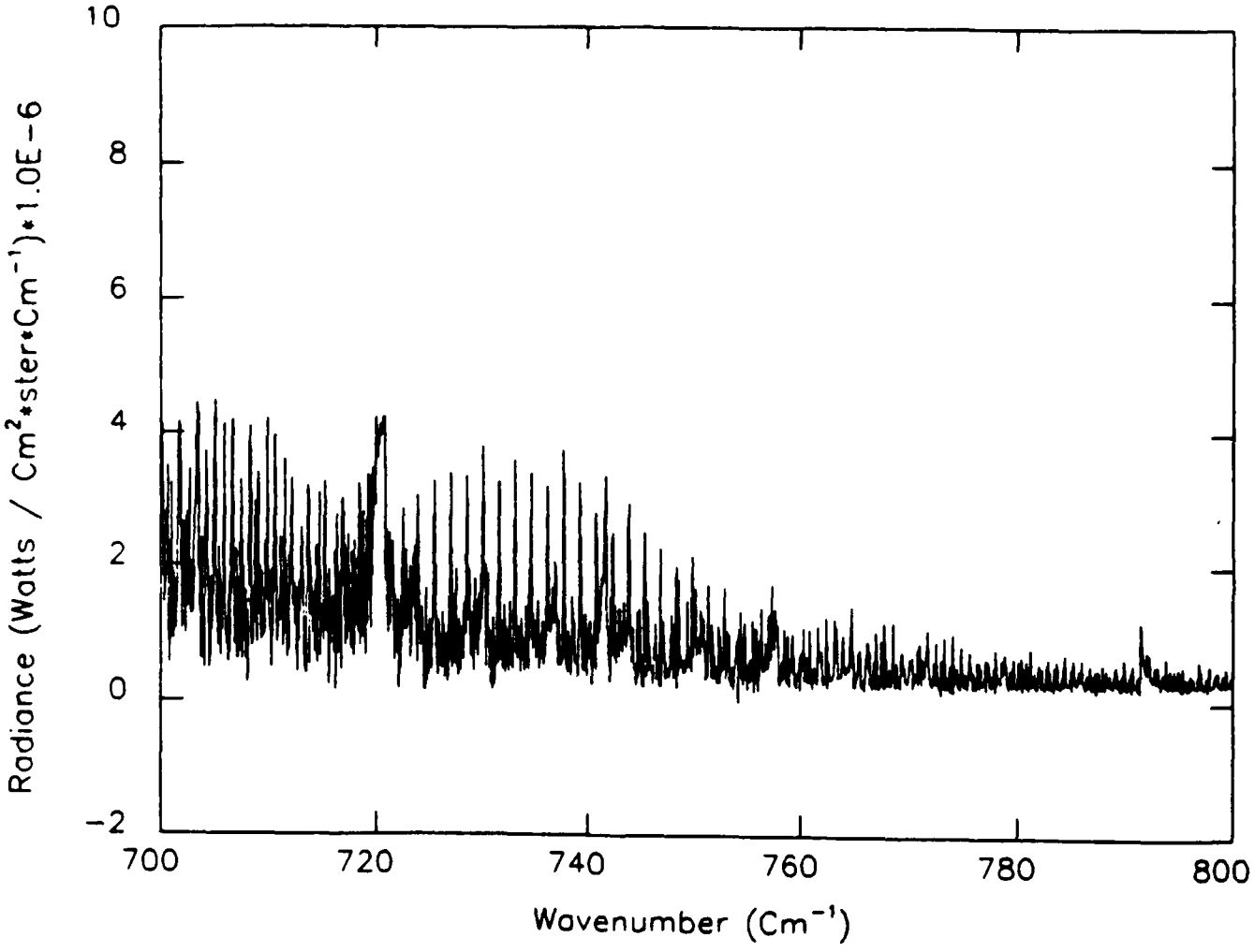

Figure B-2b. Spectrum SC844 from 700 to 800 cm^{-1}.

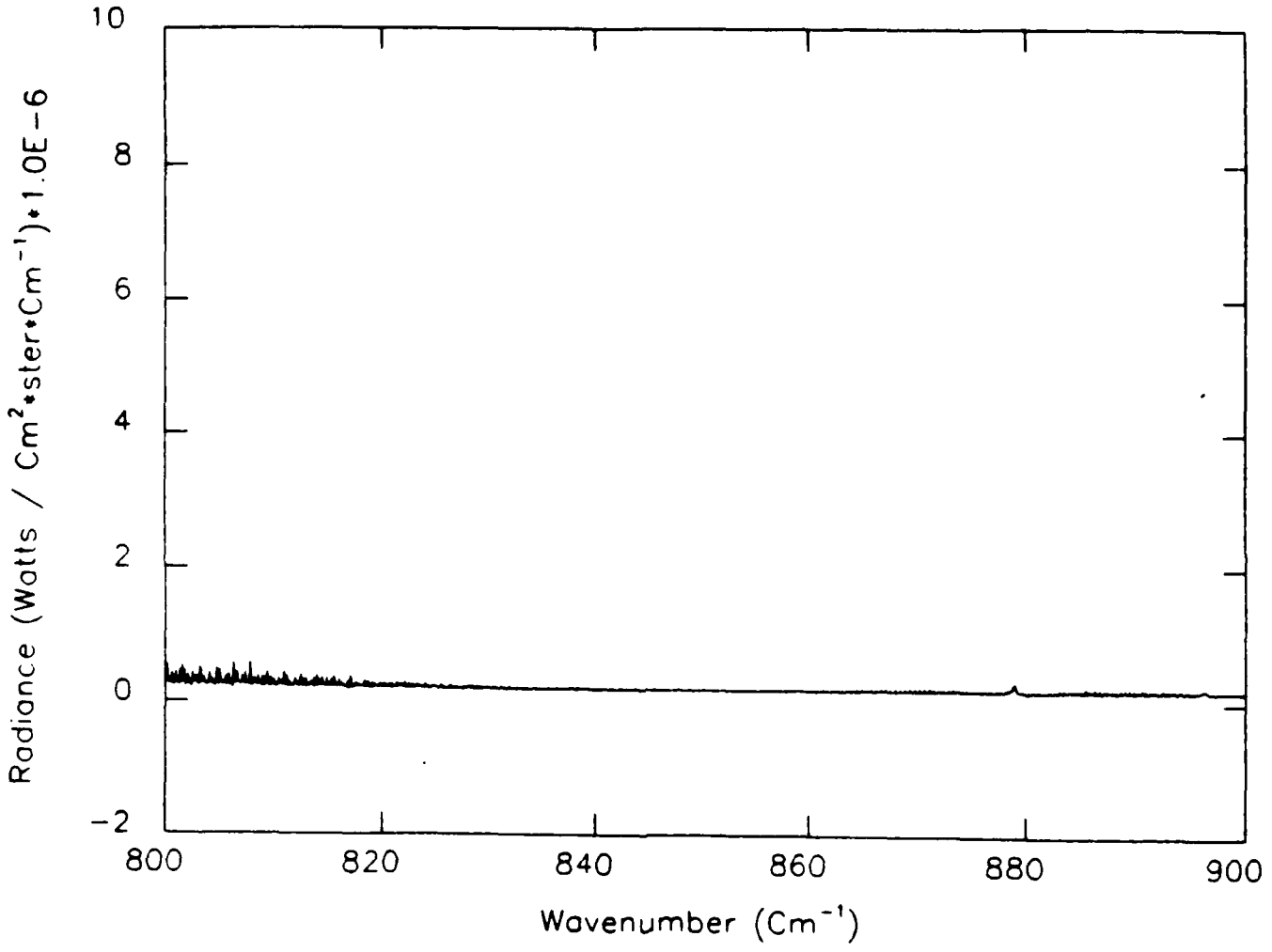

Figure B-2c. Spectrum SC844 from 800 to 900 cm^{-1}.

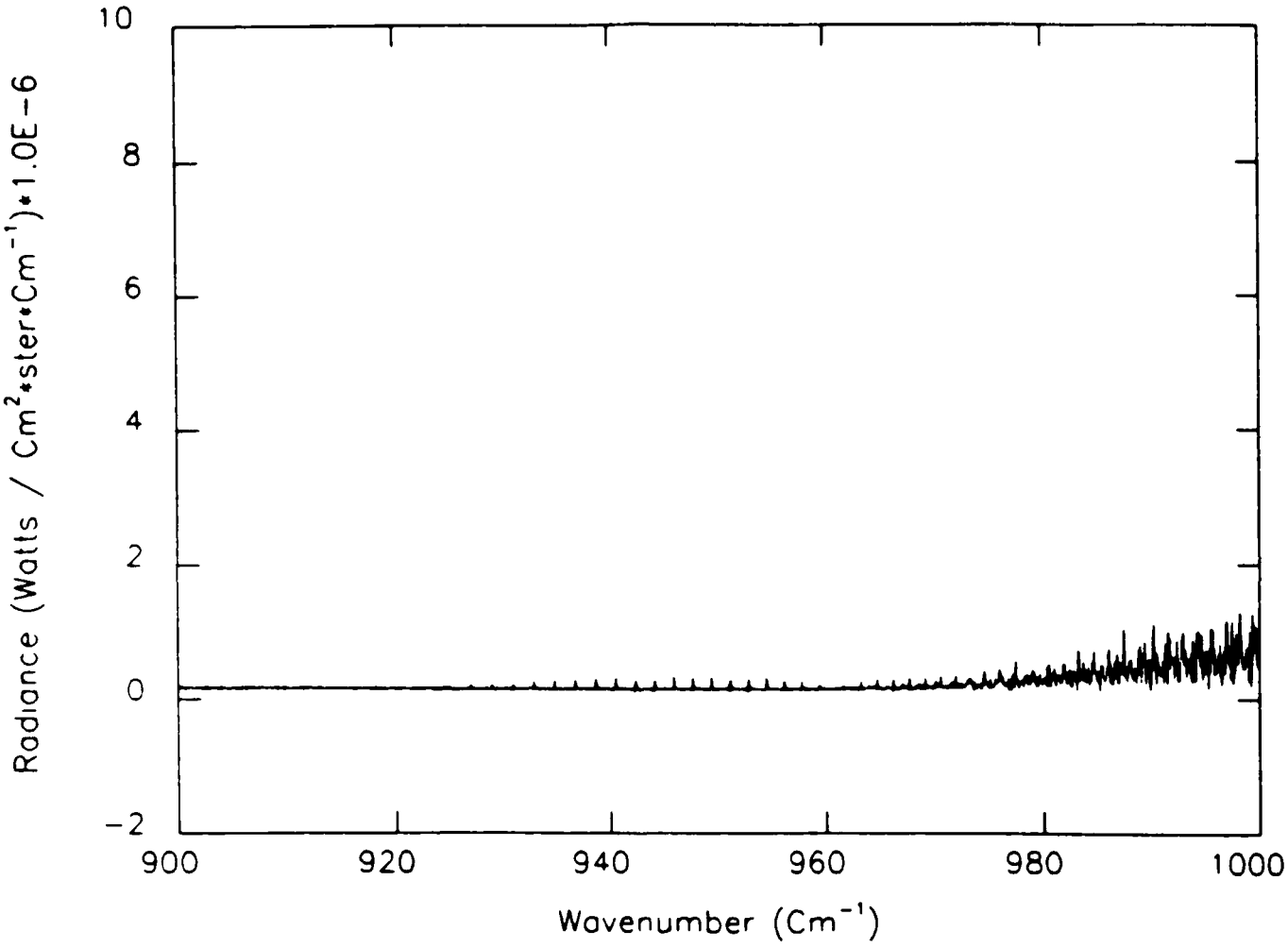

Figure B-2d. Spectrum **SC844** from 900 to 1000 cm^{-1}.

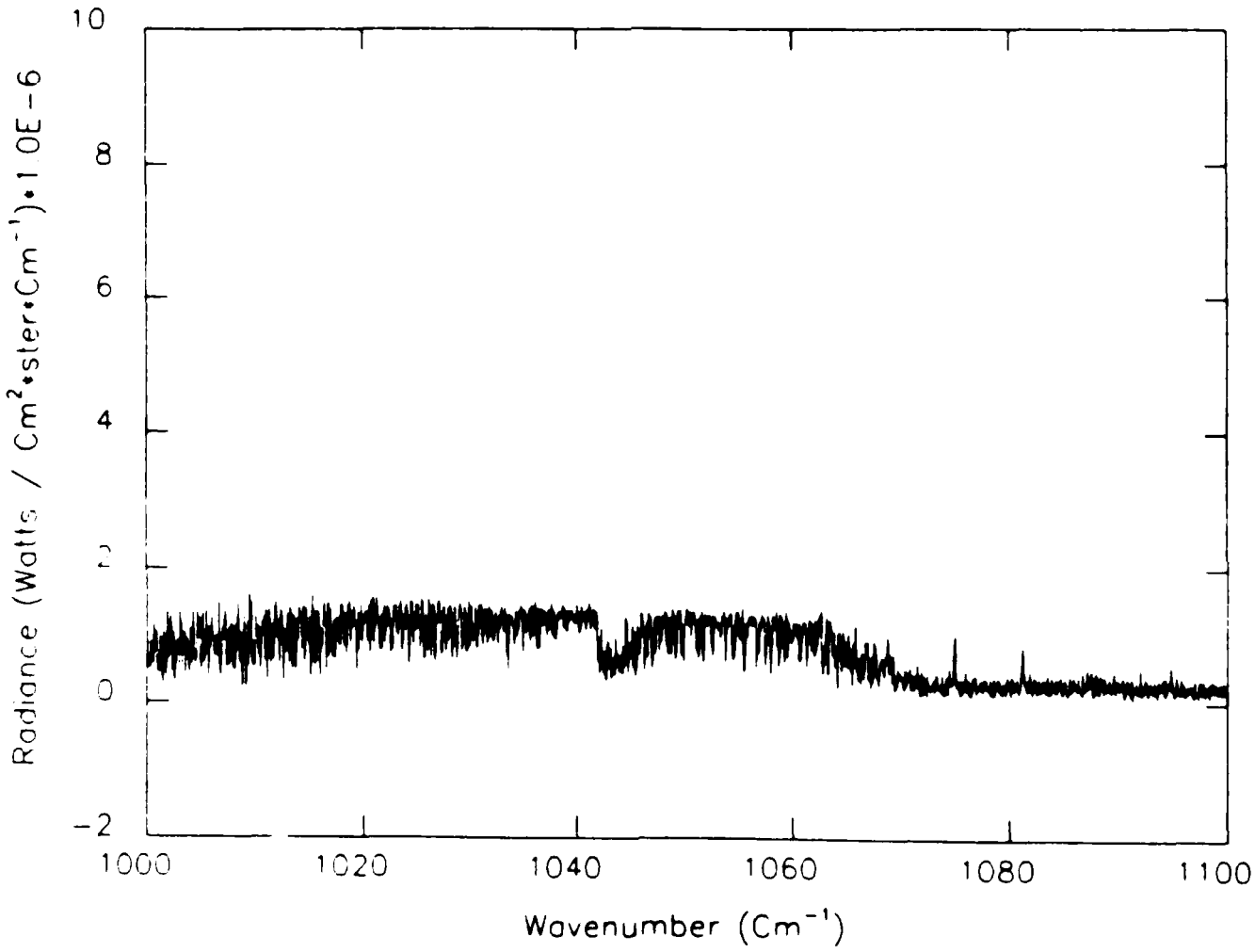

Figure B-2e. Spectrum SC844 from 1000 to 1100 cm^{-1}.

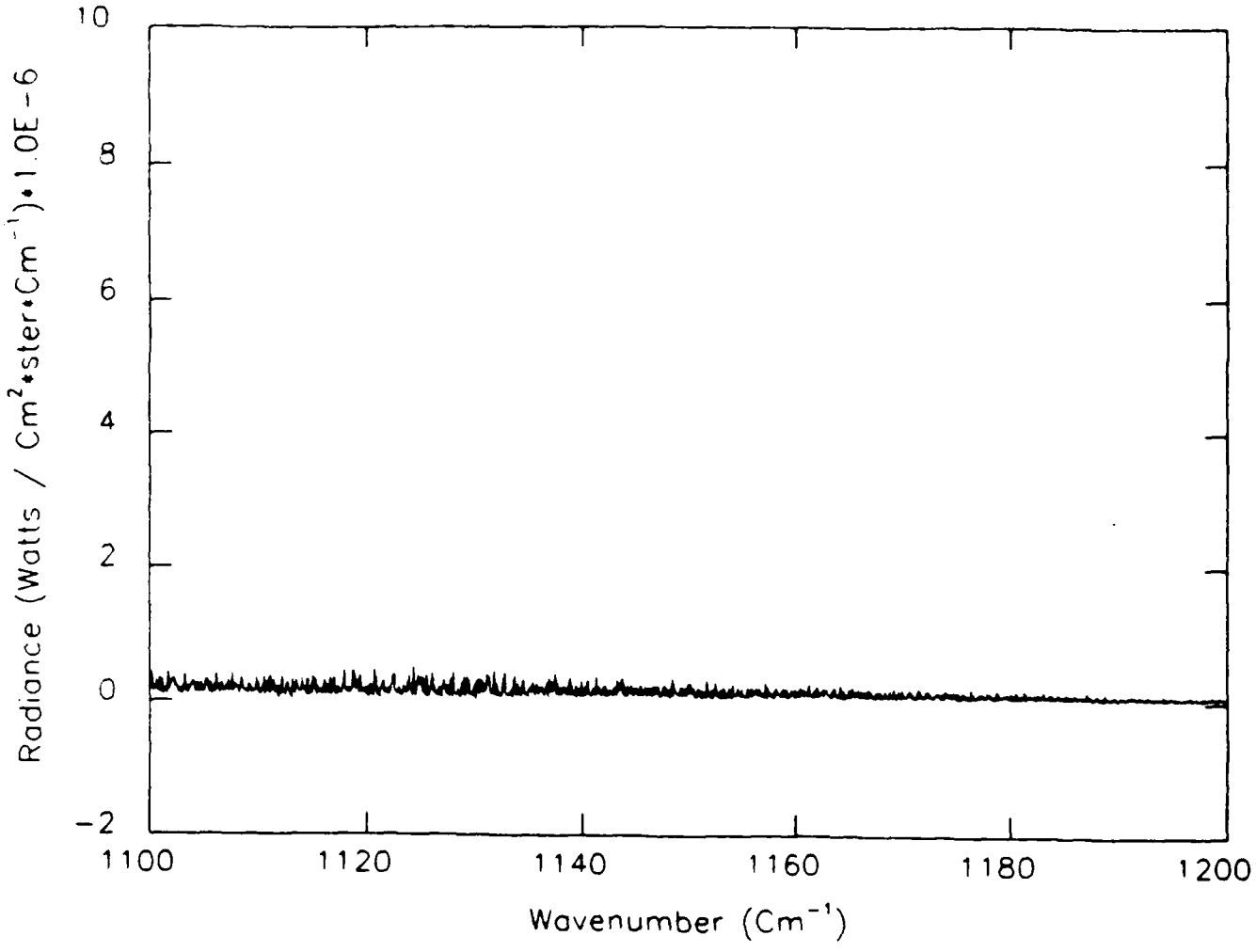

Figure B-2f. Spectrum **SC844** from 1100 to 1200 cm^{-1}.

END

9-87

DTIC